LOCKHEED MARTIN ENERGY RESEARCH LIBRARIES

3 4456 0515405 2

CENTRAL RESEARCH LIBRARY

ORNL-4800

cy. 1

NEUTRON PHYSICS DIVISION

Annual Progress Report

Period Ending May 31, 1972

OAK RIDGE NATIONAL LABORATORY
CENTRAL RESEARCH LIBRARY
DOCUMENT COLLECTION
LIBRARY LOAN COPY
DO NOT TRANSFER TO ANOTHER PERSON
If you wish someone else to see this
document, send in name with document
and the library will arrange a loan.

LCN-7969
(3 3-67)

OAK RIDGE NATIONAL LABORATORY
OPERATED BY UNION CARBIDE CORPORATION • FOR THE U.S. ATOMIC ENERGY COMMISSION

Printed in the United States of America. Available from
National Technical Information Service
U.S. Department of Commerce
5285 Port Royal Road, Springfield, Virginia 22151
Price: Printed Copy $3.00; Microfiche $0.95

This report was prepared as an account of work sponsored by the United States Government. Neither the United States nor the United States Atomic Energy Commission, nor any of their employees, nor any of their contractors, subcontractors, or their employees, makes any warranty, express or implied, or assumes any legal liability or responsibility for the accuracy, completeness or usefulness of any information, apparatus, product or process disclosed, or represents that its use would not infringe privately owned rights.

ORNL-4800
UC-34 — Physics

Contract No. W-7405-eng-26

NEUTRON PHYSICS DIVISION
ANNUAL PROGRESS REPORT
For Period Ending May 31, 1972

F. C. Maienschein, Director
R. G. Alsmiller, Associate Director
C. E. Clifford, Associate Director
R. W. Peelle, Associate Director

AUGUST 1972

OAK RIDGE NATIONAL LABORATORY
Oak Ridge, Tennessee 37830
operated by
UNION CARBIDE CORPORATION
for the
U.S. ATOMIC ENERGY COMMISSION

LOCKHEED MARTIN ENERGY RESEARCH LIBRARIES
3 4456 0515405 2

Reports previously issued in this series are as follows:

ORNL-2081	Period Ending September 10, 1956
ORNL-2389	Period Ending September 1, 1957
ORNL-2609	Period Ending September 1, 1958
ORNL-2842	Period Ending September 1, 1959
ORNL-3016	Period Ending September 1, 1960
ORNL-3193	Period Ending September 1, 1961
ORNL-3360	Period Ending September 1, 1962
ORNL-3499, Vols. I and II	Period Ending August 1, 1963
ORNL-3714, Vols. I and II	Period Ending August 1, 1964
ORNL-3858, Vols. I and II	Period Ending August 1, 1965
ORNL-3973, Vols. I and II	Period Ending May 31, 1966
ORNL-4134	Period Ending May 31, 1967
ORNL-4280	Period Ending May 31, 1968
ORNL-4433	Period Ending May 31, 1969
ORNL-4592	Period Ending May 31, 1970
ORNL-4705	Period Ending May 31, 1971

Contents

1. NEUTRON CROSS SECTIONS 1

1.0 Introduction – R. W. Peelle 1

1.1 Neutron Elastic- and Inelastic-Scattering Cross Sections for Oxygen in the Energy Range 4.34 to 8.56 MeV – W. E. Kinney and F. G. Perey 1

1.2 Neutron Elastic and Inelastic Cross-Section Measurements at ORELA – W. E. Kinney, T. A. Love, R. L. Macklin, F. G. Perey, and J. W. McConnell 3

1.3 Neutron Fission and Absorption Cross-Section Measurements for ^{239}Pu and ^{241}Pu – L. W. Weston and J. H. Todd 4

1.4 Measurement of Neutron Fission Cross Section for ^{239}Pu and ^{235}U from 0.02 eV to 200 keV – R. Gwin, E. G. Silver, and R. W. Ingle 4

1.5 Simultaneous Measurements of the Neutron Fission and Capture Cross Sections for ^{235}U for Neutron Energies from 8 eV to 10 keV – R. B. Perez, G. de Saussure, E. G. Silver, R. W. Ingle, and H. Weaver 7

1.6 Averaged ^{238}U Capture Cross Sections between 100 and 1200 eV – E. G. Silver, G. de Saussure, and R. B. Perez 7

1.7 The 150-Meter Time-of-Flight Facility at ORELA – E. G. Silver, R. W. Ingle, G. de Saussure, R. B. Perez, H. Weaver, and R. J. Robson 8

1.8 Preparations for Precision Measurements of Fission Cross Sections for ^{235}U and ^{239}Pu – R. W. Peelle, L. W. Weston, R. W. Ingle, J. H. Todd, and F. E. Gillespie 10

1.9 Resonance Reaction Formalisms for Fissile Nuclei – G. de Saussure 12

1.10 Multilevel Analyses of the ^{235}U Fission and Capture Cross Sections – G. de Saussure, R. B. Perez, and W. Kolar 12

1.11 The Generation of Kapur-Peierls Parameters from R-Matrix Parameters by the Invariant Imbedding Techniques – R. B. Perez and G. de Saussure 12

1.12 Calculation of the Perturbation Caused by Neutron Interactions with Structural Material on Measured Values of ^{233}U, ^{235}U, and ^{239}Pu Fission Cross Sections for the Neutron Energy Range 5 to 500 keV – D. E. Bartine, J. V. Pace III, and F. R. Mynatt 14

1.13 A Deterministic Method for Multiple Scattering Corrections – N. M. Greene, R. L. Childs, G. de Saussure, and R. B. Perez 14

1.14 A General Formalism for Computing the Transition Matrix of Nuclear Reaction Theory, and Its Application to the Treatment of the Coupled Channel Equations – R. B. Perez 15

1.15 Status Report of the Oak Ridge Electron Linear Accelerator (ORELA) – J. A. Harvey, T. A. Lewis, F. C. Maienschein, and H. A. Todd 15

1.16 Techniques Used at Oak Ridge National Laboratory for Unfolding Neutron and Gamma-Ray Pulse-Height Spectra – R. W. Peelle 17

1.17 Compilation of Phenomenological Optical-Model Parameters – C. M. Perey and F. G. Perey 17

1.18 Reevaluation of Carbon Neutron Cross Sections in ENDF/B Format – C. M. Perey and F. G. Perey 17

2. REACTOR AND WEAPONS RADIATION SHIELDING 19

2.0 Introduction – C. E. Clifford 19

2.1 FFTF Related Studies in the ORNL-LMFBR Shielding Program – F. R. Mynatt, C. E. Clifford, F. J. Muckenthaler, R. E. Maerker, M. L. Gritzner, L. R. Williams, and J. L. Rathbun 21

2.2 Experimental Investigation of Neutron Streaming through the Grid-Plate Shield of the Fast Flux Test Facility – C. E. Clifford, F. R. Mynatt, and P. N. Stevens 21

2.3 FFTF Coolant Duct Streaming Experiment – B. J. McGregor and F. J. Muckenthaler 21

2.4 Fast Reactor Shielding Monthly Progress Reports, 189a No. 10028, Activity No. 40 01 61 – F. R. Mynatt, M. L. Gritzner, R. E. Maerker, B. J. McGregor, R. M. Freestone, Jr., K. M. Henry, Jr., J. L. Hull, J. Lewin, J. J. Manning, J. N. Money, F. J. Muckenthaler, and L. R. Williams 23

2.5 Some Tests Related to the Use of Proton-Recoil Proportional Counters for Neutron-Flux Measurements – E. A. Straker, T. A. Love, C. E. Burgart, R. M. Freestone, Jr., and G. L. Morgan 23

2.6 Monte Carlo Calculations of the Response Functions of Bonner Ball Neutron Detectors – C. E. Burgart and M. B. Emmett 23

2.7 SWANLAC, a Computer Code Utilizing Perturbation Theory for Cross-Section Sensitivity Analysis – D. E. Bartine, F. R. Mynatt, and E. Oblow 24

2.8 Cross-Section Sensitivity Studies for the LLL Pulsed-Sphere Experiments – S. N. Cramer, F. G. Perey, R. W. Roussin, and E. Oblow 24

2.9 Identification of Radiation Streaming Paths in the Minuteman Missile Silo – T. J. Hoffman, J. V. Pace III, F. R. Mynatt, and C. E. Burgart 24

2.10 The Effect of the Ground on the Steady-State and Time-Dependent Transport of Neutrons and Secondary Gamma Rays in the Atmosphere – E. A. Straker 25

2.11 Effects of Air-Density Perturbations on the Transport of Neutrons and Secondary Gamma Rays Produced by Point Neutron Sources – B. J. McGregor 25

2.12 Analysis of GGA Measurements of the Time-Dependent Transport of Neutrons and Secondary Gamma Rays through Concrete – G. W. Morrison and E. A. Straker 26

2.13 A Study of the Effect of Source Asymmetry on Time-Dependent Neutron and Secondary Gamma-Ray Transport in Air – B. J. McGregor and E. A. Straker 26

2.14 Investigation of the Adequacy of Nitrogen Cross-Section Sets: Comparison of Neutron and Secondary Gamma-Ray Transport Calculations with Integral Experiments – E. A. Straker, M. B. Emmett, B. J. McGregor, J. V. Pace III, R. W. Roussin, H. T. Smith, and L. R. Williams 27

2.15 A Calculation of Gamma-Ray Production and Transport in Liquid Nitrogen – E. A. Straker and B. J. McGregor 27

2.16 Penetration into a Missile Silo of Neutrons and Secondary Gamma Rays Produced by Point Isotropic Neutron Sources – E. A. Straker, J. V. Pace III, M. B. Emmett, F. R. Mynatt, W. W. Engle, Jr., L. R. Williams, and L. S. Abbott 28

2.17 Neutron and Gamma-Ray Fluence Transmitted through a Slab of Borated Polyethylene – a Milestone Calculation – C. E. Burgart 28

2.18 Nuclear Weapons Initial Radiation Shield Design: A State-of-the-Art Report to Structure Designers – L. S. Abbott 29

2.19 Weapons Radiation Shielding Handbook: Status Report – L. S. Abbott, H. C. Claiborne, and C. E. Clifford 29

2.20 Collision Site Plotting Routines and Collision Density Fluence Estimates for the MORSE Monte Carlo Code – E. A. Straker and M. B. Emmett 29

2.21 Methods of Biasing Secondary Gamma-Ray Production in Coupled Neutron–Gamma-Ray Monte Carlo Calculations – M. Solomito, P. N. Stevens, E. A. Straker, C. E. Burgart, and S. N. Cramer 29

2.22 AMPX: Multigroup Coupled Neutron-Gamma Cross-Section Generator – N. M. Greene, W. E. Ford III, J. L. Lucius, J. E. White, and R. Q. Wright 30

2.23 XCHEKR – A Multigroup Cross-Section Editing and Checking Code – C. E. Burgart and E. A. Straker 32

2.24 DOMINO, a General-Purpose Discrete Ordinates to Monte Carlo Coupling Code for Radiation Transport – M. B. Emmett, C. E. Burgart, and T. J. Hoffman 32

2.25 Bracketing the Peak Primary Gamma-Ray Dose Rate from Nuclear Devices by Steady-State Transport Calculations – H. C. Claiborne and W. W. Engle, Jr. 32

2.26 Capabilities of the MORSE Multigroup Monte Carlo Code in Solving Reactor Eigenvalue Problems – C. E. Burgart 33

2.27 An Evaluation of Neutron and Gamma-Ray-Production Cross Sections for Lead – C. Y. Fu and F. G. Perey 34

2.28 On a Possible Resolution of the Nitrogen Nonelastic Neutron Cross-Section Discrepancy below 9 MeV – F. G. Perey and W. E. Kinney 34

2.29 Energies and Intensities of Gamma Rays Emitted by a ^{226}Ra Source – J. K. Dickens 34

2.30 *R*-Matrix Analysis of Differential Elastic and Inelastic Scattering of Neutrons from ^{12}C below 8.7 MeV – C. Y. Fu, F. G. Perey, and R. B. Perez 34

2.31 Self-Absorption of Gamma Rays Produced in Large Cylindrical Samples –J. K. Dickens 35

2.32 Updating of Cross-Section Files for Calcium and Lead – C. Y. Fu and F. G. Perey 35

2.33 Ca($n,x\gamma$) Reactions for $4.85 \leqslant E_n \leqslant 8.05$ MeV – J. K. Dickens 35

2.34 Doorway State in ^{206}Pb Revisited – B. J. Allen, R. L. Macklin, C. Y. Fu, and R. R. Winters 36

2.35 Gamma-Ray-Production Cross Sections of Tantalum and Carbon for Incident Neutron Energies between 0.007 and 20.0 MeV – G. L. Morgan, T. A. Love, J. K. Dickens, and F. G. Perey 36

2.36 A Comparison of Calculated and Measured Yields of Neutron-Energy-Dependent Capture Gamma Rays from ^{238}U – R. S. Booth, J. E. White, S. K. Penny, and K. J. Yost 36

2.37 Al($n,x\gamma$) Reactions for $5.3 \leqslant E_n \leqslant 9.0$ MeV – J. K. Dickens 37

2.38 Total Cross-Section Checks at the ORELA Shield Test Facility – T. A. Love, F. G. Perey, G. L. Morgan, J. W. McConnell, and R. M. Freestone, Jr. 37

2.39 Simultaneous Determination of Fast-Neutron Spectra by Time-of-Flight and Pulse-Height Unfolding Techniques – E. A. Straker, C. E. Burgart, T. A. Love, and R. M. Freestone, Jr. 37

2.40 Neutron-Induced Gamma-Ray Production in Iron for the Energy Range $0.8 \leqslant E_n \leqslant 20$ MeV – J. K. Dickens, G. L. Morgan, and F. G. Perey 38

2.41 Gamma-Ray Production Due to Neutron Interactions with Iron for Incident Neutron Energies between 0.8 and 20 MeV: Tabulated Differential Cross Sections – J. K. Dickens, G. L. Morgan, and F. G. Perey 38

2.42 The ^{23}Na($n,x\gamma$) Reaction for $4.85 \leqslant E_n \leqslant 7.5$ MeV – J. K. Dickens 38

2.43 Neutron Energy-Dependent Capture Gamma-Ray Yields in Tantalum and Tungsten – K. J. Yost, J. E. White, C. Y. Fu, and W. E. Ford III 39

2.44 Level Structure of ^{54}Mn – J. K. Dickens 39

2.45 The Testing of ^{238}U Secondary Gamma-Ray Production Data Sets from the POPOP4 Library – W. E. Ford III and J. S. Gillen 39

2.46 Comparison of ($n_{th,\gamma}$) Yields from the Current ENDF/B-III Data with Published Data – W. E. Ford III 41

2.47 Comparison of Average Secondary Gamma-Ray Production Cross Sections from ENDF/B-III Data with Published Cross Sections – W. E. Ford III 41

2.48 A Calculation of Neutron Energy-Dependent Capture Gamma-Ray Yield Spectra for Iron and Comparisons with Experiments – J. E. White, C. Y. Fu, and K. J. Yost 43

2.49 The Development and Application of a Discrete Ordinates Adjoint Difference Method for One-Dimensional Shield Weight Optimization – R. L. Childs 43

2.50 MORSE Monte Carlo Shielding Calculations for the Zirconium Hydride Reference Reactor – C. E. Burgart 43

2.51 The Relative Importance of Neutron Capture and Inelastic-Scattering Interactions to the Secondary Gamma-Ray Dose Transmitted through Laminated Tungsten and Lithium Hydride SNAP Reactor Shields – J. V. Pace III, F. R. Mynatt, and L. S. Abbott 43

2.52 Calculated Perturbations in Threshold Foil Measurements Due to Neutron Interactions in B_4C Shells – W. E. Ford III and J. S. Gillen 44

3. RADIATION SHIELDING INFORMATION CENTER 45

3.1 Introduction, Functions, and Summary of Operations – B. F. Maskewitz et al. 45

3.2 Shielding of Manned Space Vehicles Against Protons and Alpha Particles – R. G. Alsmiller, Jr., R. T. Santoro, H. C. Claiborne, and J. Barish 50

3.3 Extensions to PLOTFB, A Plotting Program for ENDF/B Data – R. Q. Wright and J. L. Lucius 51

3.4 Modification of PLOTFB for DNA Phase I Data Testing Program – J. E. White and R. Q. Wright 51

3.5 Coupled Calculations of the Transport of Neutrons and Secondary Gamma Rays through Concrete for Neutron Sources with Energies between 15 and 75 MeV – R. W. Roussin, R. G. Alsmiller, Jr., and J. Barish 52

3.6 Revisions to UKE – A Computer Program for Translating Neutron Cross Section Data from the UKAEA Nuclear Data Library to the Evaluated Nuclear Data File – R. Q. Wright 52

3.7 Revision to VIXEN – A Computer Program for Performing Physics Checks of Gamma-Ray Production Data in ENDF Format – J. B. Wright, R. Q. Wright, and W. E. Ford III 52

3.8 CDC Version of SUPERTOG, A Multigroup Neutron Cross-Section Generator – R. Q. Wright 53

3.9 Abstracts of the Data Library Packages Assembled by the Radiation Shielding Information Center (RSIC) – R. W. Roussin 53

3.10 CHECKER Code Modification – R. Q. Wright and J. L. Lucius 53

3.11 Calculation of Neutron Fluence-to-Kerma Conversion Factors Based on the ENDF/B Neutron Cross Section Library – Mohamed Abdou and R. Q. Wright 53

3.12 The MAINTAIN Code for Use in Maintaining CRBE Files on Tape – D. K. Trubey 53

3.13 Multigroup Negative Fluxes in Reflection Geometry – R. W. Roussin and D. K. Trubey 54

3.14 A Review of Calculations of Radiation Transport in Air – Theory, Techniques, and Computer Codes (Proceedings of a Seminar, November 15–17, 1971) – Compiled by D. K. Trubey and H. E. Comolander 55

3.15 A Computer Code Center – Experience and Operations – B. F. Maskewitz 56

3.16 The Maintenance of EDITOR: An ENDF/B Processing Code – J. E. White and S. K. Penny 56

3.17 Computer Codes for Shielding and Related Calculations – 1972 – B. F. Maskewitz, Francis H. Clark, and D. K. Trubey 57

4. THEORETICAL STUDIES OF MEDIUM- AND HIGH-ENERGY RADIATION TRANSPORT 58

4.0 Introduction – R. G. Alsmiller, Jr. 58

4.1 Nonelastic Interactions of Nucleons and π-Mesons with Complex Nuclei at Energies below 3 GeV – H. W. Bertini, Miriam P. Guthrie, and Arline H. Culkowski 58

4.2 Medium-Energy Intranuclear-Cascade Calculations: A Comparative Study – V. S. Barashenkov, H. W. Bertini, K. Chen, G. Friedlander, G. D. Harp, A. S. Iljinov, J. M. Miller, and V. D. Toneev 59

4.3 Results from Medium-Energy Intranuclear-Cascade Calculations – H. W. Bertini and Miriam P. Guthrie 59

4.4 The Calculation of Heavy-Ion Interactions – H. W. Bertini, T. A. Gabriel, R. T. Santoro, and J. D. Hunt 59

4.5 Monte Carlo Calculations of High-Energy Nucleon-Meson Cascades and Comparison with Experiment – T. W. Armstrong, R. G. Alsmiller, Jr., K. C. Chandler, and B. L. Bishop 60

4.6 Calculations of the Long-Lived Activity in Soil Produced by 500-GeV Protons – T. A. Gabriel and R. T. Santoro 60

4.7 Nucleon and Charged-Pion Albedo Spectra in an Accelerator Cave from 200-GeV Proton Interactions in Iron – T. A. Gabriel and R. T. Santoro 61

4.8 Energy Deposition in Ionization Spectrometers and TANC Counters for Incident High-Energy Hadrons – T. A. Gabriel, T. W. Armstrong, and K. C. Chandler 61

4.9 Calculation of Cosmogenic Radionuclides in the Moon and Comparison with Apollo Measurements – T. W. Armstrong and R. G. Alsmiller, Jr. 62

4.10 Calculation of the Lunar Photon Albedo from Galactic and Solar Proton Bombardment – T. W. Armstrong 63

4.11 Calculation of the Neutron Spectrum in the Earth's Atmosphere Produced by Galactic Cosmic Rays – T. W. Armstrong, K. C. Chandler, and J. Barish 63

4.12 Depth-Dose Distributions in a Tissue Phantom Shielded from Galactic Cosmic-Ray Protons – R. T. Santoro and R. G. Alsmiller, Jr. 65

4.13 Calculation of the Absorbed Dose and Dose Equivalent from Neutrons and Protons in the Energy Range from 3.5 GeV to 1.0 TeV – T. W. Armstrong and K. C. Chandler 66

4.14 A Calculational Method for Predicting Particle Spectra from High-Energy Nucleon and Pion Collisions (⩾3 GeV) with Protons – T. A. Gabriel, R. T. Santoro, and J. Barish 66

4.15 Operating Instructions for the High-Energy Nucleon-Meson Transport Code HETC – K. C. Chandler and T. W. Armstrong 66

4.16 Muon Transport and the Shielding of High-Energy (⩽500 GeV) Proton Accelerators – R. G. Alsmiller, Jr., F. S. Alsmiller, J. Barish, and Y. Shima 67

4.17 Low-Energy Electron Transport by the Method of Discrete Ordinates – D. E. Bartine, R. G. Alsmiller, Jr., F. R. Mynatt, W. W. Engle, Jr., and J. Barish 67

4.18 The Calculated Response of the TLND Personnel Dosimeter to Neutrons with Energies ⩽400 MeV – R. G. Alsmiller, Jr. and J. Barish 67

4.19 Calculation of the Absorbed Dose and Dose Equivalent Induced by Medium-Energy Neutrons and Protons and Comparison with Experiment – T. W. Armstrong and B. L. Bishop 69

4.20 Calculation of the Dose, Radionuclide Production, and Delayed Photon Leakage Due to Solar-Proton Bombardment of Tissue with Application to Astronaut Dosimetry – T. W. Armstrong and K. C. Chandler 69

4.21 Monte Carlo Calculations of the Dose Induced by Charged Pions and Comparison with Experiment – T. W. Armstrong and K. C. Chandler 70

4.22 Calculations for Producing Desired Depth-Dose Distributions Using Negatively Charged Pions – T. W. Armstrong, R. G. Alsmiller, Jr., and K. C. Chandler 70

4.23 Radiation Transport Codes for Potential Applications Related to Radiobiology and Radiotherapy Using Protons, Neutrons, and Negatively Charged Pions – T. W. Armstrong 71

4.24 Validity of Using Primary Protons Only in Van Allen Belt and Solar-Flare Proton Shielding Studies – R. T. Santoro, R. G. Alsmiller, Jr., and J. Barish 72

4.25 Analysis Subroutines for the Nucleon-Meson Transport Code NMTC – T. W. Armstrong and K. C. Chandler 72

4.26 TRAPP, a Computer Program for the Transport of Alpha Particles and Protons with All Nuclear-Reaction Products Neglected – J. Barish, R. T. Santoro, F. S. Alsmiller, and R. G. Alsmiller, Jr. 72

5. MEDIUM-ENERGY NUCLEON SPECTROSCOPIC STUDIES 73

5.0 Introduction – R. W. Peelle 73

5.1 Fast Forward Neutron Production in the $^7Li(p,n)^7Be$ Reaction for 40.6- and 63.8-MeV Protons – J. W. Wachter, R. T. Santoro, T. A. Love, and W. Zobel 74

5.2 Differential Cross Sections for the Production of Neutrons from the Bombardment of C and Al by 63.8-MeV Protons – J. W. Wachter, R. T. Santoro, T. A. Love, and W. Zobel 74

5.3 Measurement and Calculation of Response Functions of an NE-213 Neutron Detector for 15–61.5 MeV – J. W. Wachter, R. T. Santoro, T. A. Love, and W. Zobel 74

5.4 Differential Cross Sections for Hydrogen and Helium Particles from 30- to 60-MeV Protons on Nuclei – R. W. Peelle and F. E. Bertrand 76

5.5 A High Resolution Spectrometer System with Particle Identification for 1- through 60-MeV Hydrogen and Helium Particles – F. E. Bertrand, W. R. Burrus, N. W. Hill, T. A. Love, and R. W. Peelle 78

5.6 Elastic Scattering of 40-MeV Protons from ^{48}Ti, ^{nat}Cr, and ^{64}Zn: Tabulated Differential Cross Sections – J. K. Dickens, E. E. Gross, F. G. Perey, A. Van der Woude, and A. Zucker 78

5.7 Measurement of the Neutron Energy Spectrum at 9-g/cm^2 Residual Atmosphere – W. Zobel, T. A. Love, J. T. DeLorenzo, C. O. McNew, R. H. Baldry, and H. W. Parker 78

PUBLICATIONS AND PAPERS PRESENTED AT SCIENTIFIC MEETINGS 80

1. Neutron Cross Sections

1.0 INTRODUCTION

R. W. Peelle

Firm design of a safe and efficient liquid metal fast breeder reactor depends in part on the existence of extensive sets of accurate cross sections for all important neutron reactions. Though we perform some of the evaluation effort through which measured cross sections, theory, and integral experimental results are filtered to produce the official ENDF/B cross-section files, our effort centers on measurements of cross sections by use of neutron beams produced by the Oak Ridge Electron Linear Accelerator. Final reports are now being written for the first sets of measurements from this powerful source; preliminary data have generally already been released. The performance of ORELA itself is still being improved (paper 1.15).

In this project the workers find themselves measuring and remeasuring the quantities of most importance [such as the $^{238}U(n,\gamma)$ cross section] in the quest for correct results within narrowing confidence intervals. Our results visibly affect successive rounds of the ENDF/B cross-section sets, which are seen as underpinning for the worthwhile applied goals of the fast breeder program. To obtain the desired accuracies, systematic uncertainties are traced by analysis and removed prior to a subsequent modified experiment. When possible, it is most valuable to measure the same quantity using a totally different technique. Paper 1.3 contains encouraging preliminary results from such an independent study for the ratio of capture to fission in ^{239}Pu. The move to longer flight paths indicated in paper 1.7 is part of the process of reduction of uncertainties, since for study of cross sections for energies above ~10 keV it is important to move the observation of events in the large scintillator tank (used for neutron capture cross-section measurements) to a time interval that is sufficiently delayed after the electron burst for the large "gamma flash" detector transient to have quieted.

The delivery this year of the "Phase II" interactive-graphic data analysis system puts our data handling system another step toward the maturity to be achieved in the next year or so. When it has been programmed, its use should improve the acuity and speed with which our experimenters can examine the massive data sets through which they must slog. We are aided by several programmers from the Mathematics Division who are trying to meet the conflicting challenges of flexibility and ease of use in the graphic "application" programs.

Papers 1.12 and 1.13 reflect the valuable assistance which the neutron transport specialists of the Division's shielding groups have given in the estimation of scattering effects in our detector systems. Without this crucial support we would work much harder to obtain satisfactory handling of these experimental difficulties.

The papers in this section are arranged with some analyzed results from the Van de Graaff work of prior years first, followed by papers relating to the current experimental efforts, resonance parameter determinations, and reaction theoretical work. Two papers on cross-section evaluation appear at the end of the section.

1.1 NEUTRON ELASTIC- AND INELASTIC-SCATTERING CROSS SECTIONS FOR OXYGEN IN THE ENERGY RANGE 4.34 TO 8.56 MeV[1]

W. E. Kinney F. G. Perey

We present numerical values for neutron elastic- and inelastic-scattering cross sections for oxygen from 4.34 to 8.56 MeV. Our data are in generally good agreement with the results of others and are well described by ENDF/B evaluations (see Fig. 1.1.1).

Reference

1. Abstract of ORNL-4780 (1972).

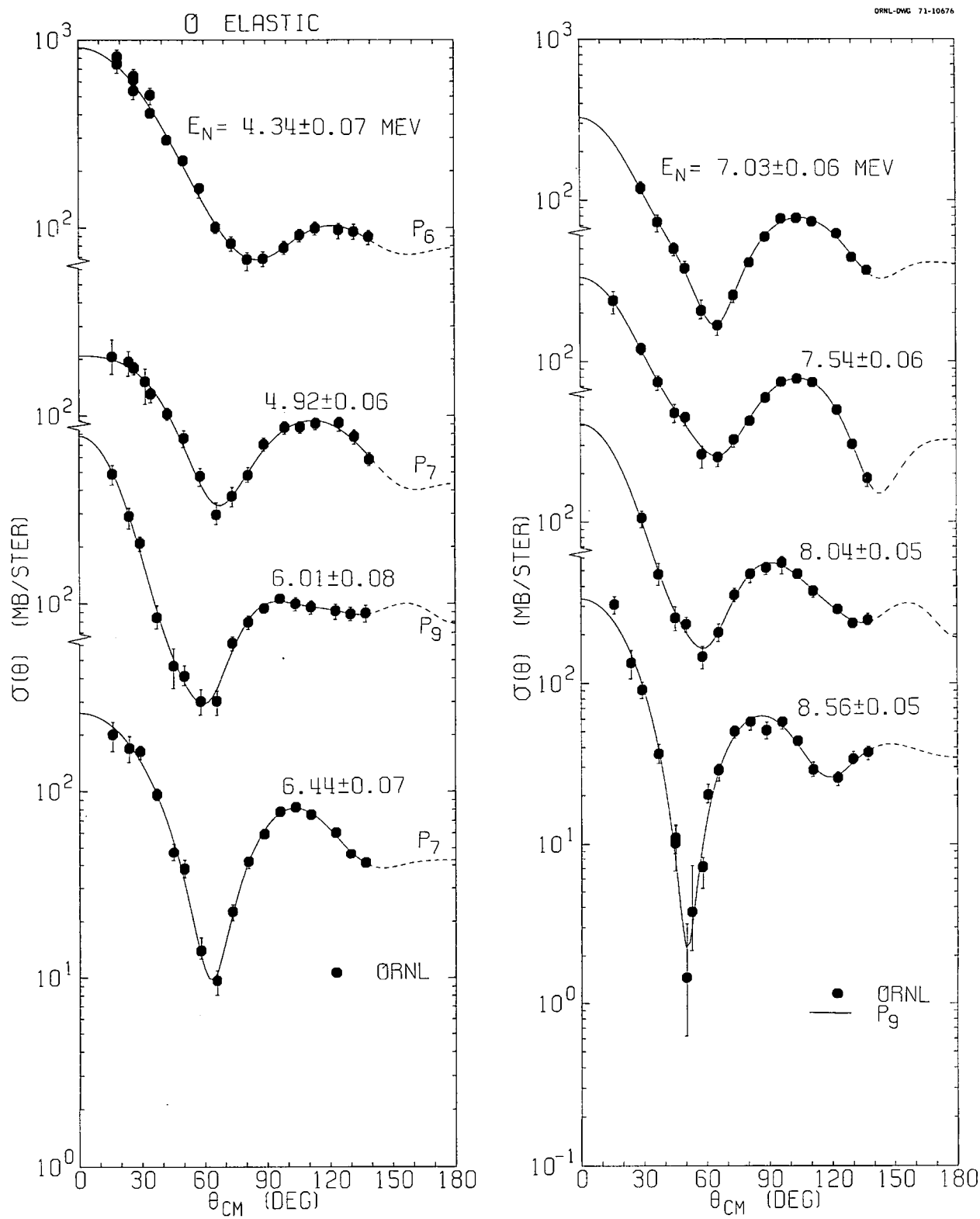

Fig. 1.1.1. Experimental oxygen differential elastic scattering cross sections compared with ENDF/B 4134 (and 1134). Some of the points from other laboratories were obtained at neutron energies significantly different from the energies used at ORNL.

1.2 NEUTRON ELASTIC AND INELASTIC CROSS-SECTION MEASUREMENTS AT ORELA

W. E. Kinney R. L. Macklin[1]
T. A. Love F. G. Perey
J. W. McConnell[2]

We have reported high-resolution cross sections for inelastic scattering to the first excited states of Na, Si, and Fe obtained at ORELA.[3] The data were taken with apparatus normally used to measure capture cross sections at the 40-m station of flight path 7 (ref. 4). In order to continue these experiments independently of the capture experiments, we have designed apparatus for installation at the 40-m station of flight path 6. We also plan to measure neutron elastic-scattering differential cross sections with a resolution similar to that of the inelastic cross sections.

The neutron beam will be collimated to a rectangle 1 in. wide and 2 in. high. Since the neutrons scattered from the beam by air would contribute appreciably to the background, the experiments will be conducted in a 4-ft nearly spherical vacuum chamber evacuated to ~1 mm.

Figure 1.2.1 shows a plan view of the (n,n) experiment in the vacuum chamber. Data will be acquired simultaneously from three detectors placed about 10 cm from the (hollow) cylindrical sample at angles ranging from 30° to 150°. The detectors will be 2-in.-diam by 2- to 4-in.-high cylinders of NE-213 (discriminating against gamma rays) mounted on RCA-8575 phototubes with the axis of the detectors parallel to the sample axis. The angular resolution will be roughly ±11° FWHM. To prevent arcing of the high voltage in the phototube bases, the detectors will be canned and mounted at atmospheric pressure.

A plan view of the $(n,n'\gamma)$ experiment in the vacuum chamber is shown in Fig. 1.2.2. The geometry is essentially the same as that of the capture experiment.[4] Two 4-in.-diam NE-213 (discriminating against neutrons) or NE-226 detectors mounted on XP-1041 phototubes will be placed as close to the sample as possible, achieving about 60% of a 4π solid angle. The detectors will be kept at atmospheric pressure by placing them in tubes capped at one end as shown.

A gamma-flash detector placed in the beam well downstream from the sample will provide a local start signal for an EGG TDC-100 clock, with the detector fast signal providing the stop. The pulse height will be digitized and sent along with the time of flight to a PDP-7 computer. Counting rates will be low enough so that the relatively slow PDP-7 movable-head disk will be adequate for any foreseeable two-dimensional storage.

ORNL-DWG 72-7095

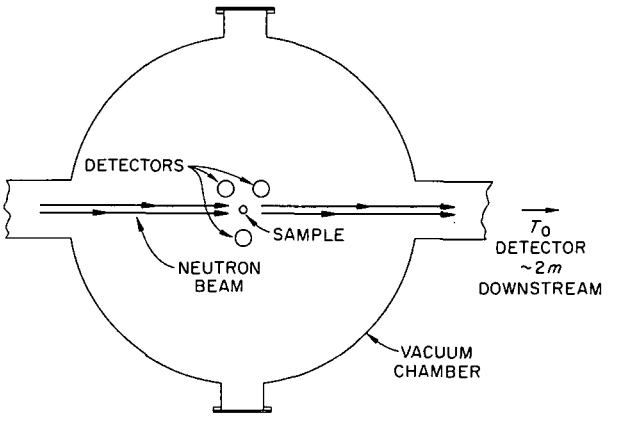

Fig. 1.2.1. Plan view of the (n,n) experiment in the vacuum chamber.

ORNL-DWG 72-7094

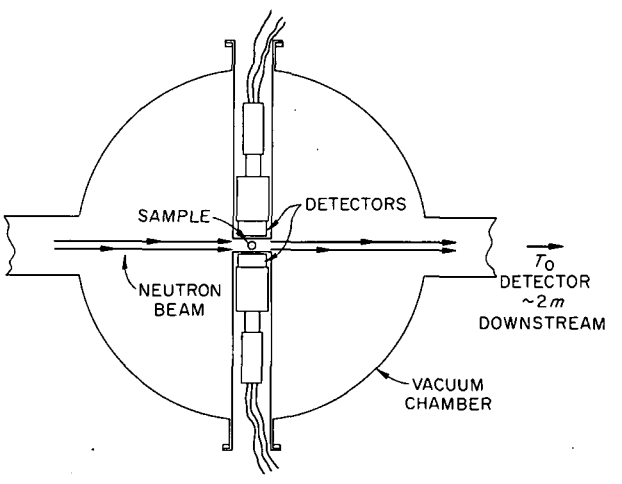

Fig. 1.2.2. Plan view of the $(n,n'\gamma)$ experiment in the vacuum chamber.

References

1. Physics Division.
2. Instrumentation and Controls Division.
3. F. G. Perey, W. E. Kinney, and R. L. Macklin, "High Resolution Inelastic Cross Section Measurements for Na, Si, and Fe," *Proceedings of the Third Conference on Neutron Cross Sections and Technology, Knoxville, Tennessee, March 15–17, 1971*, CONF-710301 (1971).
4. R. L. Macklin and B. J. Allen, *Nucl. Instrum. Methods* **91**, 565 (1971).

1.3 NEUTRON FISSION AND ABSORPTION CROSS-SECTION MEASUREMENTS FOR ^{239}Pu AND ^{241}Pu[1]

L. W. Weston J. H. Todd[2]

The neutron fission and absorption cross sections for ^{239}Pu and ^{241}Pu were measured from thermal-neutron energies to 30 keV. Since the fission and absorption cross sections were measured simultaneously, the ratio of the capture and fission cross sections, $\langle\sigma_c\rangle/\langle\sigma_f\rangle$, could be derived up to a neutron energy of 250 keV. Although data analysis is in the preliminary stages, several conclusions can already be drawn.

The Oak Ridge Electron Linear Accelerator (ORELA) was used as a source of pulsed neutrons. Capture and fission events were detected by "total energy detectors."[3] These consisted of nonhydrogenous liquid scintillator detectors (NE-226) used in such a way that their efficiency was proportional to the total prompt gamma-ray energy release. The appropriate pulse-height weighting to construct such an efficiency was done by the on-line data-taking computers, which also preserved the pulse-height information. Fast-neutron detectors (NE-213) with gamma-neutron discrimination were used to detect fission events only.

Figure 1.3.1 shows the preliminary values for $\langle\sigma_c\rangle/\langle\sigma_f\rangle$ for ^{241}Pu over the neutron energy range of 10 eV to 250 keV. Corresponding values from ENDF/B Mat 1106 are shown for comparison. The present data are normalized to the ENDF/B value at 0.025 eV. Above 30 keV the data show a more gentle decline than does ENDF/B. Below 2 keV the present data are appreciably higher than the ENDF values. The discrepancies between ENDF and the present data can be readily explained by the inadequacies of the experimental data on which the ENDF evaluation was based.

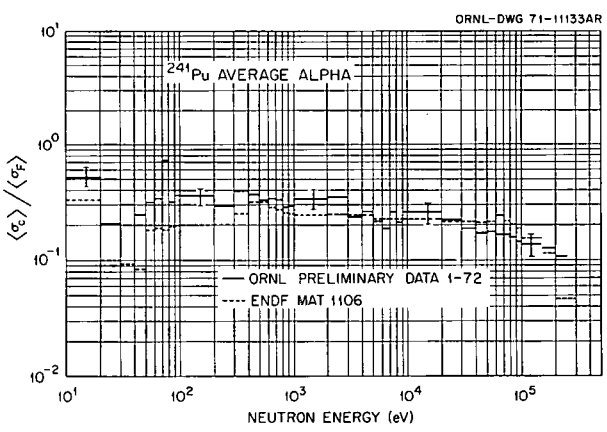

Fig. 1.3.1. ^{241}**Pu average** α.

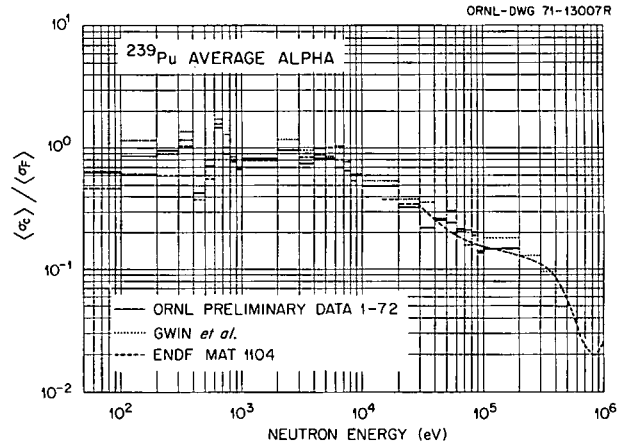

Fig. 1.3.2. ^{239}**Pu average** α.

As a check on the method, and also because of its importance to the LMFBR program, the values of $\langle\sigma_c\rangle/\langle\sigma_f\rangle$ for ^{239}Pu were also measured. The results for ^{239}Pu were in excellent agreement with the measurements of Gwin et al.[4] (see Fig. 1.3.2). This agreement is significant because of the very different techniques used. Since the more recent measurements of $\langle\sigma_c\rangle/\langle\sigma_f\rangle$ for ^{239}Pu by different experimenters using different techniques are now producing reasonably consistent agreement, much greater confidence can be placed in the knowledge of this parameter.

References

1. Summary of paper to be presented at the American Nuclear Society Meeting, June 18–22, 1972, Las Vegas, Nev.
2. Instrumentation and Controls Division.
3. R. L. Macklin and J. H. Gibbons, *Phys. Rev.* **159**, 1007 (1967).
4. R. Gwin et al., *Neutron Phys. Div. Annu. Progr. Rep. May 31, 1971*, ORNL-4705, p. 4 (1971).

1.4 MEASUREMENT OF NEUTRON FISSION CROSS SECTION FOR ^{239}Pu AND ^{235}U FROM 0.02 eV TO 200 keV[1]

R. Gwin E. G. Silver
R. W. Ingle[2]

Experiments have been performed in which the neutron fission cross sections of ^{239}Pu and ^{235}U were measured over the energy region from 0.02 eV to 200 keV. The primary goal of these experiments was to provide neutron cross-section data over a neutron energy range of importance for the design of fast breeder reactors.

The experimental technique used was essentially the same as reported previously.[3] The neutron flux was based upon the $^{10}B(n,\alpha)$ cross section suggested by Sowerby et al.[4] Normalization of the data was made at thermal energy to values given in ENDF/B II.[5] Figure 1.4.1 shows the ratio

$$\bar{\sigma}_f(^{239}Pu)/\bar{\sigma}_f(^{235}U) \; \{\bar{\sigma}_f = [\int \sigma_f(E)\, dE / \int dE]\}$$

as a function of the neutron energy; values shown for the present work which do not have error bars are in energy regions where the structural materials of the chamber interfere with the analysis of the data. Selected results of other experiments are also shown in Fig. 1.4.1.[6-9] The ENDF/B II values shown in Fig. 1.4.1 are dated January 1970 and have since then (February 1971) been revised upward by about 8% from 10 to 100 keV. This revision was accomplished by raising σ_f for ^{239}Pu.

Figure 1.4.2 shows $\bar{\sigma}_f$ for ^{235}U as a function of neutron energy for the present work along with selected results from other experiments.[6-7,10-14] Most of the results shown in Fig. 1.4.2 which are lower than the ENDF/B II values have become available after version II of the ENDF/B set was established. The present work is consistent with the ORNL-RPI[3] measurements for ^{239}Pu as indicated in Fig. 1.4.2. Figure 1.4.2 presents results which show that a decrease in $\bar{\sigma}_f$ for ^{235}U in the energy range from 10 to 100 keV would be consistent with the revised ratio $\bar{\sigma}_f(^{239}Pu)/\bar{\sigma}_f(^{235}U)$ in ENDF/B II if the ^{239}Pu cross section had not been revised upward.

The present results on $\bar{\sigma}_f$ for ^{235}U and ^{239}Pu suggest that the latest ENDF/B II (March 1971) values for these isotopes are too large. Since the ENDF/B II (March 1971) data sets are reasonably consistent with integral experiments, the present results also suggest that other ENDF/B II (March 1971) neutron cross sections may be too large [$\bar{\sigma}_\gamma(^{238}U)$ for example].

References

1. Summary of paper to be presented at the American Nuclear Society Meeting, June 18–22, 1972, Las Vegas, Nev.
2. Instrumentation and Controls Division.
3. R. Gwin et al., *Nucl. Sci. Eng.* **45**, 25 (1971).
4. M. G. Sowerby et al., *Proc. Conf. Nuclear Data for Reactors, Helsinki*, vol. I, p. 161, IAEA (1970).
5. Evaluated Nuclear Data File (ENDF/B) of the National Neutron Cross Section Center (NNCSC). For ^{239}Pu data, Material (MAT) 1104, and for ^{235}U data,

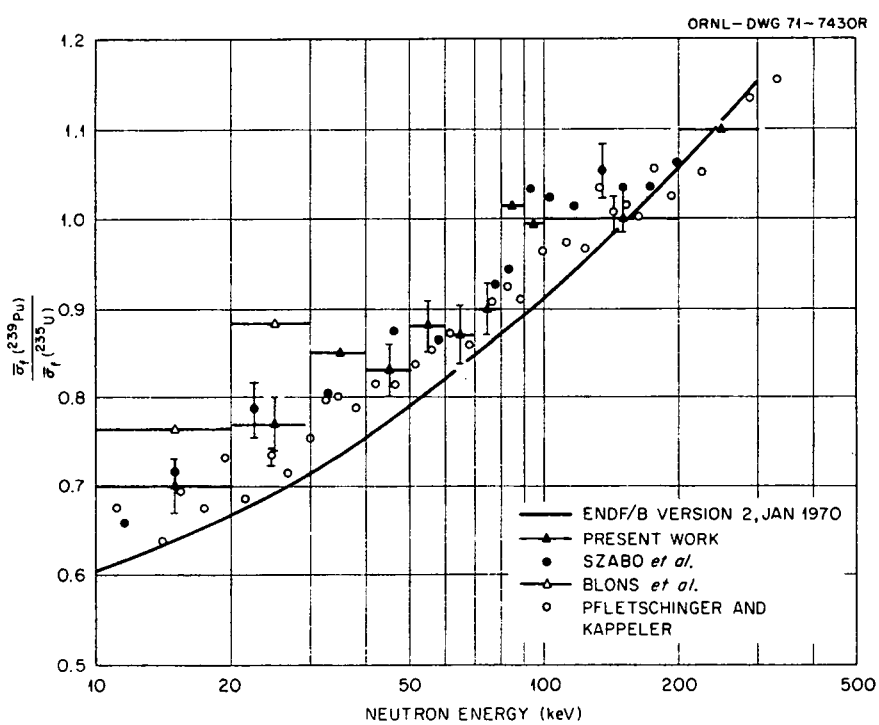

Fig. 1.4.1. Energy dependence of the ratio $\bar{\sigma}_f(^{239}Pu)/\bar{\sigma}_f(^{235}U)$ from 10 to 200 keV.

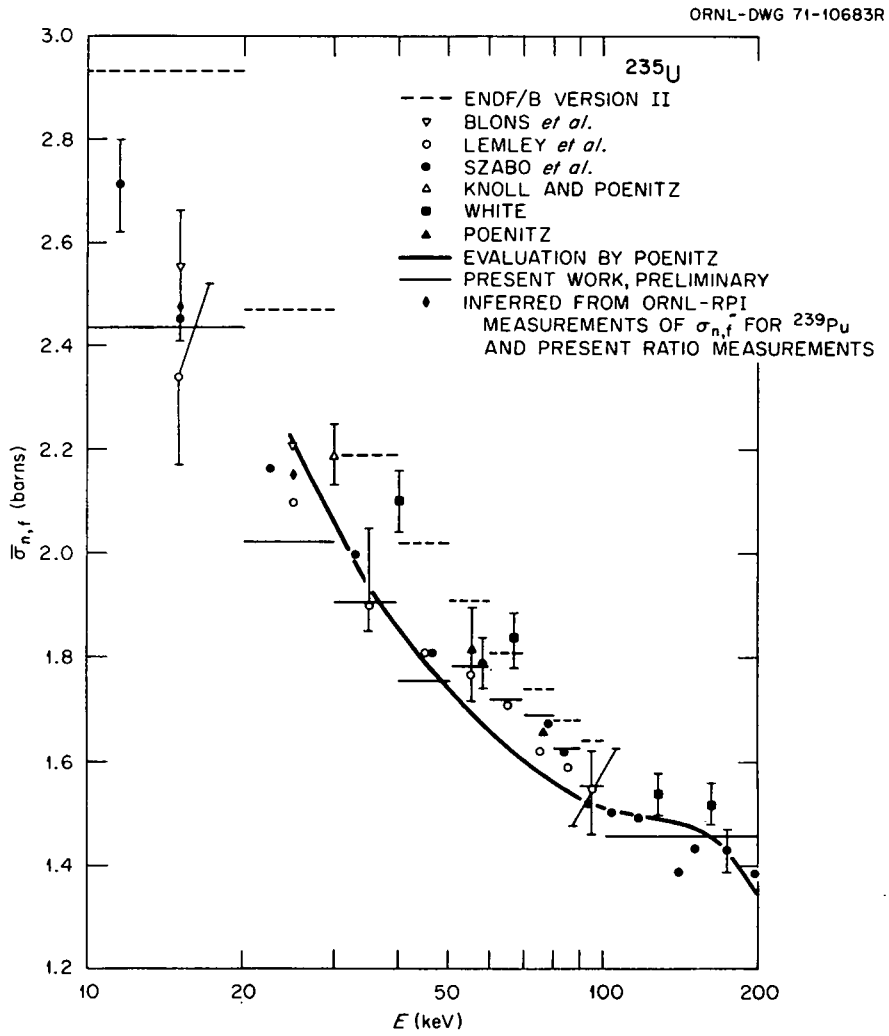

Fig. 1.4.2. Energy dependence of $\bar{\sigma}_f(^{235}U)$ over the energy range from 10 to 200 keV.

Material (MAT) 1102, Tape 201 (revised April 1970). The code SUPERTOG (April 1971) was used to obtain the data on the ENDF/B tape. The ENDF/B values for the ratio $\sigma_f(^{239}Pu)/\sigma_f(^{235}U)$ were taken from the evaluation of ^{239}Pu by N. M. Greene et al., *An Evaluation and Compilation of the Fission and Capture Cross Sections of ^{239}Pu in the Energy Range 25 keV–15 MeV*, ORNL-TM-2797, ENDF-131 (1970).

6. I. Szabo et al., *Proc. Conf. Neutron Cross Sections and Technology*, CONF-710301, vol. II, p. 573 (1971).

7. J. Blons et al., *Proc. Conf. Nuclear Data for Reactors, Helsinki*, vol. I, p. 469, IAEA (1970).

8. J. Blons et al., *Proc. Conf. Nuclear Data for Reactors, Helsinki*, vol. I, p. 481, IAEA (1970).

9. E. Pfletschinger and F. Kappeler, *Nucl. Sci. Eng.* **40**, 375 (1970).

10. J. R. Lemley, *Nucl. Sci. Eng.* **43**, 281 (1971).

11. G. F. Knoll and W. P. Poenitz, *J. Nucl. Energy* **21**, 643 (1967).

12. P. H. White, *J. Nucl. Energy A/B* **19**, 325 (1965).

13. W. P. Poenitz, *Proc. Conf. Neutron Cross Sections and Technology*, vol. I, p. 503 (1968).

14. W. P. Poenitz, "Interpretation and Intercomparison of Standard Cross Sections," *Proc. Conf. Neutron Standards and Flux Normalization*, p. 331 (1971).

1.5. SIMULTANEOUS MEASUREMENTS OF THE NEUTRON FISSION AND CAPTURE CROSS SECTIONS FOR ^{235}U FOR NEUTRON ENERGIES FROM 8 eV TO 10 keV[1]

R. B. Perez E. G. Silver
G. de Saussure R. W. Ingle[2]
H. Weaver

Simultaneous measurements of the neutron fission and capture cross sections of ^{235}U have been performed at the Oak Ridge Electron Linear Accelerator (ORELA) for neutrons with energies between 8 eV and 10 keV. These cross sections were measured relative to the standard ^{10}B(n,α) reaction cross section.

Comparisons of the present ^{235}U capture cross sections with values from other available sources show that below 200 eV there is general agreement within an error band of ±5%. In the keV energy region, the average difference observed rises to ±12%. The fission cross section results presented here agree with a worldwide compilation of fission data typically within a 3% error in the entire range of neutron energies investigated in this work.

The values of α, the capture-to-fission ratio, exhibit a remarkable amount of structure superimposed on the featureless behavior predicted by Bohr's fission channel theory.

References

1. Abstract of ORNL-TM-3696 (1972); also submitted to *Nuclear Physics.*
2. Instrumentation and Controls Division.

1.6 AVERAGED ^{238}U CAPTURE CROSS SECTIONS BETWEEN 100 AND 1200 eV[1]

E. G. Silver G. de Saussure
R. B. Perez

Where reactor physics calculations require averaged values of the ^{238}U capture cross sections, these can be obtained either by averaging directly over the results of an experimental capture measurement, such as we have previously reported,[2] or by constructing the cross sections from tables of resonance parameters, such as the set in ENDF/B II, the set published by Rahn et al.,[3] or the set compiled by C. Durston[4] for ENDF/B III. Very significant differences result, probably due at least partly to missed small levels, so that direct averages over experimental data are to be preferred.

Directly measured values must be corrected for the finite thickness of the sample, which causes both resonance self-shielding and multiple scattering. Our results have been corrected for these effects by performing Monte Carlo calculations, using the ENDF/B II parameter set for the experimental sample thicknesses (3 and 25 mils), and making zero-thickness calculations with the same parameter set. The ratio of the averaged results gives the correction factor.

Table 1.6.1 lists the averages over our experimental results, without correction, in columns A and B. Column C gives the results of the zero-thickness calculation, using the ENDF/B II parameter set. Columns D and E list the measured average values, corrected as described. Columns F and G show the constructed average results obtained by using the Rahn et al. parameters in a Monte Carlo calculation, corrected in the same way as the directly measured values using the ENDF/B II parameters. Since the Monte Carlo calculation includes the multiple scattering effect, the discrepancies between D, E and F, G cannot be due to this factor. These differences are as large as 33% at 1.2 keV.

The relative magnitude of the resonance self-shielding and multiple scattering effects is shown in columns H and I, which list the ratio of the values calculated from the ENDF/B II parameter set including multiple scattering [using the quantity $\sigma_c(1 - e^{-N\sigma_t})/N\sigma_t)$]. This ratio gives the magnitude of the multiple scattering effect estimated from ENDF/B II.

Column J gives the ENDF/B III average cross sections analogous to those in column C for ENDF/B II, and columns K and L give the measured values corrected on the basis of the ENDF/B III parameter set. Note that the disagreement between the corrected thick-sample and thin-sample results, which averaged about 2.0% using the ENDF/B II parameters, is reduced to 0.6% when the Durston parameter set is used. This high consistency supports the correctness of both the present measurements and the Durston (ENDF/B III) parameter set. There are 5–10% differences between the corrected experimental values and the ENDF/B III average cross sections, though this set is seen to be much superior to the ENDF/B II set.

The large differences observed between results of a direct measurement and of constructed value sets indicate the importance of using directly measured values.

References

1. Updated summary of a paper presented at the American Nuclear Society Meeting, Oct. 17–21, 1971, Miami Beach, Fla. (Edited by R. W. Peelle in author's absence.)

Table 1.6.1. ^{238}U capture cross sections and correction ratios

Energy range (eV)	Averaged cross section (b)							Correction ratio		Averaged cross section (b)		
	A	B	C	D	E	F	G	H	I	J	K	L
100–200	13.59	6.53	16.36	18.30	18.29	17.56	17.16	1.130	1.389	17.69	18.83	18.86
200–300	8.87	5.81	8.23	9.79	9.72	8.91	8.46	1.026	1.115	8.78	9.85	9.80
300–400	3.02	2.10	2.56	3.23	3.05	3.13	2.82	1.017	1.079	3.14	3.32	3.33
400–500	3.09	2.84	2.29	3.12	3.04	2.17	2.15	1.011	1.063	2.67	3.13	3.08
500–600	5.17	4.00	4.56	5.38	5.17	4.58	4.42	1.020	1.059	5.10	5.42	5.43
600–700	3.88	3.19	3.14	4.01	3.93	3.46	3.37	1.013	1.071	3.72	4.03	4.00
700–800	2.06	2.03	1.48	2.06	2.06	1.43	1.44	1.011	1.064	1.95	2.06	2.05
800–900	3.22	2.82	2.73	3.28	3.25	2.72	2.75	1.018	1.091	3.21	3.29	3.30
900–1000	4.30	3.41	3.75	4.50	4.55	3.98	3.89	1.016	1.070	4.37	4.53	4.60
1000–1100	2.12	2.01	1.54	2.12	2.09	1.80	1.76	1.011	1.061		2.13	2.12
1100–1200	4.04	3.63	3.23	4.09	4.10	3.09	3.06	1.020	1.088		4.10	4.09

Columns A and B: Averages over experimental results, no corrections for 3- and 25-mil samples, respectively.

Column C: Average over σ_c calculated from ENDF/B II resonance parameters for zero sample thickness.

Columns D and E: Averages over the experimental results corrected for sample-thickness effects by use of Monte Carlo calculations using ENDF/B II resonance parameters.

Columns F and G: Averages over the result of Monte Carlo calculations using the Rahn et al. resonance parameters, corrected as in columns D and E.

Columns H and I: Ratios of total correction to self-shielding correction for 3- and 25-mil samples, calculated from ENDF/B II parameters.

Column J: Average over σ_c calculated from ENDF/B III resonance parameters for zero sample thickness.

Columns K and L: Averages over the experimental results corrected for sample-thickness effects by use of Monte Carlo calculations using ENDF/B III resonance parameters.

2. E. G. Silver, G. de Saussure, R. B. Perez, and R. W. Ingle, "Measurement of Neutron Cross Sections in ^{238}U and ^{235}U below 100 keV at the ORELA," *Third Conference on Neutron Cross Sections and Technology, March 15–18, 1971, Knoxville, Tennessee.*

3. F. J. Rahn, H. Camarda, G. Hacken, W. W. Havens, Jr., H. I. Liou, J. Rainwater, M. Slagowitz, S. Wynchank, J. Arbo, and C. Ho, "Cross Section and Neutron Resonance Parameters of ^{238}U," *Third Conference on Neutron Cross Sections and Technology, March 15–18, 1971, Knoxville, Tennessee.*

4. C. Durston, private communication.

1.7 THE 150-METER TIME-OF-FLIGHT FACILITY AT ORELA[1]

E. G. Silver R. B. Perez
R. W. Ingle[2] H. Weaver
G. de Saussure R. J. Robson[3]

Flight path 6, an underground neutron time-of-flight facility located normal to the electron beam in the Oak Ridge Electron Linear Accelerator (ORELA),[4] has recently been extended from a 40-m length to a 150-m length. This extension of the underground flight path required the construction of an additional collimating station at 80 m from the neutron source and an underground experiment station at 150 m. Figure 1.7.1 shows the general features of the extended flight path.

In April 1972, this facility was completed, and the ORELAST,[5] the 800-gal liquid scintillator gamma-ray detector, was dissassembled and moved to the 150-m station, where it was reassembled.

This 3.9-fold increase in the length of the flight path was undertaken mainly to permit extension of the capture and fission cross-section measurements, previously carried out at the 40-m station, to higher energy. At the 40-m station the upper limit of measurable neutron energy was about 200 keV, due to a gamma-flash-induced overloading of the photomultipliers, preamplifiers, and linear amplifiers, as a result of which the system was inactivated for about 8 μsec. Even after the amplifiers recover, a gain shift persists, which limits the useful range to less than 100 keV. This shift occurs in the photomultipliers and is due to increased electron multiplication immediately following intense light bursts. This gain change is particularly important when both high-bias and low-bias measurements are made simultaneously, since the effective threshold bias thus changes with neutron energy, that is, time of flight.

At the 150-m distance not only is the dead-time cutoff above 1.5 MeV, but the 15-fold reduction in

ORNL-DWG 72-6259

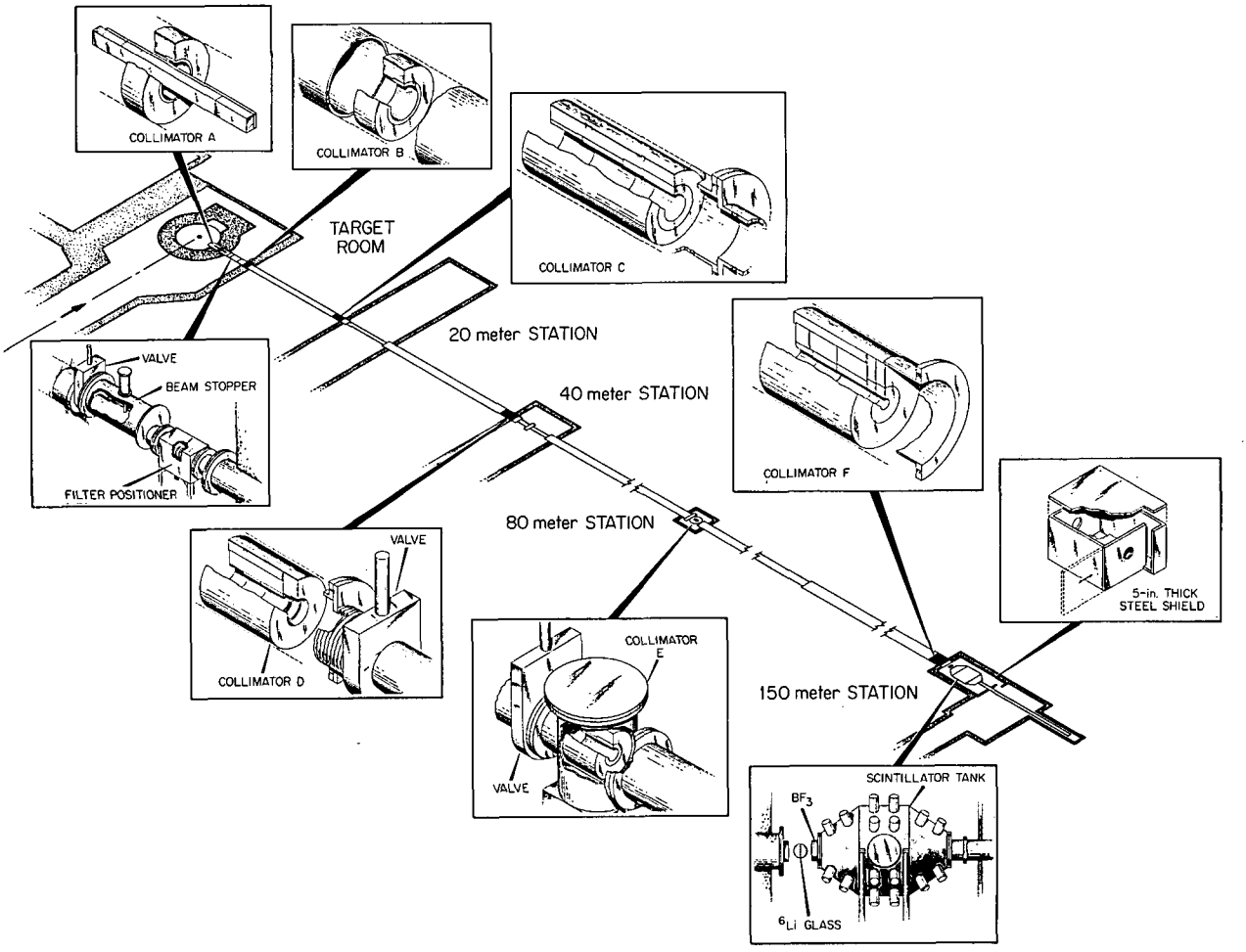

Fig. 1.7.1. The 150-meter time-of-flight facility at ORELA.

gamma intensity almost completely eliminates the gain-shift problem encountered at 40 m.

Additional advantages are the improved time-of-flight resolution and the almost complete elimination of the induced-rf noise in the signal circuits which had existed at the 40-m station. The benefits are offset, of course, by reduced intensity.

Two additional collimators have been added to the system, at 80 m in a separate cubicle and at the entrance to the 150-m station.

The collimator system is so designed that neutrons from the target cannot scatter in a single collision off the flight tube walls into the sample area.

The collimator design allows relatively easy beam-diameter changes up to 6-in.-diam beam size. A special set of collimator inserts was made to allow use of the existing high-isotopic-purity 4.375-in.-diam ^{238}U transmission samples at the 40-m station for total cross section and self-indication measurements. The entire collimator system was aligned by use of a focused He-Ne laser beam, with evacuated light path.

A 5-in.-thick shield of low-activity steel surrounds the ORELAST in its new location. This shield reduced the tank-halves coincidence background counting rate by a factor of 12 relative to the rate observed in the 40-m station without local shielding.

At the time the move from the 40-m station to the 150-m station was made, the water-filled aluminum container which surrounded the LINAC target and served as the source of moderated neutrons was replaced with a similar target can made of beryllium. This change smoothes out the neutron spectrum, which

had been noticeably perturbed at 6, 35, and 87 keV due to the aluminum resonances, since in beryllium the lowest resonance is above 600 keV.

The first experiments at the 150-m station are in progress and include measurements of $^{238}U(n,\gamma)$, $^{235}U(n,f)$, and $^{235}U(n,\gamma)$ reactions.

References

1. Summary of paper to be presented at the Informal Session of the Reactor Physics Division at the American Nuclear Society Meeting, June 18–22, 1972, Las Vegas, Nev.
2. Instrumentation and Controls Division.
3. Plant and Equipment Division.
4. N. C. Pering and T. A. Lewis, "Performance of 140-MeV High-Current Short Pulse LINAC at ORNL," *IEEE Trans. Nucl. Sci.* **NS16**(3), 316 (1969).
5. E. G. Silver, J. H. Todd, and J. Lewin, *Assembly and Initial Operation of the ORELAST*, ORNL-4433, p. 11 (1969).

1.8 PREPARATIONS FOR PRECISION MEASUREMENTS OF FISSION CROSS SECTIONS FOR ^{235}U AND ^{239}Pu

R. W. Peelle R. W. Ingle[1]
L. W. Weston J. H. Todd[1]
F. E. Gillespie[1]

Efforts continue to prepare for measurements of fission cross sections and their ratios using methods which sacrifice counting rate and perhaps resolution to obtain detector efficiencies which are stable and relate directly to the underlying energy-dependent cross sections. Since the previous report[2] the 20-m station at flight path 8 has been prepared for the experiment, the performance of a gridded ionization chamber containing boron has been evaluated as a flux monitor, initial tests have been made on a double back-to-back fission chamber, and most of the required electronic gear has been assembled. Initial measurements are planned soon to search for any apparent energy dependence in the relative (2π) counting efficiency for foils with ^{235}U deposits of various thickness.

The gridded boron chamber is designed to observe the alpha particles and ^{7}Li recoils from the $^{10}B(n,\alpha)$ and $^{10}B(n,\alpha\gamma)$ reactions which occur in ~10-mg/cm^2 evaporated ^{10}B coatings 5 cm in diameter on either side of a 1-mg/cm^2 aluminized Mylar foil. The idea of the counter is to provide good enough pulse-height resolution that one can estimate precisely the counted fraction of the $^{10}B(n,\alpha)$ reactions. The chamber is expected to be used as a flux monitor for neutron energies below 100 keV. Conventional[3] gridded ion chambers are built over each side of the boron-coated foil with a 1.6-cm cathode-grid spacing and a 2.3-cm cathode-anode spacing. The chamber is presently operated as a "flow" chamber with argon–10% methane counting gas, and with a field of ~150 V/cm at the cathode and ~500 V/cm at the anode. Under these operating conditions the chamber output is insensitive to changes in applied voltage.

Event timing is obtained from the leading edge of the ~300-nsec-wide current pulse observed at the common cathode, while the deposited energy is derived from the anode of the counter, in which the reaction product deposits energy. When the rise time of the current pulse is rolled off to about 75 nsec, electronic noise is not confused with pulses from the ^{7}Li recoils. Charge pulses from *n-p* scattering in the methane and in the Mylar electrodes die away before pulses from 100-keV neutrons occur, if $\leqslant 0.6$ μsec integrating and differentiating times are employed. Figure 1.8.1 shows a pulse-height distribution obtained from the chamber with this pulse shaping when the analysis system was made sensitive to the portions of the ORELA target's neutron spectrum below 2 keV. The lower cutoff was induced by a threshold on the cathode current signal used for triggering, the four lower peaks arise from ^{7}Li and alpha particles stopping in the chamber, and the uppermost peak is from a test pulser. A balanced diode base-line restorer (0.01 μF and 0.1 mA) was used to suppress base-line fluctuations from low-frequency microphonics from the chamber. The pulse-height resolution of the chamber is apparently more than adequate, the stability is very good, and the time resolution (60–80 nsec) is quite usable. In its present form the efficiency of the chamber is very low, but it is usable for very long experiments if the shape of the flux is smooth.

The double back-to-back fission chamber utilizes conventional parallel-plate design with fissioning deposits on 5-cm-diam regions of the cathode only. Plates with 6-mm spacing are arranged so two materials are compared twice in back-to-back geometry, with the materials ordered in each sense with respect to the beam direction. Current pulses[4] of ~130-nsec total length and rise time of ~10 nsec are observed using argon–10% methane filling, with the shapes varying between triangular and rectangular depending on the direction of fragment motion. Time resolution is expected to be narrower than 10 nsec. In application, these current pulses will be shaped with 20-nsec clipping lines to reduce alpha-particle pileup when ^{239}Pu deposits are used.

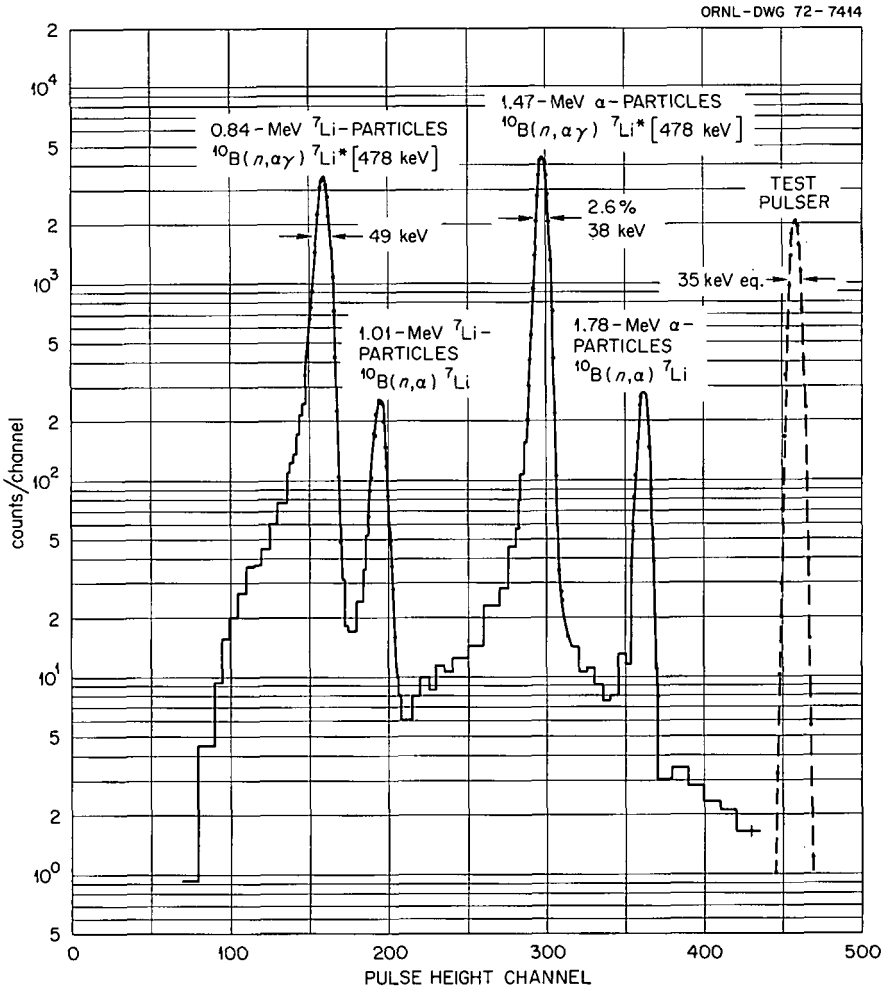

Fig. 1.8.1. Pulse-height spectrum of the $^{10}B(n,\alpha)^7Li$ reaction observed with the gridded ion chamber.

Figure 1.8.2 shows the spectrum of fully integrated charge pulses obtained in early tests using a 0.1-mg/cm^2 layer of ^{235}U. The sharp peak in the spectrum corresponds to fragments traveling normal to the electrodes, while the low-energy rise in intensity is caused by alpha particles from the decay of ^{235}U and ^{234}U. Pulses in the valley represent the very small fraction of all events in which a fragment leaves 5–20 MeV in the counting gas (each channel in the valley contains 0.015% of the fission counts). In application, only the initial portion of the current pulses will be integrated for pulse-height analysis, so the shape of the observed spectrum will be markedly modified to widen the apparent gap between the largest pulses from alpha particles and the smallest pulses from fission fragments.

A series of high-isotopic-purity ^{235}U deposits of ~0.04 and 0.1 mg/cm^2 on 0.5-mil Al foils were prepared by vacuum evaporation of UO_2 under direct heating by electron bombardment;[5] a comparable set of ~0.1 and ~0.4-mg/cm^2 deposits were prepared by electrodeposition.[6] For the thinner foils the evaporated deposits seem preferable. The deposits are being intercompared by gamma-ray[7] and in some cases alpha-particle counting techniques. Efforts to obtain comparable deposits of ^{239}Pu ($\leq$0.1 mg/cm^2) are under way.

References

1. Instrumentation and Controls Division.
2. R. W. Peelle and L. W. Weston, *Neutron Phys. Div. Annu. Progr. Rep. May 31, 1971*, ORNL-4705, p. 21.
3. O. Bunemann, T. E. Cranshaw, and J. A. Harvey, *Can. J. Res.* **27A**, 191 (1949).
4. H. Rösler, J. K. Millard, and N. W. Hill, *Nucl. Instrum. Methods* **99**, 1 (1972).

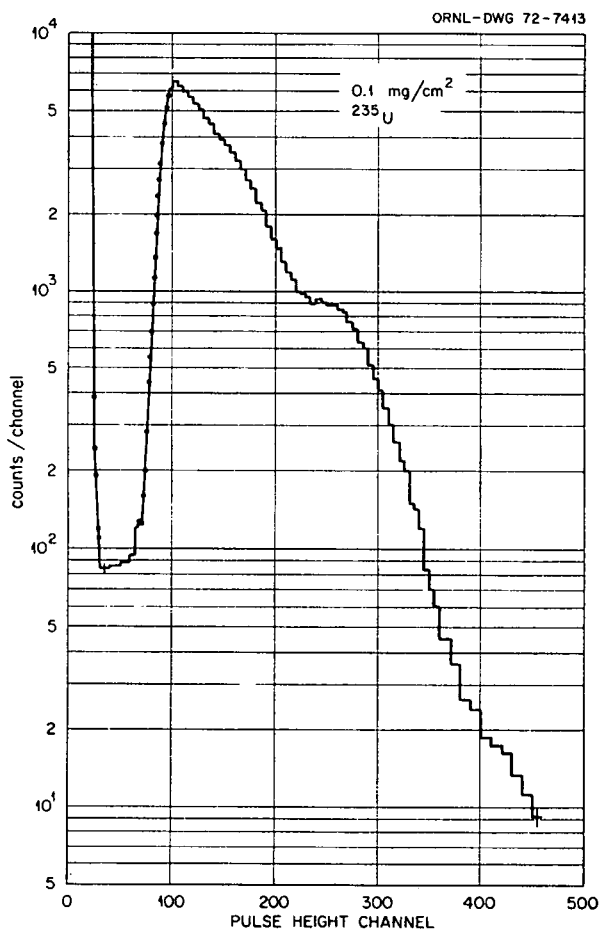

Fig. 1.8.2. Spectrum of integrated charge pulses for ^{235}U fission. A 0.1-mg/cm^2 deposit was placed on the negative electrode of a parallel plate ion chamber with ~6-mm spacing.

5. H. Adair, Isotopes Division.
6. T. McMullins, ORGDP, Laboratory Division.
7. J. Eldridge, Analytical Chemistry Division.

1.9 RESONANCE REACTION FORMALISMS FOR FISSILE NUCLEI[1]

G. de Saussure

This paper describes very briefly some of the multilevel formalisms most frequently used to represent the low-energy cross sections of the fissile nuclei. Some of the properties and applications of the resonance parameters are also discussed.

Reference

1. Abstract of paper presented at the Cross Section Evaluation Working Group Meeting, May 9–10, 1972, Brookhaven National Laboratory, Upton, Long Island, N.Y.

1.10 MULTILEVEL ANALYSES OF THE ^{235}U FISSION AND CAPTURE CROSS SECTIONS[1]

G. de Saussure R. B. Perez
W. Kolar[2]

The neutron capture and fission cross sections of ^{235}U were analyzed up to 60 eV with the multilevel formalism of Reich and Moore. The statistical distribution of the R-matrix parameters obtained in this analysis has been investigated in detail. After corrections for the "missed levels," the observed statistical distributions of the parameters and level spacings agree well with the expected Porter-Thomas distributions and Wigner law, respectively. The average values of the resonance parameters do not agree for the same cross sections with the values obtained by other authors on the basis of the single-level formalism.

The set of resonance parameters obtained in this work has been used to compute the fission cross section at liquid-nitrogen temperature, for comparison with existing measurements, and to "mock up" the cross sections in the unresolved resonance region near 1 keV, where *S*-wave processes still dominate.

References

1. Abstract of paper to be presented at the American Nuclear Society Meeting, June 18–22, 1972, Las Vegas, Nev., and of ORNL-TM-3707; also submitted for publication in the *Physical Review*.
2. Central Bureau for Nuclear Measurements, Euratom, Geel, Belgium.

1.11 THE GENERATION OF KAPUR-PEIERLS PARAMETERS FROM R-MATRIX PARAMETERS BY THE INVARIANT IMBEDDING TECHNIQUES[1]

R. B. Perez G. de Saussure

The Kapur-Peierls[2] dispersion theory leads to a very convenient parameterization of the cross section. This is especially true for the fissile nuclei, where level interference and channel effects are of importance.[3] A drawback of these types of cross-section parameterizations is that very little is known about the statistical properties of the Kapur-Peierls-type parameters. However, from the existing relationships between these parameters and the R-matrix parameters, whose statistical properties are known, one can infer the sta-

tistical distribution of the former set by various techniques.[4-9]

Further work in this area is motivated by the need of generating Kapur-Peierls parameters for p-wave neutrons in order to study the effects of level interference on Doppler coefficients and self-shielding factors in the unresolved energy region.

The residues and poles in the R-matrix formalism arise from an eigenvalue problem associated with real, momentum-independent values of the logarithmic derivatives, $-B_{0,c}$, at the nuclear surface for each channel, c. In the case of the collision matrix, U, the residues and poles result from an eigenvalue problem in which the logarithmic derivatives, $B_c = -(S_c + iP_c)$, are complex and momentum dependent, where S_c and P_c are the usual shift and penetration factors respectively. In the spirit of the invariant imbedding technique,[10] one can think in terms of a family of eigenvalue problems, with logarithmic boundary conditions, $B_0(\tau)$, defined in the form

$$B_c(\tau) = -[(S_c - B_{0,c}) + iP_c]\tau - B_{0,c} , \qquad (1)$$

where the parameter τ varies between zero and unity. In this case, it has been shown that the transition T matrix as a function of τ is given by the differential equation[11]

$$\frac{d}{d\tau} T_{cc'}(\tau) = -\frac{i}{2}\sum_{c''} P_{c''}^{-1}\, T_{cc''}(\tau) \times \left[\frac{d}{d\tau} B_{c''}(\tau)\right] T_{c''c'}(\tau) . \qquad (2)$$

The result, Eq. (2), defines the trajectories in configuration space described by the transition matrix elements as the parameter τ varies between zero and unity. In order to find the corresponding equations for the complex level widths $g_{\lambda c}$ and poles $\epsilon_\lambda = \mu_\lambda - i\nu_\lambda$, one introduces in Eq. (2) the expression

$$T_{cc'} = i \sum_\lambda \frac{g_{\lambda c}\, g_{\lambda c'}}{\epsilon_\lambda - E} , \qquad (3)$$

and one uses Eq. (1) to compute the $dB_{c''}/d\tau$ term.

After some manipulations one obtains

$$\frac{d}{d\tau} g_{\lambda c} = \frac{1}{2} \sum_{\lambda' \neq \lambda} (\epsilon_{\lambda'} - \epsilon_\lambda)^{-1}\, g_{\lambda' c} \left(\sum_{c''} P_{c''}^{-1}\, \beta_{c''}\, g_{\lambda c''}\, g_{\lambda' c''}\right) \qquad (4)$$

and

$$\frac{d}{d\tau} \epsilon_\lambda = -\frac{1}{2}\sum_{c''} P_{c''}^{-1}\, \beta_{c''}\, g_{\lambda c''}^{\,2} \qquad (5)$$

with

$$\beta_c = (S_c - B_{0,c}) + iP_c . \qquad (6)$$

The results of Eqs. (4) and (5), together with the initial conditions $g_{\lambda c}(0) = \Gamma_{\lambda c}^{\,1/2}$ and $\epsilon_\lambda(0) = E_\lambda$, form a Cauchy initial value problem, which lends itself easily to solution.[12]

There are several advantages to the method discussed here. It applies to any value of the angular momentum, and it does not involve iterative techniques or the inversion of matrices.

To demonstrate the feasibility of the method, Eqs. (4) and (5) have been coded for s-wave neutrons and its results compared with some POLLA[9] calculations.

References

1. Summary of paper to be presented at the Informal Session of the Reactor Physics Division at the American Nuclear Society Meeting, June 18–22, 1972, Las Vegas, Nev.
2. P. L. Kapur and R. E. Peierls, *Proc. Roy. Soc. (London)* **166**, 277 (1928).
3. D. B. Adler and F. T. Adler, "Neutron Cross Sections in Fissile Elements," *Proc. Conf. on Breeding, Economics, and Safety in Power Reactors, October, 1963*, ANL-6792, p. 695 (1963).
4. D. B. Adler, *LEMA-CHAMA: A FORTRAN IV Program to Calculate Neutron Cross Sections with Either Level Matrix or Channel Matrix Formalisms and with the Complex Pole Expansion of the Collision Matrix*, COO-2022-5 (1970).
5. P. A. Moldauer, *Phys. Rev.* **135**, B642 (1966); also, P. A. Moldauer, R. N. Thomas, and B. S. Garbow, *MATDIAG, a Program for Computing Multilevel S-Matrix Resonance Parameters*, ANL-7590 (1969).
6. J. D. Garrison, *Ann. Phys.* **50**, 355 (1968).
7. R. N. Hwang, *Nucl. Sci. Eng.* **36**, 67 (1969).
8. D. R. Harris, *Perturbation Transformation of Nuclear Cross Section Parameters between Wigner-Eisenbud and Kapur-Peierls Formalism: PERTA Program*, LA-4327 (1969).
9. G. de Saussure and R. B. Perez, *POLLA, a FORTRAN Program to Convert R-Matrix-Type Multilevel Resonance Parameters for Fissile Nuclei into Equivalent Kapur-Peierls-Type Parameters*, ORNL-TM-3599 (1969).

10. R. Bellman, R. Kalaba, and M. Wing, *J. Math. Phys.* **1**, 280 (1960).
11. R. B. Perez, ORNL-TM-3778 (to be published).
12. F. Ceshchino and J. Kuntzmann, *Numerical Solution of Initial Value Problems*, Prentice-Hall, 1966.

1.12 CALCULATION OF THE PERTURBATION CAUSED BY NEUTRON INTERACTIONS WITH STRUCTURAL MATERIAL ON MEASURED VALUES OF ^{233}U, ^{235}U, AND ^{239}Pu FISSION CROSS SECTIONS FOR THE NEUTRON ENERGY RANGE 5 TO 500 keV

D. E. Bartine[1] J. V. Pace III[1]
F. R. Mynatt

Calculations were made to determine the effect of aluminum structural materials in certain fission chambers on the measured fission cross section. A ^{239}Pu, a ^{235}U, and two ^{233}U chambers with differing amounts of aluminum were considered. This work was intended to obtain aluminum correction factors for the four chambers and to provide a check on the relative effects of aluminum in the two ^{233}U chambers as measured by R. Gwin.

Point cross sections were obtained from the ENDF/B files and multigrouped, then reduced to a 64-broad-group set by the one-dimensional discrete-ordinates code ANISN.[2] P_3S_8 adjoint calculations were made on each fission chamber with and without aluminum present, using the two-dimensional discrete-ordinates code DOT.[3] Since the fission cross sections were input as the source for the adjoint calculations, the resulting adjoint angular flux at the surface of the fission chamber represents the probability that an incident neutron with a given energy, traveling in a given direction, will cause a fission within the chamber. This adjoint boundary flux was multiplied by a normalized flat (equal number per kilo-electron volt) incident neutron flux spectrum and integrated over the surface on which the experimental neutron beam was incident at the most forward angle in the S_8 quadrature to obtain the fission rate as a function of incident energy. An aluminum correction factor was then obtained for each group by dividing the fission rate without aluminum by the fission rate with aluminum.

The calculations indicated that the presence of aluminum in these fission chambers caused an increase in the fission rate. This increase ranged from less than 1% up to 6%, depending on the energy of the incident neutron. It was observed that the magnitude of the correction varied directly with the aluminum elastic cross section, which describes an energy loss and an angular deflection. Since the fission cross sections investigated here were relatively constant in energy compared with the aluminum elastic cross section, this establishes that the prime effect of the aluminum was to cause the neutrons to "see" more fuel, thereby increasing the fission rate. Correction factors obtained from these calculations were in excellent agreement with those inferred from the cross-section measurements recorded by the two ^{233}U fission chambers.

References

1. Mathematics Division.
2. W. W. Engle, *A User's Manual for ANISN, a One-Dimensional Discrete Ordinates Transport Code with Anisotropic Scattering*, K-1693 (1967).
3. F. R. Mynatt, F. J. Muckenthaler, and P. N. Stevens, *Development of Two-Dimensional Discrete Ordinates Transport Theory for Radiation Shielding*, CTC-INF-952 (1969).

1.13 A DETERMINISTIC METHOD FOR MULTIPLE SCATTERING CORRECTIONS

N. M. Greene[1] G. de Saussure
R. L. Childs[1] R. B. Perez

Work has been continued on the Multiple Scattering Correction Program, MSC.[2,3] The motivation for the development of this code was to have available a "deterministic" method of calculation as opposed to the "probabilistic" Monte Carlo technique, which would allow incorporation of multiple-scattering corrections in our present fitting programs for resonance parameter analysis. Extensive comparisons of the MSC code with Monte Carlo calculations showed that, although the MSC package reproduced the main peaks in the counting rate (response function) of the ^{238}U capture in thick foils, it failed to describe properly the multiple scattering "satellite" peaks observed experimentally and well described by the Monte Carlo program.

The satellite peaks are produced by the capture of those neutrons which were scattered within a solid angle around 90° in the previous collision. The usual Legendre-polynomial expansion of the scattering kernel is not well suited to reproduce the angle-energy correlation for those scattering events, resulting in a poor description of the spurious resonances.

Following the suggestions of C. E. Clifford and F. R. Mynatt, we have developed the MSCA code, which incorporates an exact analytical description of the first-collision density into the earlier MSC program.

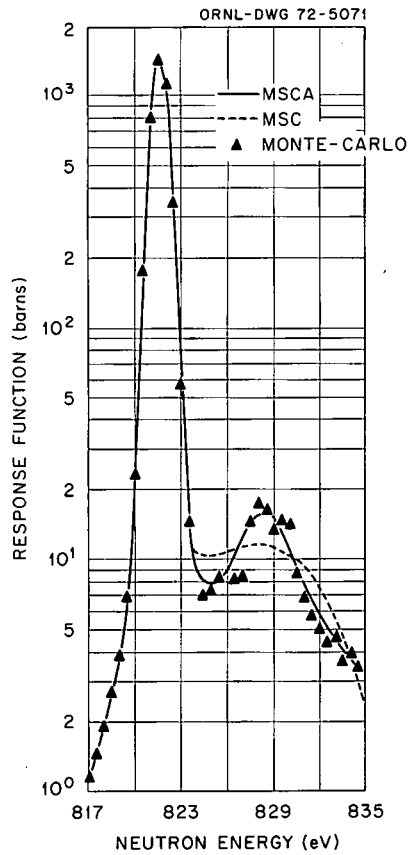

Fig. 1.13.1. The response function for the ^{238}U resonance at 821.5 eV, showing a "satellite" peak at 828 eV. The MSCA program is a "first collision" modification of the MSC program (see refs. 2 and 3 following paper 1.13).

For a 23-mil-thick ^{238}U foil, Fig. 1.13.1 shows the resonance function arising from the ^{238}U capture resonance at 821.5 eV, which exhibits a typical "satellite" peak at 828 eV. The MSC program describes the main peak correctly, but "averages out" the secondary peak. The modified MSC program (MSCA) reproduces the peak approximately.

This new program package for the computation of multiple-scattering corrections will be incorporated into fitting programs for the determination of ^{238}U resonance parameters.

References

1. Mathematics Division.
2. N. M. Greene et al., *Neutron Phys. Div. Annu. Progr. Rep. May 31, 1970,* ORNL-4592, p. 18.
3. N. M. Greene et al., *Neutron Phys. Div. Annu. Progr. Rep. May 31, 1971,* ORNL-4705, p. 25.

1.14 A GENERAL FORMALISM FOR COMPUTING THE TRANSITION MATRIX OF NUCLEAR REACTION THEORY, AND ITS APPLICATION TO THE TREATMENT OF THE COUPLED CHANNEL EQUATIONS[1]

R. B. Perez

One develops a general integrodifferential equation for the transition matrix of nuclear reaction theory in terms of the physical parameters of the nuclear reaction. On this basis, one arrives at a unified formalism which affords a great degree of flexibility regarding the boundary conditions of the basic set of eigenfunctions utilized to construct solutions of the radial coupled channel equations. One also develops, as a corollary of the main result, a system of equations which describes the motion of the poles and residues of the collision matrix as a function of the parameters entering in the reaction formalism. Various applications are shown to illustrate the present technique.

Reference

1. Abstract of ORNL-TM-3778; also submitted to the *Physical Review.*

1.15 STATUS REPORT OF THE OAK RIDGE ELECTRON LINEAR ACCELERATOR (ORELA)

J. A. Harvey[1] F. C. Maienschein
T. A. Lewis[2] H. A. Todd[2]

ORELA Operations

For the past year, operation of the Oak Ridge Electron Linear Accelerator (ORELA) has been on a rather steady basis, with current and power levels which were generally slightly below the ratings. The linac operated for experimenters a total of 5051 hr (through May 31, 1972), as shown in Table 1.15.1, an increase of 15% over the previous year.

The major limitation in the power level at ORELA has been that of heat removal in the electronics that drive the electron gun. These electronic components are operated at about 120 keV potential within the so-called gun tank. The replacement gun tank, which should remove the heat-transfer limitation and provide conservative design throughout, was installed in April 1972. It should allow an increase in repetition rate to the full 1000 pulses per second. The only other components known to be marginal are oil-filled capacitors used in the line-type modulators. All of these capacitors were replaced with new units of a higher rating during the year.[3]

Perhaps the major interference in measuring neutron cross sections in the energy range above 5 keV at ORELA has been due to the presence of an aluminum can around the neutron-producing target. The water-cooled tantalum target has been used very successfully in all other respects; therefore, a replacement target was obtained in which the aluminum can was replaced by a beryllium can. Fabrication of the beryllium can, which must contain the target cooling water under pressure, apparently pushed the state of the art of beryllium joining. However, the new target was installed in January 1972 and has continued to operate satisfactorily to date.

A new vacuum pump was installed during the year to replace the troublesome pump which had been used to evacuate the target room. The new pump provides a much better vacuum of <3 mm Hg, and it is now possible for experimenters to maintain a reasonable vacuum from the neutron-producing target all the way to their experiments.

Experience with klystron lifetimes continues to be favorable, as indicated in Table 1.15.2. As shown in Table 1.15.3, electron-gun lifetime continues to be variable, with the upper limit approximating 2500 hr.

Data-Handling System

The past year has surely been one of accumulating more data at ORELA than has been analyzed. In an attempt to anticipate this situation, which has occurred at virtually every nuclear facility in the recent past, the so-called Phase II Data Analysis System was ordered for use at ORELA. In January 1972 this system was accepted from the manufacturer, Digital Equipment Corporation. It provides three interactive graphic terminals at ORELA, together with a number of Teletypes for communication with a PDP-10 computer and a large mass store (about 2×10^8 bytes). The substantial task of building software programs for the specific use of ORELA upon the foundation provided by the equipment manufacturer started this year and will continue through the next. Already, however, limited use of the system is taking place, and it has become obvious that the large mass store will rapidly become filled with data.

The above data-analysis system has been connected to the Phase I Data Acquisition System, which continues to operate very satisfactorily in servicing many experi-

Table 1.15.1. ORELA operation from June 1, 1971, through May 31, 1972: electron beam hours for experimenters

Date	Research hours
6-1-71 to 6-30-71	633.0
7-1-71 to 7-31-71	367.6
8-1-71 to 8-31-71	507.0
9-1-71 to 9-30-71	507.6
10-1-71 to 10-31-71	646.9
11-1-71 to 11-30-71	492.4
12-1-71 to 12-31-71	420.1
1-1-72 to 1-31-72	0
2-1-72 to 2-29-72	150.0
3-1-72 to 3-31-72	593.2
4-1-72 to 4-30-72	317.2
5-1-72 to 5-31-72	416.7
Total	5051.7

Table 1.15.2. Klystron lifetimes

Klystron number	High-voltage hours	Time period
2002	1,447.0	Startup–Nov. 3, 1969[a]
2003	14,794.0	Startup–May 31, 1972[b]
2004 R1	3,868.7	Sept. 1, 1971–May 31, 1972[b,c]
2007	7,850.0	December 1969–Apr. 27, 1971[a]
2009	3,106.3	Sept. 30, 1970–Apr. 27, 1971[a]
2010	5,726.9	Apr. 27, 1971–Apr. 25, 1972[a]
2011	2,327.4	Apr. 27, 1971–Sept. 1, 1971[a]
2012	493.7	Apr. 25, 1972–May 31, 1972[b]
2013	462.9	Apr. 25, 1972–May 31, 1972[b]
		Failures
2004	3,005.7	
2008	2,324.8	Not repairable
2006	12,921.7	Now being evaluated for repair by Litton

[a]Spare.
[b]Still in accelerator.
[c]Hours since repair.

Table 1.15.3. Electron gun lifetimes

Gun number	Beam hours	Failure date
7-1	2397.2	7-26-71
4-3	2312.8	11-29-71
5-4	537.4	1-11-72
8-2	59.8	1-19-72[a]
7-2	1088.0	4-28-72[b]
4-4	419.6	5-31-72[c]

[a]Ceramic leaks.
[b]Leak in flange; plan to try on test stand to see if cathode is still good.
[c]Still on accelerator.

menters simultaneously. The PDP-10 computer is located at the ORNL Central Computing Facility, so that it can be operated by the staff of that facility. Communication between the central computer and ORELA is required over a distance of about 1 km. Taking advantage of newly developed modems has allowed an increase in data transmission rates to the displays from the specified 2400 bits/sec to 9600 bits/sec at a cost which is far less than that of the older slower modems.

References

1. Physics Division.
2. Instrumentation and Controls Division.
3. As of June 16, 1972, ORELA has operated at 1000 pulses per second and full power (50 kW in beam) for more than a week.

1.16 TECHNIQUES USED AT OAK RIDGE NATIONAL LABORATORY FOR UNFOLDING NEUTRON AND GAMMA-RAY PULSE-HEIGHT SPECTRA[1]

R. W. Peelle

Some unscrambling methods that have been used in recent years at the Oak Ridge National Laboratory are discussed and illustrated. For discrete sources, radioanalysts studying weak samples with NaI(Tl) utilize iterative least-squares spectrum resolution, while for gamma-ray spectra from $(n,n'\gamma)$ reactions another group performs peak stripping on Ge(Li) spectra with the aid of a computer-driven interactive display. To show that unfolding methods are more broadly applicable, the effect is illustrated of processing the data from two-dimensional radiodiagnostic positional scans. The energy-sensitive detector for neutron capture gamma rays is discussed as an unscrambling analysis using an inverted triangularized response matrix. For continuous spectral sources, the formulation of Burrus in terms of "window functions" is described from a simplified operational point of view. In this discussion, reference is made to comparisons with flight-time spectra and with spectra unfolded using hand-guided iterative refolding. Distinctions are made among the FERDoR, FERD, and OPTIMO codes of Burrus. Clearer documentation and more incisive procedures for error estimation are considered the greatest current needs for generally improved unfolding of continuous spectra. The method chosen for a particular problem should match its needs and the investigator's style.

Reference

1. Abstract of an invited paper presented at the American Nuclear Society Meeting, June 13–17, 1971, Boston, Mass.; also issued as ORNL-TM-3463 (August 1971).

1.17 COMPILATION OF PHENOMENOLOGICAL OPTICAL-MODEL PARAMETERS

C. M. Perey[1] F. G. Perey

At various times we have been asked to undertake a compilation of optical-model parameters and offered different reasons as to why this would be a good idea. From our own experience we realize the value and the limited utility of such compilations. The bibliography involved may be the most valuable part of the work, and we ourselves have used previous compilations for this purpose (all of them being over five years old). Because of the lack of a well-established methodology for analyzing the data and due to the many ambiguities involved in the parameters of the standard formulation of the optical model, any such compilation does not remove the need to consult the complete paper. However, it does provide the user with a valuable guide as to the end result of the analysis. Many optical-model analyses have been made in the last 20 years using a standardized form for the various parts of the potential; new analyses continue to appear in the literature, indicating that there may well be a need for such compilations. In order to test this need, the work covering two years of publications, 1969 and 1970, will soon be published in the *Nuclear Data Tables.* We report only optical-model parameters as determined from a fit to elastic-scattering data. The system is computerized and may easily be extended in scope with updated tables published regularly as our data base increases its coverage.

For future editions we plan to extend the coverage in time and incorporate, in the same format, the results of previous compilations.

Reference

1. Consultant.

1.18 REEVALUATION OF CARBON NEUTRON CROSS SECTIONS IN ENDF/B FORMAT

C. M. Perey[1] F. G. Perey

The present ENDF/B III evaluation for carbon was based on very incomplete data above 5 MeV and does

not contain any gamma-ray production cross sections. New data have become available in the last two years which indicate that a complete reevaluation for carbon is required above 5 MeV. We are in the process of performing such a reevaluation. Progress to date includes: (1) complete reevaluation of the carbon total cross sections from 4.5 to 20 MeV (the total cross-section file is based heavily on two very complete measurements due to Cierjacks et al.[2] of Karlsruhe and Schwartz et al.[3] of NBS); and (2) a complete analysis of elastic- and inelastic-scattering cross sections of two extensive data sets by Galati et al.[4] up to 7 MeV and Perey and Kinney[5] up to 7 MeV. A complete Legendre polynomial analysis of both elastic and inelastic scattering of the data has been made using the PDP-10 IACC computer.

References

1. Consultant.
2. S. Cierjacks, P. Forti, D. Kopsch, L. Kropp, J. Nebe, and H. Unseld, *High Resolution Total Neutron Cross Sections between 0.5 to 30 MeV*, USAEC report EURFNR-591 (KFK-1000, EUR-3963, and EANDC(E)-111), Institut fuer Angewandte Kernphysik (June 1968).
3. R. B. Schwartz, R. A. Schrack, and H. T. Heaton II, in *Neutron Cross Sections and Technology, Proceedings of a Conference, Washington, D.C., Mar. 4–7, 1968*, ed. D. T. Goldman, NBS Spec. Publ. 299 (vol. 2), pp. 771–781, U.S. Government Printing Office, Washington, D.C. (1968).
4. W. Galati, J. D. Brandenberger, and J. L. Weil, *Phys. Rev.* **C5**(5), 1508 (1972).
5. F. G. Perey and W. E. Kinney (to be published).

2. Reactor and Weapons Radiation Shielding

2.0 INTRODUCTION

C. E. Clifford

The objectives of the ORNL shielding program, which is supported by the AEC Space Nuclear Systems (SNS) Division, the Defense Nuclear Agency (DNA), and the AEC Division of Reactor Development and Technology program for the liquid metal fast breeder reactor (LMFBR), are the development of basic methods for solving radiation transport problems, the testing of these methods by comparison with experimental results, and the development of data and techniques that engineers can use with a high degree of confidence in designing shields to meet their requirements. Furthermore, the intent is to provide design techniques that are general in nature so that shields can be optimized not only with respect to weight, as required for the SNS program, but also with respect to cost, radiation heating, radiation damage, or any other requirement or constraint that may be imposed by the design engineers.

The LMFBR shielding development program has continued to increase in scope and is still the major reactor shielding program within the division. The highest priority effort in this program has been the work and support of the shielding design for the Fast Test Reactor (FTR), which is currently under construction. Several difficult shield design problems for this reactor have been considered from both an experimental and a calculational point of view. These problems include a study of neutron penetration through very thick layers of sodium, neutron streaming through clearance gaps for removable and rotating plugs in the top steel shield, streaming in the reactor cavity and coolant pipe chaseways, and neutron penetration through the stainless steel grid-plate shield. As a result of parametric calculations made during the study of the neutron streaming problem in the reactor cavity and vessel support system of the head, recommendations for additional shielding both in the cavity and above the top head were made in order to meet the design radiation levels. The radiation transport calculations were performed with the discrete ordinates computer code DOT using a two-dimensional representation of the reactor and shield system.

An integral experimantal program has also been carried on at the Tower Shielding Facility as a major part of the LMFBR shielding program. The purpose of these experiments is to provide an indication of errors which may be present in the shielding calculations. Validation of the calculational part of the program is achieved by comparing experimental and calculated results, the latter being obtained from the same cross-section data sets and codes used in the shield design studies. Conclusions concerning the iron and sodium penetration experiments which were completed last year have been based to date on a qualitative comparison of such experimental and calculated results. It has been shown, for instance, that 10–30% agreement can be obtained between the calculations and the measurements for deep neutron penetration in both iron and sodium. While this is considered to be very good agreement for such experiments, quantitative studies can now be made which relate even these minor disagreements directly to errors in the cross sections, and then back to errors in the real shield design problems under investigation. In many instances, a 30% disagreement between measured and calculated results in an experiment can indicate the possibility of cross-section errors which result in errors as large as a factor of 2 or 3 in an actual shield calculation. The application of this quantitative approach to the sensitivity of both the experiments and the calculations to cross-section errors has been very recently developed and has therefore been applied only in a preliminary way to the LMFBR program.

Several experiments which examine the problem of streaming in the LMFBR shield design have also been completed at the TSF. Included were a parametric study of streaming through clearance gaps in a 40-in.-thick solid steel shield, a study of neutron streaming in a mockup of the coolant pipe chaseways which included both the sodium-filled pipe and its insulation,

and a study of neutron streaming in a large steel-lined concrete vault which simulated a heat exchanger (IHX) isolation valve cavity in the FTR design. Analysis of these streaming data has allowed improvement and simplification of the methods which have been utilized to calculate streaming. In general, it has been found that the available techniques can accurately calculate these configurations, and attention is being turned toward reducing the cost of comparable calculations in design studies. For example, it has been demonstrated that as few as 5 neutron groups can be used to calculate most of the measured results for the neutron streaming through the concrete pipe chaseways rather than the 50 groups which have been utilized in the majority of transport calculations. It was found, however, that a high-order angular quadrature and a fine spatial mesh were required to obtain such accurate results.

The shielding effort being conducted for the Defense Nuclear Agency (DNA) is primarily concerned with radiation transport through the atmosphere and into shielded military systems. The analytical program has been concerned with development of a modular code system to greatly improve the processing of point cross-section data into coupled neutron gamma-ray multigroup cross-section sets. When completed, the processing code, called AMPX, will eliminate a large amount of hand labor which has been required in setting up the four and five different codes formerly used to process point data. The use of AMPX should reduce the time required for producing new multigroup cross-section data libraries from several weeks to several days.

Rather rapid progress is now being made in the sensitivity studies for DNA. A computer program has been developed to implement the data handling and data presentation that are required in sensitivity calculations with this system. A combination of forward and adjoint solutions obtained from either ANISN or DOT is used to produce an energy-dependent importance profile for the cross sections in a given problem. Such a profile illustrates, in a quantitative way, the sensitivity of the calculated results to the cross sections in each energy group for each problem being studied. This approach has allowed a quantitative study to be made of the effect of cross-section uncertainties on the neutron and gamma-ray dose resulting from neutron transport through the atmosphere.

A number of calculations of specific problems have been made as part of the DNA program. The most extensive calculational effort has been applied to the prediction of the radiation intensities inside a Minuteman silo taking into account three-dimensional streaming paths. The Monte Carlo code MORSE was used for these calculations. The discrete ordinates code DOT was utilized to calculate the radiation environment incident on the silo and also to calculate the streaming paths which could be simulated in a two-dimensional calculation. A DOT calculation was also made of the radiation transmitted through the unperturbed shield. A detailed study of the accuracy of the nitrogen cross-section data sets has required the calculation of two experimental configurations involving 14-MeV neutron sources in air or liquid nitrogen. The object of the analysis was to determine which of two data cross-section sets was most correct for use in the air transport calculations. It was found that the results of the two experiments were somewhat conflicting, and selection of the best cross-section set could not be made on the basis of these experiments alone.

The DNA program also supports an experimental program at the ORELA Shield Test Station. Two classes of experiments are conducted in this program. The first of these entails measurements of differential cross-section data, and the second is an integral experiment program designed to check transport calculational methods as well as the differential cross-section data. Experiments of the first type which have recently been completed include the measurement of gamma-ray production cross sections for tantalum and carbon, for incident neutron energies between 0.007 and 20 MeV. An experiment of the second type which has recently been completed but not reported is concerned with the measurement of the scattered neutron spectrum along the axis of a relatively thick annular ring of carbon. The experimental program also includes measurements designed to validate total cross-section data sets in the energy range from 0.5 to 20 MeV and a number of experiments to validate gamma-ray production data.

The group which is conducting the experimental program at ORELA is also heavily involved in cross-section evaluations for a number of elements for DNA. The most significant effort to date has been placed on the evaluation of iron. A complete data file containing both neutron and gamma-ray production cross-section data has resulted from this work. Portions of this data file have been substantially modified as a result of feedback from integral experiment analysis. The modified version of the file has been accepted as the iron evaluation for ENDF/B-III. First-round evaluations have also been prepared for calcium and lead, and gamma-ray production data have been provided for several elements of interest to DNA.

The SNS shielding program was considerably reduced in scope during FY 1972. The most significant

effort in this program has been shield design studies for several applications of interest both to the Air Force and NASA/Lewis. Work was continued on the shield optimization program, SHAPE. The shield optimization program is similar in approach to the one used in the sensitivity studies in that it utilizes a single set of forward and adjoint calculations and perturbation theory to obtain the derivative of the dose with respect to a shield perturbation at any point throughout the shield. This code is several times more efficient than the earlier shield optimization code ASOP and therefore may be applied to two-dimensional shield studies using DOT. The program also included some further analysis of the experiments conducted for the SNS program during FY 1971.

2.1 FFTF RELATED STUDIES IN THE ORNL-LMFBR SHIELDING PROGRAM[1-3]

F. R. Mynatt R. E. Maerker
C. E. Clifford M. L. Gritzner
F. J. Muckenthaler L. R. Williams
J. L. Rathbun[4]

This paper documents an oral presentation given in the special session on Fast Reactor Shielding sponsored by the Shielding and Dosimetry Division at the October 1971 meeting of the American Nuclear Society in Miami, Florida. The progress to date on neutron transport calculational studies of FFTF shielding design is presented, including the analysis of supporting integral experiments. The major FFTF shielding problems considered were the predictions of (1) neutron dose rates above the reactor head and (2) neutron fluence intensities at the core support grid plate.

References

1. Funded by the LMFBR Program of the Atomic Energy Commission.
2. Presented at the 1971 Winter Meeting of the American Nuclear Society, Oct. 17, 1971.
3. Abstract of ORNL-TM-3705 (1972).
4. Westinghouse Electric Corporation, Advanced Reactor Division, Waltz Mill Site, Madison, Pa. 15663.

2.2 EXPERIMENTAL INVESTIGATION OF NEUTRON STREAMING THROUGH THE GRID-PLATE SHIELD OF THE FAST FLUX TEST FACILITY[1,2]

C. E. Clifford F. R. Mynatt
P. N. Stevens[3]

An experiment was performed at the Tower Shielding Facility (TSF) to determine the effect of neutron streaming in sodium coolant holes on the peak neutron fluence transmitted through a prototype of the FTR grid-plate shield. Three grid-plate shield configurations, supplied by WADCO Corporation, a subsidiary of Westinghouse Electric Corporation, were used in the experiment, each having different hole configurations. A flux increase of about 10% was measured for straight-through holes, and a 3% increase was measured for holes having a single offset. Standard deviations of measurements obtained were approximately 2%.

References

1. Funded by the LMFBR Program of the Atomic Energy Commission.
2. Abstract of ORNL-TM-3514 (1971).
3. Present address: Oregon State University, Corvallis, Ore.

2.3 FFTF COOLANT DUCT STREAMING EXPERIMENT[1,2]

B. J. McGregor[3] F. J. Muckenthaler

The present FFTF reactor design includes sodium inlet and outlet pipes which penetrate the 4-ft-thick reactor cavity wall at a height of 19 ft above the top of the core. Hence most neutrons enter these ducts at a slant angle, and streaming subsequent to scattering in the duct contributes an important source of neutrons to the heat exchanger vaults. Streaming of neutrons can take place along the sodium in the pipes as well as along the clearance gaps and low-density insulation surrounding the pipes. Two duct streaming experiments have been designed to validate analytical methods which will be used to predict the flux levels in the heat exchanger vault and piping. The first experiment, discussed here, was a concrete duct and sodium-filled pipe mockup

placed in a collimated neutron beam at an angle of 60°. The second experiment, still in progress, consists of a steel-lined concrete-walled plenum chamber containing an inlet and outlet duct. Both experiments are being conducted at the ORNL Tower Shielding Facility.

During the first experiment, measurements were made with nine Bonner balls[4] and the Benjamin spectrometer (hydrogen counter)[5] behind a 46½-in.-long pipe positioned at an angle of 60° to the TSF beam and at a distance of 15 ft from the reactor collimator face. Measurements were taken with the pipe empty, with a central cylinder filled with sodium in the pipe, and with the sodium cylinder and insulation inside the pipe. The Bonner ball measurements included both horizontal and vertical traverses 2 ft beyond the pipe exit, as well as traverses along the pipe axis for the empty pipe configuration. The Benjamin spectrometer measurements were made 2 ft beyond the pipe exit on the center line and 1 ft north and south of the center line.

An analysis of the experiment was performed with DOT-III,[6] using the 50-group structure cross-section library maintained at ORNL for FFTF shielding analy-

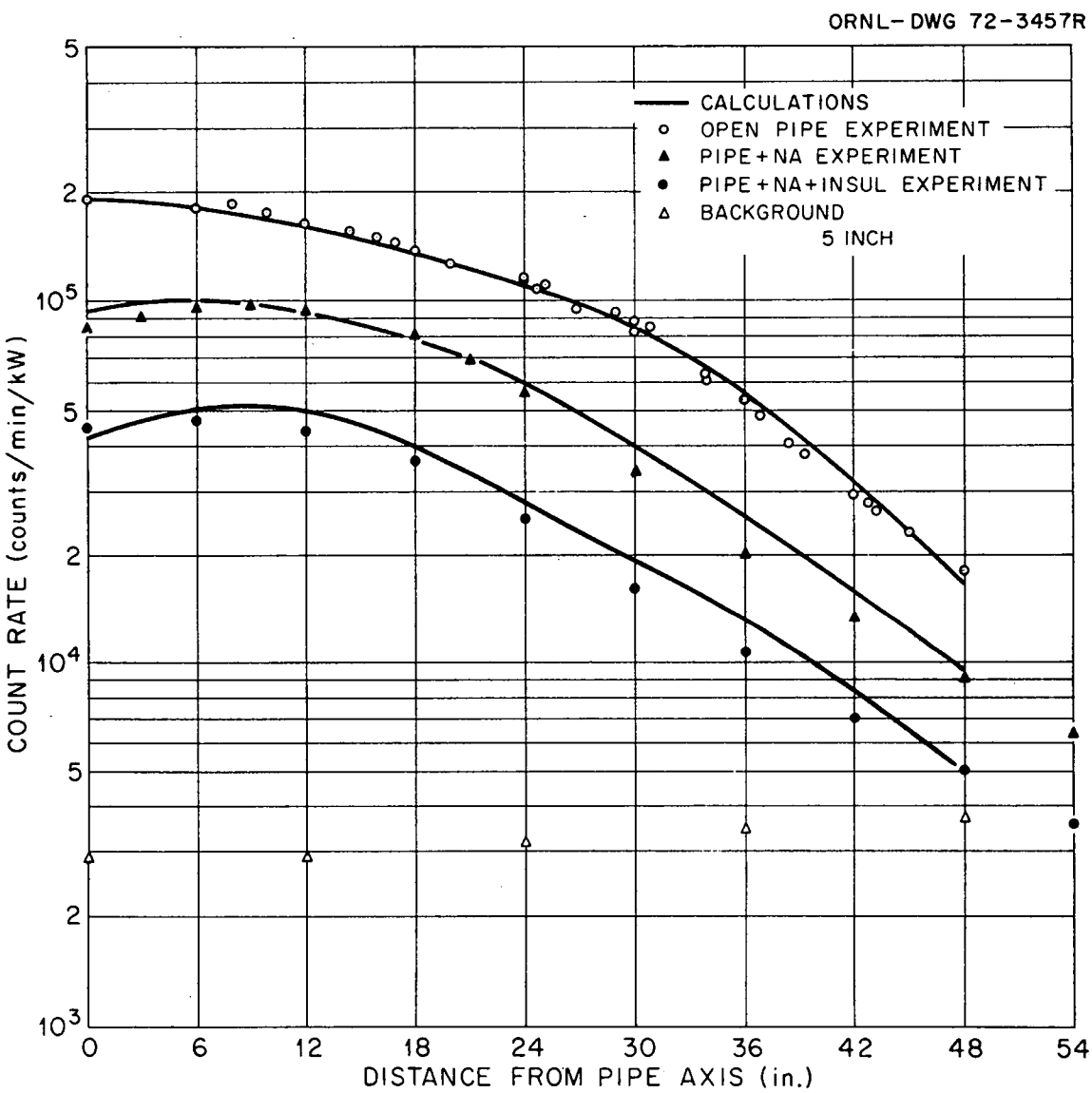

Fig. 2.3.1. Comparison of calculated values with measurements made beyond sodium-filled pipe mockup with 5-in. Bonner ball. Horizontal traverse 24 in. beyond the pipe.

ses. A special quadrature set was developed to handle this type of problem. With this quadrature set and a relatively fine axial mesh in the pipe assembly, good agreement with the experiment was obtained for all three configurations for seven Bonner balls ranging from 12 in. to 3 in. in diameter. The calculated results are lower than the measured results for the Cd-covered ball and the bare BF_3 counter. The calculation of the energy spectrum is in good agreement with the unfolded experimental spectrum from 50 keV to 1.5 MeV obtained from the Benjamin spectrometer.

Figure 2.3.1 shows a comparison of calculation and experiment for the 5-in. Bonner ball traverse.

References

1. Funded by the LMFBR program of the Atomic Energy Commission.
2. To be presented at the American Nuclear Society Topical Meeting on New Developments in Reactor Physics and Shielding, Kiamesha Lake, N.Y., Sept. 12–15, 1972.
3. On assignment from the Australian Atomic Energy Commission.
4. R. E. Maerker, L. R. Williams, F. R. Mynatt, and N. M. Greene, *Response Functions for Bonner Ball Neutron Detectors*, ORNL-TM-3451 (1971).
5. P. W. Benjamin, C. D. Kemshall, and J. Redfearn, "A High Resolution Spherical Proportional Counter," *Nucl. Instrum. Methods* **59**, 77–85 (1968).
6. F. R. Mynatt, F. J. Muckenthaler, and P. N. Stevens, *Development of Two-Dimensional Discrete Ordinates Transport Theory for Radiation Shielding*, Union Carbide Corporation report CTC-INF-952 (1969).

2.4 FAST REACTOR SHIELDING MONTHLY PROGRESS REPORTS, 189a NO. 10028, ACTIVITY NO. 40 01 61[1,2]

F. R. Mynatt — J. L. Hull
M. L. Gritzner — J. Lewin
R. E. Maerker — J. J. Manning
B. J. McGregor[3] — J. N. Money
R. M. Freestone, Jr. — F. J. Muckenthaler
K. M. Henry, Jr. — L. R. Williams

These reports summarize the progress made by the ORNL Neutron Physics Division in Fast Reactor Shielding Research during the months of June 1971 through May 1972.

References

1. Funded by the LMFBR Program of the Atomic Energy Commission.
2. Abstracts of ORNL-TM's 3521, 3538, 3573, 3606, 3639, 3666, 3695, 3746, 3786, 3800, 3857, and 3881.
3. On assignment from the Australian Atomic Energy Commission.

2.5 SOME TESTS RELATED TO THE USE OF PROTON-RECOIL PROPORTIONAL COUNTERS FOR NEUTRON-FLUX MEASUREMENTS[1,2]

E. A. Straker[3] — C. E. Burgart[3]
T. A. Love — R. M. Freestone, Jr.
G. L. Morgan

Several tests have been made in order to check the accuracy of neutron-flux measurements obtained with a spherical proton-recoil counter. The results indicate such measurements are valid for neutron energies as low as 10 keV.

References

1. Abstract of ORNL-TM-3631 (1971).
2. Funded by the LMFBR Program of the Atomic Energy Commission.
3. Now at Science Applications, Inc.

2.6 MONTE CARLO CALCULATIONS OF THE RESPONSE FUNCTIONS OF BONNER BALL NEUTRON DETECTORS[1,2]

C. E. Burgart[3] — M. B. Emmett[4]

Adjoint MORSE calculations were performed to verify the response functions of Bonner ball neutron detectors. Bare 3-in.- and 6-in.-diam Bonner balls were considered. These calculations utilized 123-group cross sections with 30 groups of thermal upscatter and also 104-group cross sections with a single thermal group. The response function shapes are in good agreement, and the magnitudes are within 10% of previously reported results.

References

1. Abstract of ORNL-TM-3739 (1972).
2. Funded by the LMFBR Program of the Atomic Energy Commission.
3. Now at Science Applications, Inc.
4. Mathematics Division.

2.7. SWANLAC, A COMPUTER CODE UTILIZING PERTURBATION THEORY FOR CROSS-SECTION SENSITIVITY ANALYSIS[1,2]

D. E. Bartine[3] F. R. Mynatt
E. Oblow

A computer code has been developed to provide cross-section sensitivity analysis for one-dimensional radiation transport problems. The forward and adjoint flux solutions to a given problem are utilized to obtain in one sensitivity calculation the effects of changing each, any, or all the cross sections which were involved in the transport calculation.

The code itself uses a special output tape produced by ANISN[4] and is compatible with all ANISN options. This report documents the code for users, including discussion of the calculations, description of input and output, and a sample problem. As a representative application of the code, results are presented for the sensitivity analysis of an air-transport problem in which the tissue dose from neutrons and gamma rays is calculated at a 2000-m range for 14-MeV, thermonuclear, and fission spectrum sources. An additional use of the sensitivity analysis is demonstrated in the formation of an improved energy grid structure for air cross sections.

References

1. Funded by the Defense Nuclear Agency under Subtask PC 104-03.
2. Abstract of ORNL-TM-3809 (to be published).
3. Mathematics Division.
4. W. W. Engle, Jr., *A User's Manual for ANISN, a One-Dimensional Discrete Ordinates Transport Code with Anisotropic Scattering,* K-1693 (1969).

2.8 CROSS-SECTION SENSITIVITY STUDIES FOR THE LLL PULSED-SPHERE EXPERIMENTS[1]

S. N. Cramer[2] R. W. Roussin
F. G. Perey E. Oblow

The calculations of the LLL pulsed-sphere experiments[3] have been extended to include sensitivity studies of the cross-section data in an effort to determine which specific areas of the data have an important effect on the final results. Primary attention has been given to the iron data, where the calculations show the poorest agreement with experiment. Other experiments investigated included the nitrogen, oxygen, and water spheres.

The O6R Monte Carlo code[4] is being used in these studies owing to its applicability in isolating specific aspects of the transport and collision processes. In this manner the results at various times can be analyzed with respect to (1) reaction type, (2) secondary energy distribution, (3) reaction energy, and (4) number of collisions. The MORSE Monte Carlo code[5] has been used to a lesser degree in order to verify the results from O6R. Although the two codes process basic cross sections by entirely different methods, the calculated time-dependent count rates compare favorably in all cases.

Calculations for the iron spheres indicate that the fast spectrum above 2 MeV is highly sensitive to uncollided neutrons from the source and the partial cross sections and secondary energy distribution of nonelastic reactions at source energies. An analysis of the data for these reaction processes has provided useful information to the evaluation effort on iron at ORNL.

References

1. Funded by the Defense Nuclear Agency under Subtask PC104-03.
2. Mathematics Division.
3. R. W. Roussin et al., "O6R Calculations of Nitrogen and Iron LRL Pulsed Sphere Experiments," *Trans. Amer. Nucl. Soc.* **14**(2), 925–26 (1971).
4. C. L. Thompson and E. A. Straker, *O6R-ACTIFK, Monte Carlo Neutron Transport Code,* ORNL-CF-69-8-36 (1969).
5. E. A. Straker et al., *The MORSE Code – a Multigroup Neutron and Gamma-Ray Monte Carlo Transport Code,* ORNL-4585 (1970).

2.9 IDENTIFICATION OF RADIATION STREAMING PATHS IN THE MINUTEMAN MISSILE SILO[1]

T. J. Hoffman[2] F. R. Mynatt
J. V. Pace III[2] C. E. Burgart[3]

The initial approach to the problem of radiation streaming in the Minuteman silo has consisted of a time-independent study of the transport of neutrons and gamma rays through suspected streaming paths in the silo closure. Both the Monte Carlo code MORSE[4] and the discrete ordinates code DOT[5] have been used in the analysis of the streaming problem.

A discrete ordinates calculation of the radiation environment exterior to the silo was made using the DOT code. This air-ground calculation used an unclassified thermonuclear source[6] at a specified source height.

DOT calculations were made of a Minuteman silo without streaming penetrations using as sources the external environment at several ground ranges as defined by the previous DOT calculation. The effects of radiation streaming through slots and gaps in the three-dimensional calculation were compared with these results.

Monte Carlo and discrete ordinates calculations of suspected streaming paths in the silo have also been made, and the study is being documented.

References

1. Funded by the Defense Nuclear Agency under Subtask PB050-03.
2. Mathematics Division.
3. Now at Science Applications, Inc.
4. E. A. Straker et al., *The MORSE Code – a Multigroup Neutron and Gamma-Ray Monte Carlo Transport Code,* ORNL-4585 (1970).
5. F. R. Mynatt et al., *Development of Two-Dimensional Discrete Ordinates Transport Theory for Radiation Shielding,* CTC-INF-952 (1969).
6. E. A. Straker and M. L. Gritzner, *Neutron and Secondary Gamma-Ray Transport in Infinite Homogeneous Air,* ORNL-4464 (1969).

2.10 THE EFFECT OF THE GROUND ON THE STEADY-STATE AND TIME-DEPENDENT TRANSPORT OF NEUTRONS AND SECONDARY GAMMA RAYS IN THE ATMOSPHERE[1,2]

E. A. Straker[3]

Calculations have been made of the space, energy, angle, and time dependence of the neutron and secondary gamma-ray fields produced in the atmosphere by several neutron sources, and the results for a 12.2- to 15-MeV source and a fission source are compared in this paper. They include steady-state and time-dependent results at ranges out to 1500 m for both an infinite-air medium and an air-over-ground medium, the latter for source heights of 15 and 343 m. The data show that the neutron doses and dose rates from the 12.2- to 15-MeV source are higher than those from the fission source in all geometries and time intervals. While the secondary gamma-ray doses produced by the 12.2- to 15-MeV source also are higher than those produced by the fission source in all geometries, the secondary dose rates are higher only for times less than 10^{-3} sec, after which the dose rates from the two sources are comparable. The effects of the ground are to enhance both the neutrons and the secondary gamma rays at ranges close to the source and to act as an absorber at ranges far from the source. These effects decrease with increasing source height.

References

1. Funded by the Defense Nuclear Agency under Subtask PB050-03.
2. Abstract of *Nucl. Sci. Eng.* **46**, 334–355 (1971) and of ORNL-TM-3754 (1972).
3. Now at Science Applications, Inc.

2.11 EFFECTS OF AIR-DENSITY PERTURBATIONS ON THE TRANSPORT OF NEUTRONS AND SECONDARY GAMMA RAYS PRODUCED BY POINT NEUTRON SOURCES[1,2]

B. J. McGregor[3]

Several calculations have been performed to investigate the effect that changes in the air density produced by one weapon detonation will have on the transport of radiation from a second weapon detonated within the next few seconds. Both weapons were assumed to be detonated at an altitude of 9.15 km, at which the density of the unperturbed air was taken to be 4.5×10^{-4} g/cc. In all cases the density profile of the perturbed air was assumed to be spherically symmetric around the point of detonation of the first weapon.

Two density profiles were used: one describing the air density as a function of distance from the first burst at a time 1 sec after the burst, and another giving the same information for a time 3.16 sec after the burst. The second weapon was always assumed to be a point isotropic neutron source emitting neutrons of specified energies at given distances from the first source. The response functions calculated were the neutron displacement (damage equivalent to that produced by 1-MeV neutrons in Si) and secondary gamma-ray ionization (rads – Si) at distances between 1 and 1.5 km from the second source within solid angles measured from an axis passing through both sources. The effects of the perturbed air were deduced from comparisons of the responses calculated for the perturbed and unperturbed atmospheres. Most of the calculations were performed with the MORSE Monte Carlo code, with check calculations made with the ANISN discrete ordinates code in both the forward and adjoint modes. In all cases the medium was assumed to be infinite air. The cases calculated were the following:

Case	Density profile	Second source	Distance between sources (m)
1	At 3.16 sec	Standard thermonuclear	1500
2	At 3.16 sec	Standard thermonuclear	1100
3A	At 1 sec	Standard thermonuclear	800
3B	At 1 sec	14 MeV	800
3C	At 1 sec	Fission	800
3D	At 1 sec	14 MeV	600
3E	At 1 sec	14 MeV	300
3F	At 1 sec	14 MeV	0

In general, the effects of the density perturbations for cases 1 and 2 were small. This was expected, since the perturbations reflected in the 3.16-sec density profile itself were small except for a small void at the detonation center, which did not subtend a large solid angle at the second source. For cases 3A through 3F, the effects were greater for all sources. This, too, was expected, since the 1-sec density profile has much larger perturbations and the second source is closer to the first source in all cases; thus, the void formed at the center of the first source subtends a larger solid angle at the second source. All neutron responses calculated for positions immediately beyond the first burst were about 50% higher than those obtained at the same positions in the unperturbed atmosphere; lesser increases were obtained as the angle from the axis of symmetry was increased. The secondary gamma-ray responses also were higher, with the increases being approximately one-half of increases of the neutron responses at the same positions. When the two detonations occurred at the same position (case 3F), the neutron responses between 1000 and 1500 m were about 19% higher than those in the unperturbed atmosphere, and the gamma-ray responses were 9% higher.

References

1. Abstract of ORNL-TM-3864 (to be published).
2. Funded by the Defense Nuclear Agency under Subtask PB050-03.
3. On assignment from the Australian Atomic Energy Commission.

2.12 ANALYSIS OF GGA MEASUREMENTS OF THE TIME-DEPENDENT TRANSPORT OF NEUTRONS AND SECONDARY GAMMA RAYS THROUGH CONCRETE[1]

G. W. Morrison[2] E. A. Straker[3]

Earlier O6R-OGRE Monte Carlo calculations of the time-dependent neutron and gamma-ray count rates behind slabs of concrete of various thicknesses have underestimated the long time (>5 μsec) gamma-ray count rates.[4] One explanation offered for this discrepancy was the failure to include the secondary gamma rays produced by thermal-neutron captures in the concrete. As a test of this hypothesis, a one-velocity thermal treatment was added to O6R. Several test calculations were performed on slabs of borated polyethylene to verify that the one-velocity thermal treatment was working properly. These calculations of the neutron and gamma-ray fluences agreed with other Monte Carlo calculations and S_n transport calculations.[5]

The 40.64-cm-thick concrete slab was rerun with the one-velocity thermal treatment to generate thermal capture gamma rays. Results of the calculations showed that thermal capture gamma rays should be included in the long time count rates. However, the calculated count rates are still lower than the measured count rates at long times.

The possibility of replacing the point detector used in the calculations with an actual detector geometry is being investigated.

References

1. Funded by the Defense Nuclear Agency under Subtask PE083-05.
2. Mathematics Division.
3. Now at Science Applications, Inc.
4. E. A. Straker and G. W. Morrison, *Trans. Amer. Nucl. Soc.* **14**(2), 919 (1971).
5. C. E. Burgart, *Neutron and Gamma-Ray Fluence Transmitted through a Slab of Borated Polyethylene – a Milestone Calculation,* ORNL-TM-3517 (1972).

2.13 A STUDY OF THE EFFECTS OF SOURCE ASYMMETRY ON TIME-DEPENDENT NEUTRON AND SECONDARY GAMMA-RAY TRANSPORT IN AIR[1,2]

B. J. McGregor[3] E. A. Straker[4]

The effects of source asymmetry on the time-dependent and steady-state transport of 12.2- to 15-MeV neutrons and fission neutrons in air have been determined. The response functions considered were air kerma, nonionizing silicon kerma, and tissue dose for neutrons, and air kerma, silicon kerma, and tissue dose for gamma rays. Monte Carlo calculations were made to determine the time-dependent responses. Adjoint discrete ordinates results were obtained to compare with

the time-integrated Monte Carlo data. The use of the one-dimensional adjoint solution to investigate source asymmetry effects is discussed in detail.

References

1. Funded by the Defense Nuclear Agency under Subtask PE080-01.
2. Abstract of ORNL-4741 (1972).
3. On assignment from the Australian Atomic Energy Commission.
4. Now at Science Applications, Inc.

2.14 INVESTIGATION OF THE ADEQUACY OF NITROGEN CROSS-SECTION SETS: COMPARISON OF NEUTRON AND SECONDARY GAMMA-RAY TRANSPORT CALCULATIONS WITH INTEGRAL EXPERIMENTS[1-3]

E. A. Straker[4] J. V. Pace III[5]
M. B. Emmett[5] R. W. Roussin
B. J. McGregor[6] H. T. Smith[4]
L. R. Williams

Two sets of cross sections for neutron interactions and secondary gamma-ray production in nitrogen, one recently evaluated by P. G. Young and D. G. Foster and another assembled in 1968 by Straker, have been tested in transport calculations corresponding to integral experiments. The experiments are Operation HENRE, during which measurements were made of the neutron and gamma-ray doses produced in the atmosphere by an accelerator emitting approximately 14-MeV neutrons, and two experiments in which liquid-nitrogen-filled dewars were pulsed with approximately 14-MeV neutrons. One of the nitrogen-dewar experiments, performed at Gulf Radiation Technology, yielded the energy spectra of fast and intermediate energy neutrons and secondary gamma rays within the nitrogen, and the other, performed at Lawrence Livermore Laboratory, gave time-dependent count rates due to neutrons leaking from the nitrogen. The comparisons of the calculated and measured results showed that for Operation HENRE both cross-section sets were adequate for calculating the neutron doses but that only the old set correctly predicted the gamma-ray doses, the new set giving results that are 30 to 50% lower than the data. Conversely, the comparisons for the GRT nitrogen-dewar experiment showed that the new set gives gamma-ray spectral data that are in reasonable agreement with the data, whereas the old set overpredicts by as much as a factor of 2. For both nitrogen-dewar experiments, the new cross sections give better predictions of the neutron spectra and time-dependent neutron count rates than the old cross sections. Additional calculations with both sets of cross sections for an infinite-air medium show that the two sets give identical neutron and secondary gamma-ray doses for a fission source; they also give very similar neutron doses for a 12.2- to 15-MeV neutron source, but the secondary gamma-ray doses are in disagreement, those obtained with the newer set being 30 to 50% lower. "Sensitivity" calculations indicate that for high-energy neutron sources most of the secondary gamma rays are produced by neutrons having energies greater than 10 MeV, and the greatest difference between the two cross-section sets is in their gamma-ray production probabilities at high neutron energies. On the basis of the various comparisons, it appears that the new neutron cross sections give better predictions of neutron quantities, but that a choice between the gamma-ray production cross sections is not obvious since each set agrees with one of the two gamma-ray experiments.

References

1. Presented by E. A. Straker at TTCP Working Panel N-6, London, England, Sept. 21–24, 1971, and at the RSIC Seminar Workshop on Radiation Transport in Air, Nov. 15–17, 1971.
2. Funded by the Defense Nuclear Agency under Subtask PE083-05.
3. Abstract of ORNL-TM-3768 (1972).
4. Science Applications, Inc.
5. Mathematics Division.
6. On assignment from the Australian Atomic Energy Commission.

2.15 A CALCULATION OF GAMMA-RAY PRODUCTION AND TRANSPORT IN LIQUID NITROGEN[1,2]

E. A. Straker[3] B. J. McGregor[4]

The gamma rays produced by neutron collisions with nitrogen comprise the major component of the secondary gamma-ray dose in air. To determine the adequacy of gamma-ray production cross sections, calculations using the ENDF/B material 506 version of neutron and gamma-ray cross sections for nitrogen are compared to results of a secondary gamma-ray measurement made at Gulf General Atomic for a 14-MeV neutron source in a very large nitrogen dewar.

References

1. Funded by the Defense Nuclear Agency under Subtask PE080-01.
2. Abstract of ORNL-TM-3635 (1971).
3. Now at Science Applications, Inc.
4. On assignment from the Australian Atomic Energy Commission.

2.16 PENETRATION INTO A MISSILE SILO OF NEUTRONS AND SECONDARY GAMMA RAYS PRODUCED BY POINT ISOTROPIC NEUTRON SOURCES[1,2]

E. A. Straker[3] F. R. Mynatt
J. V. Pace III[4] W. W. Engle, Jr.
M. B. Emmett[4] L. R. Williams
L. S. Abbott

The radiation fields produced in a missile silo by two low-altitude point isotropic neutron sources having weapons energy spectra have been calculated for three thicknesses of the silo concrete cover (40, 50, and 60 in.). The purpose of the calculations was twofold: to predict the radiation-induced displacement and ionization in the silicon components of electronic systems in the silos; and to illustrate possible techniques for coupling Monte Carlo and discrete ordinates transport methods to obtain the most efficient solution to this type of problem. Both time-integrated and time-dependent results were obtained, the latter to determine silicon response rates. The time-dependent calculations were performed in three successive steps corresponding to the radiation transport through air over ground, through the silo cover, and within the silo proper. The first and second steps were performed in slab geometry with the MORSE Monte Carlo code and the TDA discrete ordinates code respectively, and the third step was done in cylindrical geometry with MORSE; in each case the output from one code was used as the source term for the next. The time-integrated calculations were carried out in two steps, the first describing the transport through air over ground, and the second describing the transport through the cover and down into the silo. Both steps were performed in cylindrical geometry with the DOT discrete ordinates code. A few additional calculations were done with the ANISN discrete ordinates code, which used the DOT air-transport results as the source for calculating the penetration through the silo cover in slab geometry. When integrated over time, the MORSE-TDA-MORSE results were in good agreement with the DOT-DOT and DOT-ANISN results at common detector points, indicating that the coupling techniques were successful. The various calculations show that for the 50-in. cover the peak silicon ionization rates produced in the silo by secondary gamma rays are always at least a factor of 20 higher than those produced by neutrons. Photons produced outside the silo and those produced within the concrete cover contribute approximately equally to these peak rates; however, only the photons produced in the cover are important to the total gamma-ray ionization, which exceeds the total neutron ionization within the silo by factors of 350 to 600. The calculations also show that the attenuation in the silo cover of the various silicon responses is the same for both sources.

References

1. Abstract of ORNL-TM-3599 (1971) (SRD).
2. Funded by the Defense Nuclear Agency under Subtask PE072-02.
3. Now at Science Applications, Inc.
4. Mathematics Division.

2.17 NEUTRON AND GAMMA-RAY FLUENCE TRANSMITTED THROUGH A SLAB OF BORATED POLYETHYLENE – A MILESTONE CALCULATION[1,2]

C. E. Burgart[3]

A multigroup Monte Carlo code, a two-dimensional discrete ordinates code, and a one-dimensional discrete ordinates code were utilized in a milestone radiation transport calculation. The neutron energy spectrum and the neutron and gamma-ray fluence at points located a large distance from a slab of borated polyethylene were calculated. A line beam of neutrons with a ^{235}U fission spectrum is assumed normally incident on the slab. Identical multigroup cross sections were employed, providing a rigorous comparison of the transport methods alone. A pseudo-energy point cross-section Monte Carlo code was also utilized. This provided a check on the cross-section processing codes. The methods yield nearly identical results for points located within 30° of a normal to the slab. The agreement becomes less satisfactory at greater angles. However, possible explanations for the observed discrepancies are given.

References

1. Funded by the Defense Nuclear Agency under Subtask PE074-02.

2. Abstract of ORNL-TM-3517 (1972).
3. Now at Science Applications, Inc.

2.18 NUCLEAR WEAPONS INITIAL RADIATION SHIELD DESIGN: A STATE-OF-THE-ART REPORT TO STRUCTURE DESIGNERS[1]

L. S. Abbott

At the request of the U.S. Army Corps of Engineers, a chapter discussing the state of the art of shield design for protection against the initial radiation produced by nuclear weapons has been written for inclusion in a book being prepared by the U.S. Army Engineer Waterways Experiment Station, Corps of Engineers, Vicksburg, Mississippi. The book will be entitled *State-of-the-Art Evaluation of Vulnerability and Hardness Analyses for Ballistic Missile Defense Facilities.* This chapter is written for engineers who without a background of nuclear physics must consider the effects of initial nuclear radiations from an in-air detonation on the integrity and usefulness of various types of structures. It describes the radiation sources, summarizes the methods most frequently used to calculate the penetration of radiation through the atmosphere and into shielded structures, and discusses the calculational techniques that have been used to evaluate specific structures. It also guides the engineer to the limited amount of engineering data that are available. The primary purpose of the chapter is to acquaint the structure designer with the many factors that must be considered in radiation shield design so that he can better determine the best approach to his particular problem.

Reference

1. Funded by Omaha District Corps of Engineers, Omaha, Neb. under order number PS-72.

2.19 WEAPONS RADIATION SHIELDING HANDBOOK: STATUS REPORT[1]

L. S. Abbott H. C. Claiborne[2]
C. E. Clifford

During the past year a revised and enlarged version of Chap. 3 of the Weapons Radiation Shielding Handbook was issued. Entitled "Methods for Calculating Neutron and Gamma-Ray Attenuation," and identified as DNA-1892-3, Rev. 1, the chapter was authored by P. N. Stevens and D. K. Trubey.

No other Handbook work was performed during the year, and Chaps. 8 and 1 are yet to be published. Chapter 8 will present an engineering method for predicting doses in aboveground structures, and Chap. 1 will be an introduction to the entire Handbook.

References

1. Funded by the Defense Nuclear Agency under Subtask PB052-02.
2. Chemical Technology Division.

2.20 COLLISION SITE PLOTTING ROUTINES AND COLLISION DENSITY FLUENCE ESTIMATES FOR THE MORSE MONTE CARLO CODE[1,2]

E. A. Straker[3] M. B. Emmett[4]

Routines for use with the Monte Carlo transport code MORSE have been written to provide collision site plots – that is, plots of the locations of collisions occurring during the random walk process. The plots can be made either on the on-line printer or, through a collision tape, on a pen and ink or cathode-ray plotter. The user must decide what type of events and over what spatial range the collisions are to be plotted. Also, an output routine has been added to take advantage of the collision counter information in MORSE in providing a region-averaged estimate of the fluence. Printer plots of the resulting energy spectra for both neutrons and gamma rays are part of the output. This output may be obtained for both forward and adjoint calculations. These routines can also be utilized in other Monte Carlo codes.

References

1. Funded by the Defense Nuclear Agency under Subtask PE080-01.
2. Abstract of ORNL-TM-3585 (1971); previously referred to as ORNL-4722 before it was published.
3. Now at Science Applications, Inc.
4. Mathematics Division.

2.21 METHODS OF BIASING SECONDARY GAMMA-RAY PRODUCTION IN COUPLED NEUTRON–GAMMA-RAY MONTE CARLO CALCULATIONS[1–3]

M. Solomito[4] E. A. Straker[6]
P. N. Stevens[5] C. E. Burgart[6]
S. N. Cramer[7]

Methods for applying importance sampling techniques to secondary gamma-ray generation in coupled neutron–gamma-ray Monte Carlo transport calculations

have been developed and evaluated. The Boltzmann transport equation is presented in an integral-matrix form which defines a set of coupled neutron–gamma-ray multigroup equations and provides the basis for the coupled Monte Carlo random walk. Three methods of biasing the production of secondary gamma rays which make use of importance functions obtained from discrete ordinates adjoint calculations are formalized. These methods employ importance sampling techniques which include alteration of the gamma-ray generation probabilities, nonabsorption weighting, and a combination of splitting and Russian roulette. These three methods are evaluated using the multigroup Monte Carlo code MORSE in the solution of a deep-penetration shielding problem in concrete. All three methods are shown to be more efficient than the standard method of biasing the secondary gamma-ray production in the MORSE code. The methods varied from a factor of 1.3 to 40.0 better than the standard method, based on the running time of the code and variance of the answer obtained.

References

1. Jointly funded by the Defense Nuclear Agency under Subtask PE080-01 and the Space Nuclear Systems Division of the Atomic Energy Commission.
2. Abstract of ORNL-TM-3530 (1971).
3. A dissertation presented to the Graduate Council of the University of Tennessee in partial fulfillment of the requirements for the degree of Doctor of Philosophy for M. Solomito.
4. Present address: 3699 South Galloway Drive, Memphis, Tenn.
5. University of Tennessee.
6. Now at Science Applications, Inc.
7. Mathematics Division.

2.22 AMPX: MULTIGROUP COUPLED NEUTRON-GAMMA CROSS-SECTION GENERATOR[1]

N. M. Greene[2] J. L. Lucius[2]
W. E. Ford III[2] J. E. White[2]
R. Q. Wright[2]

A system of interfaced computer codes which will automate the processing of neutron and gamma-ray point cross sections into coupled sets of multigroup cross sections is being developed. The system is called AMPX, and the phase I development has been defined as that development required to collect state-of-the-art techniques for producing coupled cross-section sets into a usable system. In most cases, considerable tailoring was required to make individual techniques fit the design features of this system, of which the most important are:

1. Flexible dimensioning of all large arrays.
2. Cross section library formats general enough to describe neutron, gamma-ray, or coupled sets without normal restrictions as to number of processes, scattering orders, etc.
3. Multipath flexibility – any module in the system executable as a stand-alone code and any combination of modules executable in any order.
4. Free-form FIDO input to all modules.

In addition, AMPX should occupy little more core than its longest module. At this time, it meets these requirements.

Figure 2.22.1 illustrates the original design chart for AMPX. The features of each module are noted. All modules except XSDRNPM have been tailored to the AMPX requirements and are operational. Most of the modifications to the original XSDRN program to create XSDRNPM have been programmed, and debugging should commence soon. Nevertheless, as it stands, AMPX will make coupled cross-section sets and can output them in ANISN formats through an option provided in the NITAWL module. To date, the following coupled sets have been processed:

1. A 100-neutron-group, 18-gamma-group aluminum set.
2. A 22-neutron-group, 18-gamma-group oxygen set.
3. A 22-neutron-group, 18-gamma-group nitrogen set.
4. A 22-neutron-group, 18-gamma-group aluminum set.

The 22-18 sets were all processed from DNA evaluations and are being visually compared with sets produced by pre-AMPX procedures. These sets will also be used in ANISN transport calculations to obtain more significant verification of their "correctness." All of the DNA evaluations will be processed, probably in the 22-18 structure, to be sure that all modules will handle them, and where feasible, other calculational checks will be made with the data.

Most of the AMPX modules will need some development work in FY 73. A large fraction of the modifications are required to include new and improved treatments not used in present-day programs. The possible areas, ranked roughly by importance are given below.

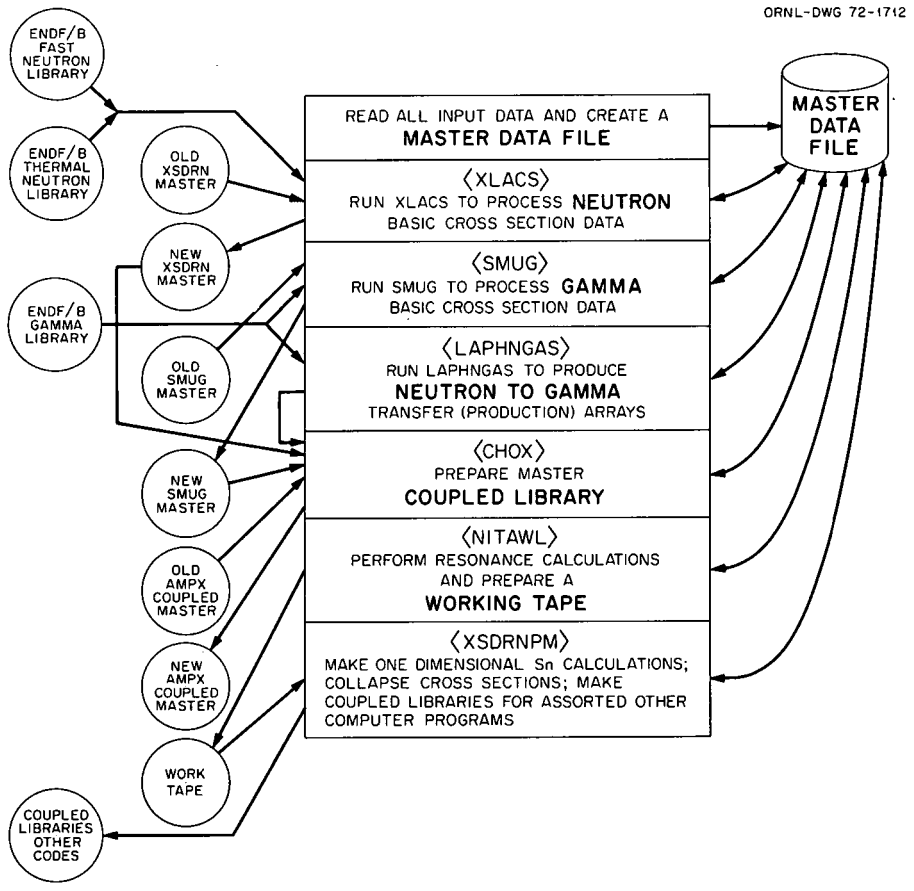

Fig. 2.22.1. AMPX flow chart.

XLACS:

1. Treat inelastic processes anisotropically.
2. Weight higher order cross-section matrices over better approximations for the higher flux moments.
3. Include processing for Adler-Adler and Reich-Moore resonance parameters.
4. Modify elastic routines to process tabulated angular distribution data, when given in this form.
5. Include a more efficient and accurate means of calculating free gas thermal kernels.

LAPHNGAS:

1. Make the code read a binary ENDF/B tape (the original code reads only the BCD form).
2. Include all the weighting options used in XLACS into this code (it presently assumes a flat flux in energy).
3. Produce P_l scattering matrices.

SMUG:

1. Include processing of form factor data.
2. Possibly allow other flux weighting options.

CHOX:

1. Provide general maintenance.

NITAWL:

1. Modify resonance treatments to handle Adler-Adler and Reich-Moore data.

XSDRNPM:

1. Complete debugging.
2. Include adjoint calculation.
3. Interface to DRDT library format.

New module A: Work is presently under way to include a module in AMPX to output cross sections for use with point cross-section techniques. This may, at some future time, provide a very detailed and accurate way of weighting cross sections.

New module B: The cross-section sensitivity processing may be built in, when it is worked into production form.

References

1. Funded by the Defense Nuclear Agency under Subtask PE074-02.
2. Mathematics Division.

2.23 XCHEKR – A MULTIGROUP CROSS-SECTION EDITING AND CHECKING CODE[1,2]

C. E. Burgart[3] E. A. Straker[3]

XCHEKR is a multigroup cross-section editing and checking code. Cross sections in either ANISN or DTF-IV format may be read from cards or binary magnetic tape. These cross sections may be for neutrons only, for gamma rays only, or they may be coupled neutron and gamma-ray cross sections, all with full or partial downscatter and/or upscatter. XCHEKR produces a highly readable edit of the P_0 portion of the cross sections, as well as tables of evaluated angular distributions for each group-to-group transfer. Checks are performed to determine if the Legendre coefficients are possible.

References

1. Funded by the Defense Nuclear Agency under Subtask PE074-01.
2. Abstract of ORNL-TM-3518 (1971).
3. Science Applications, Inc.

2.24 DOMINO, A GENERAL-PURPOSE DISCRETE ORDINATES TO MONTE CARLO COUPLING CODE FOR RADIATION TRANSPORT[1,2]

M. B. Emmett[3] C. E. Burgart[4]
T. J. Hoffman[3]

A method of coupling two-dimensional discrete ordinates calculations with Monte Carlo calculations is incorporated in the DOMINO code. In particular, the DOT[5] code, a two-dimensional discrete ordinates code, has been coupled with MORSE,[6] a Monte Carlo code.

The discrete ordinates calculation is limited to an *r-z* geometry. Either the DOT boundary angular fluxes or the angular fluxes at internal surfaces may be input to DOMINO. Any amount of surface may be used in DOMINO, that is, from all mesh points down to a portion of one interval. The radii, axes, and quadrature set must be read into DOMINO. Appropriate cumulative probability distributions are calculated from the angular fluxes and written on a DOMINO tape. Four different types of DOMINO tapes may be written for use in Monte Carlo codes – upward from a disk, downward from a disk, inward from a cylindrical surface, and outward from a cylindrical surface. The DOMINO tape contains all necessary coupling information for use by the Monte Carlo code. The MORSE calculation may utilize this data in four ways: (1) as a source for a forward MORSE case, (2) as a scoring function for an adjoint MORSE case, (3) as a source for an adjoint MORSE case, or (4) as a scoring function for a forward MORSE case.

A detailed discussion of the coupling operation as well as a sample problem are included in the appendices. Logical flow charts of the routines add to the understanding of the code.

References

1. Funded by the Defense Nuclear Agency under Subtask PE074-01.
2. Abstract of an ORNL report to be published.
3. Mathematics Division.
4. Now at Science Applications, Inc.
5. F. R. Mynatt, F. J. Muckenthaler, and P. N. Stevens, *Development of Two-Dimensional Discrete Ordinates Transport Theory for Radiation Shielding,* CTC-INF-952 (1969).
6. E. A. Straker, P. N. Stevens, D. C. Irving, and V. R. Cain, *The MORSE Code – a Multigroup Neutron and Gamma-Ray Monte Carlo Transport Code,* ORNL-4585 (1970).

2.25 BRACKETING THE PEAK PRIMARY GAMMA-RAY DOSE RATE FROM NUCLEAR DEVICES BY STEADY-STATE TRANSPORT CALCULATIONS[1,2]

H. C. Claiborne[3] W. W. Engle, Jr.

Electronic components can be affected by the dose rate from gamma rays delivered during the first few shakes of an exploding nuclear device. Determining such dose rates generally requires expensive time-dependent calculations. This paper demonstrates that relatively inexpensive steady-state transport calculations can be used to bracket the time-dependent peak dose rates with meaningful upper and lower limits.

The model configuration consisted of a sphere of air surrounded by a spherical annulus of concrete with an isotropic source of gamma rays from fissioning ^{235}U located at the geometric center. Steady-state calcula-

tions were made with the discrete ordinates code ANISN and the time-dependent calculations with TDA (time-dependent ANISN). The upper limit dose rates were obtained by dividing the steady-state total dose by the pulse width of the device. This is equivalent to assuming that the uncollided and air-scattered fluxes arrive at the shield simultaneously. For a lower limit calculation, only the uncollided flux was considered incident on the shield.

Calculations were made for a 120-cm-thick concrete shield for ranges of 500, 1000, and 5000 m and for step-function burst pulse widths of 1 through 8 shakes. The results from the steady-state calculations generally bracketed the peak time-dependent dose rates within an acceptably narrow band except for the 500-m range at the back end of the shield, where the peak time-dependent dose rates were highest for all pulse widths. This apparent anomaly is explained on the basis of using a moving boundary condition in the time-dependent solution, and the effect is shown to be of no consequence.

References

1. Funded by the U.S. Army Corps of Engineers, Huntsville Division, Huntsville, Ala.

2. Abstract of *Nucl. Technol.* 13, 209–215 (1972); included last year as abstract of ORNL-TM-3462 (1971).

3. Chemical Technology Division.

2.26 CAPABILITIES OF THE MORSE MULTIGROUP MONTE CARLO CODE IN SOLVING REACTOR EIGENVALUE PROBLEMS[1-3]

C. E. Burgart[4]

A multigroup Monte Carlo code, MORSE, has been utilized in solving many nonmultiplying fixed source radiation transport problems. Time-dependent and coupled neutron–gamma-ray problems have been considered in complex geometries. The capabilities of MORSE in solving reactor eigenvalue problems have not previously been described or demonstrated.

MORSE utilizes multi-energy-group cross sections identical to those used by several discrete ordinates codes. Thermal upscattering may be included. Legendre polynomial expansions of the angular distributions for each group-to-group transfer are utilized when anisotropic scattering is considered. Both a general geometry module capable of describing any combination of quadratic surfaces and special geometry modules for simplified slab, cylindrical, or spherical systems are available. Albedo boundary conditions may be applied at any surfaces. Calculations may be performed in the forward as well as the adjoint mode.

Two additional features are of particular interest in reactor calculations. First is the "fictitious scattering" method of choosing path lengths. With this method, pseudocollision sites are chosen using the maximum total cross section in the system. A rejection technique based on the ratio of the actual total cross section at the pseudocollision site to the maximum cross section is utilized to determine if this is a real collision. If the test fails, a new pseudocollision site is chosen. The "fictitious scattering" method avoids much of the geometry tracking usually encountered in complex reactor calculations. Thus, the calculation time does not increase proportionately to the geometric detail. Another feature of interest is the "point cross-section" option. MORSE can utilize "point" total, scattering, and fission cross sections in selecting path lengths, in nonabsorption weighting, and in producing fission neutrons. These cross sections are defined at numerous energy points in a variable supergroup-subgroup structure. The energy degradation and outgoing direction are chosen as in a conventional MORSE calculation. However, for the purpose of cross-section lookup, the energy within a given multigroup is chosen from a constant frequency function. This point cross-section option allows considerably more detail in the cross sections to be utilized with relatively little penalty in computer core storage. Some of the disadvantages of multigroup cross-section weighting may thus be avoided.

The quantities routinely calculated for reactor eigenvalue problems include, in addition to k_{eff}, the mean time to birth and the mean time to death. Average reaction rates in specified spatial regions may also be determined. These quantities have been calculated for several critical configurations, and the usefulness of some of the above capabilities are discussed.

References

1. Funded by the Space Nuclear Systems Division of the Atomic Energy Commission.

2. Abstract of ORNL-TM-3662 (1971).

3. Presented at the IAEA Seminar on Numerical Reactor Calculations, Vienna, Austria, Jan. 17–21, 1972.

4. Now at Science Applications, Inc.

2.27 AN EVALUATION OF NEUTRON AND GAMMA-RAY-PRODUCTION CROSS SECTIONS FOR LEAD[1,2]

C. Y. Fu[3] F. G. Perey

A survey was made of the available information on neutron and gamma-ray-production cross-section measurements of lead. Evaluated nuclear data sets in the ENDF/B format were prepared for lead covering the energy range from 0.00001 eV to 20.0 MeV. The cross-section sets were based on experimental results available to June 1971 and on nuclear model calculations. This evaluation received MAT. No. 4136 in the DNA Library and 1136 in the CSEWG files.

References

1. Abstract of ORNL-4765 (1972).
2. Funded by the Defense Nuclear Agency under Subtask PC102-04.
3. University of Tennessee.

2.28 ON A POSSIBLE RESOLUTION OF THE NITROGEN NONELASTIC NEUTRON CROSS-SECTION DISCREPANCY BELOW 9 MeV[1,2]

F. G. Perey W. E. Kinney

New measurements of differential elastic-scattering cross sections of neutrons from nitrogen at six energies between 6.0 and 8.5 MeV yield nonelastic cross sections which are in essential agreement with the sum of the measured nonelastic partial cross sections. The new data give results systematically lower than those obtained from previous measurements, thereby removing the discrepancy in the nonelastic cross sections of nitrogen below 9 MeV.

References

1. Abstract of *Nucl. Sci. Eng.* **46**, 428–431 (1971).
2. Jointly funded by the Defense Nuclear Agency under Subtask PC102-04 and the Division of Reactor Development and Technology of the Atomic Energy Commission.

2.29 ENERGIES AND INTENSITIES OF GAMMA RAYS EMITTED BY A ^{226}Ra SOURCE[1,2]

J. K. Dickens

Energies and intensities of 64 gamma rays emitted by ^{226}Ra and its decay products have been measured for gamma-ray energies between 186 and 2979 keV. The tabulated results are of primary use for efficiency calibration of Ge(Li) detectors.

References

1. Abstract of ORNL-TM-3509 (1971).
2. Jointly funded by the Defense Nuclear Agency under Subtask PC101-05 and the Division of Reactor Development and Technology of the Atomic Energy Commission.

2.30 *R*-MATRIX ANALYSIS OF DIFFERENTIAL ELASTIC AND INELASTIC SCATTERING OF NEUTRONS FROM ^{12}C BELOW 8.7 MeV[1]

C. Y. Fu[2] F. G. Perey
R. B. Perez

We have attempted to use the multilevel multichannel *R*-matrix theory[3] to describe the differential elastic- and inelastic-scattering cross sections of ^{12}C for E_n below 8.7 MeV. Inelastic scattering in this energy range is characterized by the excitation of the 4.43-MeV level. From 5 to 8.7 MeV the data used are those measured by Perey and Kinney.[4] The hard-sphere phase shifts are, for the time being, multiplied by the functions $a_l + b_l E_n$ to approximate the effect of ignored distant levels.

First the total and differential cross sections below the inelastic threshold were visually fitted by adjusting the level energies and widths using the known[5] J^π and by adjusting the channel radius and the parameters a_l and b_l. The parameters a_l and b_l for $l \leqslant 2$ were determined by fitting the differential cross sections at off-resonance energies.

Above the inelastic threshold the problem gets overwhelmingly complex for straightforward fitting because of unknown levels, known levels with unknown J^π, strongly overlapping resonances, and the dependence of the differential inelastic scattering on the signs of the reduced width amplitudes. To simplify it we temporarily set aside the differential inelastic data. From the relative strengths of each resonance in the various Legendre coefficients of differential elastic data, we could readily assign spin limits to some of the levels of unknown J^π. From the interference patterns of a state of firmly established J^π with its nearby or underlying neighbors we could assign J^π values to the latter. With considerable trials and errors we arrived at a set of tentative resonance levels and parameters approximately fitting the total elastic and inelastic and the differential elastic-scattering cross sections up to 8.7 MeV.

Our next step is to see if we can fit the differential inelastic data by adjusting the signs of the reduced width amplitudes and their relative strengths in various channel configurations. If we succeed, then the code and/or method may be refined by adding one or more of the following: (1) an automatic search for fine adjustment of the level positions and widths, (2) a potential model for fitting the off-resonance phase shifts, and (3) a complex phase-shift analysis for further testing the assumed J^{π} values.

References

1. Funded by the Defense Nuclear Agency under Subtask PC102-04.
2. University of Tennessee.
3. A. M. Lane and R. G. Thomas, *Rev. Mod. Phys.* **30**, 257 (1958).
4. F. G. Perey and W. E. Kinney (to be published).
5. F. Ajzenberg-Selove, *Nucl. Phys.* **A166**, 1 (1971).

2.31 SELF-ABSORPTION OF GAMMA RAYS PRODUCED IN LARGE CYLINDRICAL SAMPLES[1,2]

J. K. Dickens

An exact expression is derived for the self-absorption of gamma rays produced uniformly throughout large cylindrical samples (i.e., diameter > 1 mean-free path). The calculated self-absorption of gamma rays emitted by ^{110m}Ag is compared with observed absorption by a 2-cm-diam Pb sample. The calculated self-absorption of gamma rays produced by 7-MeV neutron interactions with ^{208}Pb agrees with estimates based upon Monte Carlo computations.

References

1. Abstract of *Nucl. Instrum. Methods* **98**, 451 (1972).
2. Jointly funded by the Defense Nuclear Agency under Subtask PC101-05 and the Division of Reactor Development and Technology of the Atomic Energy Commission.

2.32 UPDATING OF CROSS-SECTION FILES FOR CALCIUM AND LEAD[1]

C. Y. Fu[2] F. G. Perey

The evaluations of calcium (Material 4152)[3] and lead (Material 4136)[4] cross sections sponsored by the Defense Nuclear Agency have been updated and/or revised. The new cross-section files are available at RSIC as Modification III of the corresponding material numbers.

The major revisions for calcium include:

1. Extension of the lower energy limit from 0.001 eV to 0.00001 eV.
2. Reevaluation of $\sigma(n,n')$, $\sigma(n,p)$, $\sigma(n,\alpha)$, $\sigma(n,np)$, and $\sigma(n,n\alpha)$ above 9 MeV.
3. Reevaluation of the energy distributions of secondary neutrons.
4. Gamma-ray production cross sections for (n,γ), (n,n'), (n,p), and (n,α) reactions, previously combined for nonelastic reactions, are now separately given.
5. Addition of gamma-ray production cross sections for (n,np) and $(n,n\alpha)$ reactions.

The capture cross sections for lead from 1 keV to 1 MeV have been completely reevaluated based primarily on a recent high-resolution measurement of capture cross sections for the lead isotopes 204, 206, 207, and 208 by Allen et al.[5] Approximately 75% of the capture cross sections in the range from 1 keV to 200 keV were given explicitly as resonances. Correlation of these resonances with the total cross sections enables us to refine the resonance widths and areas of the total cross sections as well. Corresponding changes have been made in the elastic-scattering and nonelastic cross sections.

References

1. Funded by the Defense Nuclear Agency under Subtask PC102-04.
2. University of Tennessee.
3. Evaluated by F. G. Perey, C. Y. Fu, and W. E. Kinney.
4. C. Y. Fu and F. G. Perey, *An Evaluation of Neutron and Gamma-Ray Production Cross Sections for Lead,* ORNL-4765 (March 1972).
5. B. J. Allen, R. L. Macklin, R. R. Winters, and C. Y. Fu, Oak Ridge National Laboratory (to be published).

2.33 Ca$(n,x\gamma)$ REACTIONS FOR $4.85 \leq E_n \leq 8.05$ MeV[1,2]

J. K. Dickens

Gamma-ray spectra have been obtained for reactions involving neutron interactions with a sample of natural calcium. Gamma rays were observed which are associated with the reactions ^{40}Ca$(n,n'\gamma)^{40}$Ca, ^{40}Ca$(n,p\gamma)^{40}$K, ^{40}Ca$(n,\alpha\gamma)^{37}$Ar, and ^{42,44}Ca$(n,n'\gamma)^{42,44}$Ca. Incident neutron energies were

E_n = 4.85, 5.4, 6.45, 7.0, 7.5, and 8.05 MeV, and the scattering angle was θ_γ = 125°. The gamma rays were detected using a 45-cm^3 coaxial Ge(Li) detector placed at 100 cm from the sample; the time-of-flight technique was used with the gamma-ray detector to discriminate against pulses due to neutrons and background gamma radiation. The sample was 20 g of natural calcium metal in the form of a right circular cylinder. The incident neutron beam was produced by bombarding a deuterium-filled gas cell with the pulsed deuteron beam of appropriate energy from the ORNL 6-MV Van de Graaff. The resulting neutron beam was monitored with a scintillation counter; a time-of-flight spectrum from this detector was recorded simultaneously with the gamma-ray data. These data have been studied to obtain absolute cross sections for the production of gamma rays from Ca for the incident neutron energies quoted above.

More than 50 gamma rays were correlated with transitions among the residual nuclei; these assigned gamma rays have >90% of the total gamma-ray production cross section for $E_n \leqslant 6.45$ MeV. All unplaced gamma rays have small cross sections and are most likely associated with transitions in ^{40}K. The cross sections have been compared, where possible, with previously measured values and with results of the most recent evaluation for calcium with generally good agreement. Several important differences with previous data are discussed.

References

1. Abstract of ORNL-TM-3584 (1971) and of *Nucl. Sci. Eng.* **48**, 78–86 (1972).

2. Jointly funded by the Defense Nuclear Agency under Subtask PC103-01 and the Division of Reactor Development and Technology of the Atomic Energy Commission.

2.34 DOORWAY STATE IN ^{206}Pb REVISITED[1]

B. J. Allen[2] C. Y. Fu[4]
R. L. Macklin[3] R. R. Winters[5]

The neutron capture cross section of ^{206}Pb(n,γ) has been measured with high resolution at the Oak Ridge Electron Linear Accelerator. The capture results show that the reported $s_{1/2}$ doorway in ^{206}Pb is not observed in the photon channel.

References

1. Partially funded by the Defense Nuclear Agency under Subtask PC102-04.

2. Present address: Australian Atomic Energy Commission, Lucas Heights.
3. Physics Division.
4. The University of Tennessee.
5. Guest Assignee from Denison University, Granville, Ohio.

2.35 GAMMA-RAY-PRODUCTION CROSS SECTIONS OF TANTALUM AND CARBON FOR INCIDENT NEUTRON ENERGIES BETWEEN 0.007 AND 20.0 MeV[1,2]

G. L. Morgan J. K. Dickens
T. A. Love F. G. Perey

Cross sections for neutron-induced gamma radiation from tantalum have been measured as a function of both neutron and gamma-ray energy. The neutron energies ranged from 0.007 to 20.0 MeV while gamma-ray energies from 1.0 to 10.5 MeV were measured. Data were taken at angles of 90° and 125° with respect to the incident neutrons. Similar measurements were made for natural carbon, and these results demonstrate the efficacy of the data acquisition and reduction systems.

References

1. Abstract of ORNL-TM-3702 (1972).

2. Funded by the Space Nuclear Systems Division of the Atomic Energy Commission.

2.36 A COMPARISON OF CALCULATED AND MEASURED YIELDS OF NEUTRON-ENERGY-DEPENDENT CAPTURE GAMMA RAYS FROM ^{238}U[1,2]

R. S. Booth[3] S. K. Penny[4]
J. E. White[4] K. J. Yost[5]

The gamma-ray energy spectra resulting from neutron capture in ^{238}U were calculated using the gamma-ray cascade code DUCAL for incident neutrons in the energy range $0.0 \leqslant E \leqslant 1.1$ MeV. The overall spectral shapes generated for thermal and epithermal neutron capture agree quite favorably with an integral measurement. Absolute comparisons of the generated spectra with differential capture yield measurements exhibit general agreement. Variations in the spectral shape with neutron energy are noticeable above 3.0 MeV.

References

1. Funded by the Space Nuclear Systems Division of the Atomic Energy Commission.

2. Abstract of *Nucl. Sci. Eng.* **47**, 8 (1972).
3. Instrumentation and Controls Division.
4. Mathematics Division.
5. Purdue University.

2.37 Al($n,x\gamma$) REACTIONS FOR $5.3 \leqslant E_n \leqslant 9.0$ MeV[1,2]

J. K. Dickens

Interactions of neutrons with aluminum have been studied by measuring gamma-ray-production cross sections. Spectra were obtained for incident mean neutron energies E_n = 5.35, 5.85, 6.4, 6.9, 7.45, 7.95, 8.5, and 9.0 MeV. The gamma rays were detected using a coaxial Ge(Li) detector of 30-cm^3 active volume. Data were obtained for gamma-ray scattering angles of 55° for all E_n, 90° for all E_n except 5.35 MeV, and 75° for E_n = 6.4 and 7.45 MeV. Time of flight was used with the detector to discriminate against pulses due to neutrons and background radiation. Absolute cross sections for production of gamma rays were obtained for the incident neutron energies quoted above. The cross sections have been compared, where possible, with previous measurements with good agreement. The spectra were studied for gamma rays which could be associated with deexcitation of nuclear levels having unknown decay modes. Gamma rays were found having energies appropriate for ground-state decay of levels at excitation energies E_x = 5.155, 5.414, 5.434, 6.514, 6.821, 6.956, 7.290, 7.411, 7.471, 7.56 (doublet), 7.655, 8.148, and 8.184 MeV.

References

1. Partially funded by the Defense Nuclear Agency under Subtask PC068.
2. Abstract of *Phys. Rev. C* **5**, 100 (1972); included in last year's annual as abstract of ORNL-TM-3284 (1971).

2.38 TOTAL CROSS-SECTION CHECKS AT THE ORELA SHIELD TEST FACILITY[1]

T. A. Love G. L. Morgan
F. G. Perey J. W. McConnell[2]
R. M. Freestone, Jr.

The ORELA Shield Test Facility was instrumented to perform total cross-section checks using the 47-m flight path. A sample changer was installed at the 28-m station and was interfaced with the PDP-9 computer. An NE-110 plastic scintillator is used as the detector. Because of the superior light transmission characteristics of NE-110, it is possible to set the bias to a level below that of a 100-keV neutron energy. The system was thoroughly tested while performing total cross-section measurements on carbon. Excellent agreement was found with the KAPL[3] evaluation of the total cross section below 2 MeV down to 200 keV. Our results agree well with the measurements of Cierjacks et al.[4] and Schwartz et al.[5] at higher energies. The system is now considered to be fully operational and will be used shortly to test the ENDF evaluations for N, O, Si, Al, Ca, and Fe.

References

1. Funded by the Space Nuclear Systems Division of the Atomic Energy Commission.
2. Instrumentation and Controls Division.
3. N. C. Francis, C. R. Lubitz, J. T. Reynolds, C. J. Slavik, and R. G. Stieglitz, "Carbon as a Cross-Section Standard between 0 and 2 MeV," *Neutron Standards and Flux Normalization Symposium, October 21–23 (1970)*, p. 166.
4. S. Cierjacks, P. Forti, D. Kopsch, L. Kropp, J. Nebe, and H. Unseld, *High Resolution Total Neutron Cross Sections between 0.5 to 30 MeV*, USAEC report EURFNR-591 [KFK-1000, EUR-3963, and EANDC(E)-111], Institut fuer Angewandte Kernphysik (June 1968).
5. R. B. Schwartz, R. A. Schrack, and H. T. Heaton II, in *Neutron Cross Sections and Technology, Proceedings of a Conference, Washington, D.C., March 4–7, 1968*, ed. D. T. Goldman, Nat. Bur. Stand. (U.S.) Spec. Publ. 299 (vol. 2), pp. 771–781, U. S. Government Printing Office, Washington, D.C. (1968).

2.39 SIMULTANEOUS DETERMINATION OF FAST-NEUTRON SPECTRA BY TIME-OF-FLIGHT AND PULSE-HEIGHT UNFOLDING TECHNIQUES[1,2]

E. A. Straker[3] T. A. Love
C. E. Burgart[3] R. M. Freestone, Jr.

Proton-recoil spectrometers have frequently been used in the past few years to measure spectra for neutron energies greater than approximately 1 MeV, with the results depending strongly on the adequacy of the response matrix used in unfolding pulse-height spectra. By simultaneously measuring a fast-neutron spectrum by time of flight and by pulse-height unfolding, the adequacy of the response matrix and unfolding code could be determined. Spectra of several

shapes and measurements with different time-of-flight resolutions were used to validate the spectra obtained by unfolding the pulse-height spectrum.

References

1. Funded by the Defense Nuclear Agency under Subtask PE075.
2. Abstract of *Nucl. Instrum. Methods* **97**, 275 (1971); included in last year's annual as abstract of ORNL-TM-3371 (1971).
3. Now at Science Applications, Inc.

2.40 NEUTRON-INDUCED GAMMA-RAY PRODUCTION IN IRON FOR THE ENERGY RANGE $0.8 \leqslant E_n \leqslant 20$ MeV[1,2]

J. K. Dickens G. L. Morgan
F. G. Perey

Cross sections for production of gamma rays due to neutron interactions with iron have been measured as a function of both neutron and gamma-ray energy. Two experimental configurations were used to obtain the data: a NaI-spectrometer system using the Oak Ridge Linear Accelerator as the neutron source and a Ge(Li)-spectrometer system using a pulsed Van de Graaff and the D(*d,n*) reaction as the neutron source. The NaI-spectrometer system is described completely in this report, since it is new. It was used to acquire data for $0.8 \leqslant E_n \leqslant 20$ MeV and $\theta_\gamma = 125°$, which was unfolded to obtain $d^2\sigma/d\omega dE$ values for gamma-ray energies between 0.7 and 10 MeV. The Ge(Li) system was used as before to obtain high-resolution information on the production of discrete-line $d\sigma/d\omega$ values for $4.85 \leqslant E_n \leqslant 9.0$ MeV and $\theta_\gamma = 55$, 75, and 90°. Our data are compared with previously reported experimental data and with the current ENDF/B evaluation. Although there is generally reasonable agreement, important differences among these data are discussed.

References

1. Abstract of ORNL-TM-3850 (to be published).
2. Funded by the Defense Nuclear Agency under Subtask PC101-05.

2.41 GAMMA-RAY PRODUCTION DUE TO NEUTRON INTERACTIONS WITH IRON FOR INCIDENT NEUTRON ENERGIES BETWEEN 0.8 AND 20 MeV: TABULATED DIFFERENTIAL CROSS SECTIONS[1,2]

J. K. Dickens G. L. Morgan
F. G. Perey

Numerical values of differential cross sections for gamma rays produced by neutron reactions with iron have been obtained for neutron energies between 0.8 and 20 MeV. The data are primarily for $\theta_\gamma = 125°$ with supporting data at $\theta_\gamma = 35$, 75, and 90°. These data consist of (*a*) discrete-line values of $d\sigma/d\omega$ for 45 observed transitions due to neutron interactions with natural iron and (*b*) neutron gamma-ray-production group cross-section values of $d^2\sigma/d\omega dE$ for $0.7 \geqslant E_\gamma \leqslant 10.5$ MeV, with gamma-ray group sizes ranging from 20 keV for $E_\gamma \leqslant 1$ MeV to 160 keV for $E_\gamma \leqslant 9$ MeV. The $d\sigma/d\omega$ values were obtained for $4.85 \leqslant E_n \leqslant 9.0$ MeV using a Ge(Li) spectrometer. Additional discrete-line $d\sigma/d\omega$ values for $4.85 \leqslant E_n \leqslant 6.45$ MeV at $\theta_\gamma = 125°$ have been tabulated for 66 observed transitions due to neutron interactions with an iron sample enriched in the isotope ^{54}Fe. The $d^2\sigma/d\omega dE$ values were obtained for $0.8 \leqslant E_n \leqslant 20$ MeV using a NaI spectrometer.

References

1. Abstract of ORNL-4798 (1972).
2. Funded by the Defense Nuclear Agency under Subtask PC101-05.

2.42 THE ^{23}Na($n,x\gamma$) REACTION FOR $4.85 \leqslant E_n \leqslant 7.5$ MeV[1,2]

J. K. Dickens

Interactions of neutrons with sodium have been studied by measuring gamma-ray-production cross sections. Spectra were obtained for incident mean neutron energies $E_n = 4.85$, 5.4, 5.9, 6.45, 7.0, and 7.5 MeV. Data were obtained at angles of 125° and 55° using Ge(Li) detectors. The time-of-flight technique was used to discriminate against pulses due to neutrons and background radiation. Absolute cross sections for production of gamma rays were obtained for the incident neutron energies, and the data have been compared with previous inelastic neutron scattering results and with evaluated cross sections with good agreement. The

spectra were studied for gamma rays which could be associated with deexcitation of nuclear levels having unknown decay modes. Gamma rays were found which have energies appropriate for decay of levels at excitation energies E_x = 5762, 5934, 5967, 6115, 6576, and 6866 keV.

References

1. Abstract of ORNL-TM-3737 (1972).
2. Funded by the Defense Nuclear Agency under Subtask PC101-05.

2.43 NEUTRON ENERGY-DEPENDENT CAPTURE GAMMA-RAY YIELDS IN TANTALUM AND TUNGSTEN[1,2]

K. J. Yost[3] C. Y. Fu[5]
J. E. White[4] W. E. Ford III[4]

Gamma-ray yields as a function of neutron energy for tantalum and tungsten have been generated with a combined experimental and theoretical approach. The results are presented in a format that would facilitate use in coupled neutron–gamma-ray transport calculations. In the case of tungsten, pronounced variations in the capture yield spectra were noticed above 3.0 MeV. On the other hand, only slight variations in the yield spectra were evident for tantalum. The results have been compared with integral gamma-ray yield measurements, and the agreement is favorable.

References

1. Funded by the Space Nuclear Systems of the Atomic Energy Commission.
2. Abstract of *Nucl. Sci. Eng.* **47**, 209 (1972).
3. Purdue University.
4. Mathematics Division.
5. University of Tennessee.

2.44 LEVEL STRUCTURE OF ^{54}Mn[1,2]

J. K. Dickens

Properties of levels in ^{54}Mn have been studied using the ^{54}Fe$(p,n\gamma)^{54}$Mn reaction. These data alone were not sufficient to determine spin and parity assignments, but when correlated with data from prior experimental investigations of the ^{54}Mn nucleus, a set of unique J^π assignments for the lowest five excited states was determined. These assignments are consistent with nearly all presently available experimental data and are in good agreement with shell-model calculations. The level excitation energies and J^π values obtained are: ground-state, 3^+; 54.3 keV, 2^+; 156.9 keV, 4^+; 367.6 keV, 5^+; 407.5 keV, 3^+; and 839.0 keV, 4^+. Transitions from higher lying states were observed and possible J^π values were obtained.

References

1. Abstract of ORNL-TM-3674 (1972).
2. Jointly funded by the Defense Nuclear Agency under Subtask PC101-05 and the Division of Reactor Development and Technology of the Atomic Energy Commission.

2.45 THE TESTING OF ^{238}U SECONDARY GAMMA-RAY PRODUCTION DATA SETS FROM THE POPOP4 LIBRARY[1,2]

W. E. Ford III[3] J. S. Gillen[3]

The uranium nonfission capture, fission capture, and inelastic scattering data sets included in the POPOP4 library of neutron-induced secondary gamma-ray yield and cross-section data were "tested" for use in the preparation of ^{238}U secondary gamma-ray production cross sections (SGRPXS's). The data sets were "tested" over various neutron energy ranges by comparing calculated secondary gamma-ray pulse-height spectra with previously measured spectra resulting from the exposure of a 30-mil-thick depleted uranium foil to bare, thermal, and Cd-, ^{10}B-, (Cd-^{10}B)-, and (Cd-1.377^{10}B)-filtered neutron beams from the ORNL TSR-II reactor.

Uranium-238 nonfission capture data sets 928109, 928112, and 928113 and the total SGRPXS data set 928901 are adequate for use in shielding calculations when used over the neutron and gamma-ray energy ranges for which the data are defined. In the absence of suitable ^{236}U fission capture and inelastic scattering data sets, ^{238}U data sets 925801 and 925301 were found to be adequate for these reactions in the preparation of ^{238}U SGRPXS's.

References

1. Funded by the Space Nuclear Systems Division of the Atomic Energy Commission.
2. Abstract of ORNL-TM-3482 (1972).
3. Mathematics Division.

Table 2.46.1. Comparison of Na (MAT 1156) thermal capture yields with previous results

Data source	Photons per 100 captures in gamma-ray energy range of –															% BE[a]
	0.0–0.5 MeV	0.5–0.98 MeV	0.98–1.0 MeV	1.0–1.5 MeV	1.5–2.0 MeV	2.0–2.5 MeV	2.5–3.0 MeV	3.0–3.5 MeV	3.5–4.0 MeV	4.0–4.5 MeV	4.5–5.0 MeV	5.0–5.5 Mev	5.5–6.0 MeV	6.0–6.5 MeV	>6.5 Mev	
MAT 1156	151.1	43.8	0.0	17.0	9.0	24.8	43.5	17.2	37.2	2.8	0.5	1.1	6.2	22.1	0.0	97
Maerker and Muckenthaler[b]				14.8	11.9	26.9	47.6	14.2	34.0	6.4	2.65	2.2	5.9	21.5	0.0	89[c]
Greenwood[d]	152.2	40.6	0.0	15.0	9.9	21.4	43.6	16.2	36.4	5.25	2.55	1.1	4.9	20.5	0.0	96
Barfield et al.[e]		8	0.0	>1.9	15.1	18.7	26.1	11.0	32.3	4.2	1.8	1.2	4.4	17.8	0.0	68
Groshev[f]	74.0	53.3	0.0	6.5	17.0	29.5	36.5	14.5	42.4	4.7	2.1	0.8	6.0	22.0	0.0	100
Rasmussen, Orphan, et al.[g]				2.8	17.7	34.7	38.0	20.8	44.5	2.7	0.5	1.2	5.2	22.4	0.0	100
POPOP4 110101[h]				14.8	11.9	26.9	47.6	14.2	34.0	6.4	2.65	2.2	5.9	21.5	0.0	90
Reactor Handbook[i]	96 (0–1 MeV)			27 (1–2 MeV)		87 (2–3 MeV)			70 (3–5 MeV)				31 (5.6 MeV)		0.0	110

[a]Na binding energy = 6.96 MeV.
[b]Ref. 3, p. 124; no data given for $E_\gamma \leq 1.0$ eV.
[c]Does not include ~13% contribution from energies below 1 MeV.
[d]Ref. 4, pp. 402–404.
[e]Ref. 4, pp. 402–404; no data given for $E_\gamma < 0.783$ MeV.
[f]Ref. 4, pp. 402–404.
[g]Ref. 5, p. 20; spectrum normalized to binding energy, including contribution from energies below 1 MeV; observed % BE = 83.7.
[h]POPOP4 (refs. 6, 7) data from ref. 3, p. 124; no data given for $E_\gamma \leq 1.0$ eV.
[i]Ref. 8, p. 45.

Table 2.46.2. Comparison of Al (MAT 1135) thermal capture yields with previous results

Data source	Photons per 100 captures in gamma-ray energy range of –																		% BE[a]
	0.5–0.98 MeV	0.98–1.0 MeV	1.0–1.5 MeV	1.5–2.0 MeV	2.0–2.5 MeV	2.5–3.0 MeV	3.0–3.5 MeV	3.5–4.0 MeV	4.0–4.5 MeV	4.5–5.0 MeV	5.0–5.5 MeV	5.5–6.0 MeV	6.0–6.5 MeV	6.5–7.0 MeV	7.0–7.5 MeV	7.5–8.0 MeV	8.0–8.5 MeV	>8.5 MeV	
MAT 1135	0.3	10.0	2.5	7.9	12.8	18.6	13.9	16.5	19.5	20.3	9.5	1.7	7.9	5.3	3.0	26.5	0.0	0.0	99
Hardell et al.[b]	2.4	1.9	7.6	7.0	12.7	20.5	17.3	13.6	16.3	18.8	6.5	2.3	6.4	1.5	0.1	33.0	0.0	0.0	94
Draper et al.[c]	2.7	0.0	7.7	5.4	13.0	10.0	17.0	7.0	15.0	16.0	0.0	0.0	0.0	0.0	0.0	32.0	0.0	0.0	72
Bartholomew et al.[d]						4.6	13.5	6.9	10.7	7.6	3.3	2.5	3.4	1.5	0.5	20.0	0.0	0.0	52
Groshev et al.[e]					8.1	15.0	10.9	11.8	13.1	15.4	5.5	0.8	5.3	1.7	0.0	24.0	0.0	0.0	71
Greenwood et al.[f]	0.0	9.2	4.9	4.3	8.0	0.0	0.0	0.0	0.0	0.0	0.0	0.0	0.0	0.0	0.0	37.0	0.0	0.0	43
POPOP4 130102[g]	0.0	0.0	60.1[h]	88.8[h]	50.7	31.5	27.2	22.9	22.9	22.9	5.4	5.4	5.4	5.9	7.2	7.2	7.2	1.4	145[h]
POPOP4 130103[i]	0.0	0.0	12.9[h]	93.1[h]	14.3	19.9	16.3	14.5	16.4	17.8	7.0	3.1	6.3	2.3	1.1	34.3	0.0	0.0	118[h]
Rasmussen et al.[j]	0.0		6.3	7.8	15.3	15.9	12.8	13.2	17.9	19.2	6.6	1.5	5.4	4.9	3.2	35.5	0.0	0.0	100
Maerker and Muckenthaler[k]	0.0		18.6	10.4	13.1	20.5	15.9	14.3	16.1	17.6	6.8	2.8	6.0	2.2	0.7	32.4	0.0	0.0	95
Reactor Handbook[l]	95 (0.5–1.5 MeV)				69 (2–3 MeV)		62 (2.5–5 MeV)				19 (5–7 MeV)				19 (7–8.5 MeV)				122

[a]Al binding energy = 7.724 MeV.
[b]Ref. 9, pp. 392–400.
[c]Ref. 4, p. 415.
[d]Ref. 4, p. 415; no data given for $E_\gamma < 2.84$ MeV.
[e]Ref. 4, p. 415; no data given for $E_\gamma < 2.12$ MeV.
[f]Ref. 4, p. 415.
[g]POPOP4 data taken from ref. 10, p. 74.
[h]Includes 1.78-MeV activation gamma rays in ^{28}Si following beta decay of ^{28}Al.
[i]POPOP4 data taken from ref. 3, p. 74.
[j]Ref. 5, p. 21; spectrum normalized to binding energy indicates contribution from $E_\gamma < 0.98$ MeV; observed % BE = 83.7.
[k]Ref. 3, p. 74.
[l]Ref. 8, p. 45; top gamma group is 7–9 MeV.

2.46 COMPARISON OF (n_{th},γ) YIELDS FROM THE CURRENT ENDF/B-III DATA WITH PUBLISHED DATA[1]

W. E. Ford III[2]

Due to the infancy of the ENDF/B photon production data and of the processing codes to prepare secondary gamma-ray production cross sections, both the data and the codes are subject to evaluation. As a first check of the latest ENDF/B-III photon production data available as of June 1972, LAPHNGAS was used to calculate the number of photons per thermal-neutron capture (yields) for the 12 ENDF/B-III data sets which have photon production data – ^{1}H (MAT 1148), ^{9}Be (1154), ^{14}N (1133), ^{16}O (1134), ^{23}Na (1156), ^{27}Al (1135), Si (1151), Cl (1149), K (1150), Ca (1152), Fe (1180), and Pb (1136). The calculated yields were then compared with published data. The ENDF/B data were obtained on magnetic tape from the Radiation Shielding Information Center. Examples of the data checks for Na and Al are shown in Tables 2.46.1 and 2.46.2 respectively.

References

1. Funded by the Defense Nuclear Agency under Subtask PE047-02.
2. Mathematics Division.
3. R. E. Maerker and F. J. Muckenthaler, *Gamma-Ray Spectra Arising from Thermal Neutron Captures in Elements Found in Soils, Concretes, and Structural Materials,* ORNL-4382 (August 1969).
4. K. Way (ed.), "Compendium of Thermal-Neutron-Capture γ-Ray Measurements, Part I. $Z \leqslant 46$," *Nucl. Data* 3(4–6) (December 1967).
5. V. J. Orphan, N. C. Rasmussen, T. L. Harper, et al., *Line and Continuum Gamma-Ray Yields from Thermal-Neutron Capture in 75 Elements,* GA-10248 (July 31, 1970).
6. W. E. Ford III and D. H. Wallace, *POPOP4 – a Code for Converting Gamma-Ray Spectra to Secondary Gamma-Ray Production Cross Sections,* CTC-12 (May 1969).
7. W. E. Ford III, *The POPOP4 Library of Neutron-Induced Secondary Gamma-Ray Yield and Cross Section Data,* CTC-42 (1970).
8. E. P. Blizard and L. S. Abbott (eds.), *Reactor Handbook,* vol. III, Part B – *Shielding,* Interscience Publishers, New York (1962).
9. R. Hardell, S. O. Idetjarn, and H. Ahlgren, "Thermal-Neutron Capture Gamma-Rays from the ^{27}Al$(n,\gamma)^{28}$Al Reaction," *Nucl. Phys.* **A126**(2), 392–400 (Mar. 24, 1969).
10. J. H. Ray, E. S. Troubetzkoy, and G. Grochowski, *Neutron Cross Sections of Nitrogen, Oxygen, Aluminum, Silicon, Iron, Deuterium, and Beryllium,* UNC-5139 (November 1965).

2.47 COMPARISON OF AVERAGE SECONDARY GAMMA-RAY PRODUCTION CROSS SECTIONS FROM ENDF/B-III DATA WITH PUBLISHED CROSS SECTIONS[1]

W. E. Ford III[2]

As a means of obtaining a first-order check of the ENDF/B photon production data, LAPHFOR was used to calculate the average secondary gamma-ray production cross sections (SGRPXS's) for Al (MAT 1135), Si (1151), K (1150), Ca (1152), and Fe (1180). These SGRPXS's were then compared with experimentally determined data published by Maerker and Muckenthaler.[3] The experimental SGRPXS's were determined by exposing slabs of the materials of interest to a fission-like spectrum of fast neutrons. This neutron spectrum was obtained by placing a ^{10}B filter over the ORNL TSR-II reactor neutron beam port.

The point ENDF/B photon production data were first reduced to a set of SGRPXS's in 27 neutron fine groups ($0.0 \leqslant E_n \leqslant 14.9182$ MeV) and 13 gamma-ray groups ($1.0 \leqslant E_\gamma \leqslant 7.5$ MeV). For comparison with the published cross sections, the 27 neutron and 13 gamma group cross sections were then reduced to a single broad neutron group structure $1.0 \leqslant E_n \leqslant 14.9182$ MeV and the same 13 gamma groups by using the multigroup representation of the experimental ^{10}B-filtered neutron beam as a weighting function.

As examples of the results, the Al and Fe comparisons are shown in Tables 2.47.1 and 2.47.2. The experimental SGRPXS's are estimated to have an accuracy of ±30%. Also shown in the tables are previously published results from ref. 3.

References

1. Funded by the Defense Nuclear Agency under Subtask PE074-02.
2. Mathematics Division.
3. R. E. Maerker and F. J. Muckenthaler, *Gamma-Ray Spectra Arising from Fast-Neutron Interactions in Elements Found in Soils, Concretes, and Structural Materials,* ORNL-4475 (April 1970).

Table 2.47.1. Comparison of Al (MAT 1135) average secondary gamma-ray production cross sections with published data

Source	Cross section (mb) for gamma-ray energy range of –													
	1–1.5 MeV	1.5–2 MeV	2–2.5 MeV	2.5–3 MeV	3–3.5 MeV	3.5–4 MeV	4–4.5 MeV	4.5–5 MeV	5–5.5 MeV	5.5–6 MeV	6–6.5 MeV	6.5–7 MeV	7–7.5 MeV	Total
MAT 1135	197	34.3	120	35.2	44.4	7.2	6.5	9.6	3.5	2.5	1.8	1.1	0.7	463.8
Maerker and Muckenthaler[a]	181	36.3	102.5	26.3	42.4	8.8	5.8	6.9	4.9	2.0	<1.7	<1.5	<0.3	≲420
Celnik and Spielberg[a]	208	60.8	106	25.5	11.0	4.5	4.7	7.3	2.7	1.1	1.1	0.6	0	433

[a]Ref. 3, p. 57.

Table 2.47.2. Comparison of Fe (MAT 1180) average secondary gamma-ray production cross sections with published data

Source	Cross section (mb) for gamma-ray energy range of –													
	1–1.5 MeV	1.5–2 MeV	2–2.5 MeV	2.5–3 MeV	3–3.5 MeV	3.5–4 MeV	4–4.5 MeV	4.5–5 MeV	5–5.5 MeV	5.5–6 MeV	6–6.5 MeV	6.5–7 MeV	7–7.5 MeV	Total
MAT 1180	259.8	102.2	96.0	86.5	32.2	25.1	3.0	3.3	3.0	2.5	<0.7	<0.6	0.3	615
Maerker and Muckenthaler[a]	278	110	101	74	44	33	8.7	5.6	3.8	2.4	<2.1	<0.6	<1.5	≤665
Celnik and Spielberg[a]	307		198		78		14		8.5		2.0		0.4	608

[a]Ref. 3, p. 44.

2.48 A CALCULATION OF NEUTRON ENERGY-DEPENDENT CAPTURE GAMMA-RAY YIELD SPECTRA FOR IRON AND COMPARISONS WITH EXPERIMENTS[1,2]

J. E. White[3] C. Y. Fu[4]
K. J. Yost[5]

The spin-dependent gamma-ray cascade model DUCAL has been applied to calculate neutron energy-dependent capture gamma-ray spectra in iron. There are significant variations in the capture gamma-ray yield spectra with neutron energy. The results have been compared with a series of integral gamma-ray yield measurements above 1 MeV, and the agreement found was reasonably good. The yield data are presented in a neutron energy format that would facilitate the preparation of the capture component of the secondary gamma-ray-production cross sections in iron.

References

1. Funded by the Defense Nuclear Agency.
2. Abstract of ORNL-TM-3442 (1971); also submitted for journal publication.
3. Mathematics Division.
4. University of Tennessee.
5. Purdue University.

2.49 THE DEVELOPMENT AND APPLICATION OF A DISCRETE ORDINATES ADJOINT DIFFERENCE METHOD FOR ONE-DIMENSIONAL SHIELD WEIGHT OPTIMIZATION[1,2]

R. L. Childs[3]

An improved method for the weight optimization of one-dimensional layered shields has been developed. The radiation transport problem is represented by coupled neutron–gamma-ray discrete ordinates transport calculations. In the optimization procedure, forward and adjoint calculations are performed for the initial shield design. An approximate form of the perturbed adjoint is used in the adjoint difference approach to determine the effect of shield changes, and a simple closed form optimization algorithm is used as in the ASOP code.

Three realistic shield optimization problems were solved to demonstrate the capabilities of the method. A comparison between the results obtained using this method and the ASOP code showed the agreement of the two methods to be very good and the new method to be significantly faster.

References

1. Funded by the Space Nuclear Systems Division of the Atomic Energy Commission.
2. Thesis to be submitted by R. L. Childs to the University of Tennessee, Department of Nuclear Engineering.
3. Mathematics Division.

2.50 MORSE MONTE CARLO SHIELDING CALCULATIONS FOR THE ZIRCONIUM HYDRIDE REFERENCE REACTOR[1-3]

C. E. Burgart[4]

A comparison of DOT-SPACETRAN transport calculations and MORSE Monte Carlo calculations of a lithium hydride and tungsten shield for a SNAP reactor has been performed. Transport of both neutrons and gamma rays was considered. Several forms of importance sampling were utilized in the MORSE calculations. Quantities internal to the shield, as well as dose at several points outside of the configuration, were in satisfactory agreement with the DOT calculations of the same.

References

1. Funded by the Space Nuclear Systems Division of the Atomic Energy Commission.
2. Abstract of ORNL-TM-3366 (1971).
3. Presented at National Symposium on Natural and Manmade Radiation in Space, Las Vegas, Nev., Mar. 2–5, 1971.
4. Now at Science Applications, Inc.

2.51 THE RELATIVE IMPORTANCE OF NEUTRON CAPTURE AND INELASTIC-SCATTERING INTERACTIONS TO THE SECONDARY GAMMA-RAY DOSE TRANSMITTED THROUGH LAMINATED TUNGSTEN AND LITHIUM HYDRIDE SNAP REACTOR SHIELDS[1,2]

J. V. Pace III[3] F. R. Mynatt
L. S. Abbott

Calculations have been made of the spatial and neutron energy dependence of the neutron captures and inelastic scatterings that contribute to the secondary gamma-ray dose transmitted through a laminated tungsten (Hevimet) and lithium hydride shield adjacent to a SNAP reactor. Four shield configurations were considered: a 5-cm-thick slab of Hevimet alone, the Hevimet followed by a 30.5-cm thickness of LiH, the

Hevimet preceded by the LiH, and the Hevimet preceded and followed by the LiH. For each configuration both a forward calculation and an adjoint calculation were performed with the one-dimensional discrete ordinates code ANISN, the forward calculation yielding neutron fluences within the shield and the adjoint calculation yielding probabilities that a gamma ray of a given energy originating at a given position in the shield would contribute to the transmitted dose. The results from the two calculations were convoluted with gamma-ray production data to determine the spatial distribution of the neutron interactions contributing to the exit secondary gamma-ray dose. The calculations show, as was expected, that in each configuration essentially all of the exit secondary gamma-ray dose is due to neutron interactions in the Hevimet, with the contribution from the last half of the Hevimet being a factor of 3 to 5 higher than that from the first half. When LiH follows the Hevimet, 80% of the exit gamma-ray dose is produced by neutron captures, with nearly half of them occurring at neutron energies between 3.06 eV and 0.111 MeV. When LiH does not follow the Hevimet, the importance of neutron inelastic scatterings approaches that of the captures.

References

1. Funded by the Space Nuclear Systems of the Atomic Energy Commission.
2. Abstract of ORNL-TM-3270 (CTC-41) (1972).
3. Mathematics Division.

2.52 CALCULATED PERTURBATIONS IN THRESHOLD FOIL MEASUREMENTS DUE TO NEUTRON INTERACTIONS IN B_4C SHELLS[1,2]

W. E. Ford III[3] J. S. Gillen[3]

Calculations were made to determine expected perturbation effects to the measured neutron flux in B_4C shielded threshold foils resulting from neutron interactions in the B_4C. Results indicated that there is a significant increase in the measured flux below the source energy of monoenergetic neutron beams due to scattering.

The activities in a series of threshold foils encased within a B_4C shell were calculated for exposure of the shell to monoenergetic 13.57- and 1.01-MeV neutron beams incident at 0° with respect to the shell axis. Calculations were also made to determine if there would be a significant change in the measured threshold foil activities if the detector were inadvertently positioned "upside down" (beam incident at 180°) during an experiment. The difference between the 0° and 180° activities was not sufficient to distinguish which end of the detector was oriented toward the beam.

References

1. Funded by the Army Nuclear Defense Laboratory.
2. Abstract of ORNL-TM-3519 (1971).
3. Mathematics Division.

3. Radiation Shielding Information Center

3.1 INTRODUCTION, FUNCTIONS, AND SUMMARY OF OPERATIONS[1]

Betty F. Maskewitz
R. W. Roussin
F. S. Alsmiller
C. M. Anthony
J. Gurney
H. R. Hendrickson
M. W. Landay
J. B. Wright
D. K. Trubey
F. H. Clark
R. T. Santoro
H. E. Comolander
A. B. Gustin
V. Z. Jacobs
M. B. Nicholson
J. D. Needham

The Radiation Shielding Information Center (RSIC) continues to serve the international scientific community. Functioning as a scientific institute, it serves those engaged in research and development for the design of shields that provide protection from biological and physical damage due to penetrating ionizing radiation. The Center is sponsored by the Atomic Energy Commission (AEC), the Defense Nuclear Agency (DNA), and the National Aeronautics and Space Administration (NASA). In serving the interests of these agencies, RSIC is concerned with the shielding of radiation from nuclear reactors, nuclear weapons, radioisotopes, accelerators, and radiation present in space.

3.1.1 The RSIC Directory

The RSIC Storage and Retrieval Information System (SARIS)[2] is used routinely for producing lists of persons with particular interests and mailing labels for the RSIC distribution, keeping current a customer address and telephone directory and an inventory of the codes and data collections.

The directory contains over 1800 names and addresses of persons and organizations interested in shielding. About two-thirds are persons who receive the monthly newsletter and optionally receive other material such as the Selective Dissemination of Information (SDI), which provides computer-printed abstracts of added literature to those interested in particular subjects. The number of persons has been increasing slowly, even though many additions are made, since names of persons no longer interested are removed each year.

3.1.2 Literature Review and Indexing

The RSIC monthly newsletter lists the current accession of literature in the process of review. During the year, approximately 947 papers, reports, and books on reactor and weapons shielding and 217 on space and accelerator shielding were announced and subsequently reviewed. More than half of these were indexed according to the RSIC subject category lists and entered into the SARI system. An additional 314 documents describing computer codes for use in shielding research were reviewed, indexed, and announced in the newsletter.

3.1.3 Selective Dissemination of Information (SDI)

The number of persons taking advantage of the SDI service increased during the year. Currently, 376 profiles are serviced through SARIS, an increase of 42% during the year. An additional 161 retrospective searches were performed on requests received in the report period.

3.1.4 Computer Information Storage and Retrieval Development

The RSIC Storage and Retrieval Information System (SARIS) has been fully operational since 1969. It is a batch-type program running at the Oak Ridge Computing Technology Center. The data base is stored on tape. Input consists of punched cards or Magnetic Tape Selectric Typewriter (MT/ST) cartridge tapes. Programming is under way to implement several improvements to make file maintenance and search input preparation easier. In addition, key term descriptors and text information will be added to the customer data as described in ref. 3.

3.1.4.1 Computer terminal operations. An IBM-2741 communication terminal was installed to gain experience in on-line data creation, editing, and retrieval. The Conversational Remote Batch Entry (CRBE) system, operating normally on the ORNL IBM-360/75 computer, allows the terminal user to create data, edit it, store it on disk, and submit jobs. The objective is to increase efficiency by reducing the various typing and keypunching operations involved in literature control (card files, records, and ordering forms) and computer input. To this end, citations of the literature ordered since January 1972 were entered into CRBE files, corrected as necessary, printed out for the newsletter accession list, indexed by the BIRS program (see below), filed on longer-term tape storage, and processed for ADSEP input (see below). Data on the RSIC computer code collection were also entered and indexed by BIRS.

The terminal has a typewriter-like character set, which makes the creation of upper- and lower-case text information easy to implement.

Other terminals are under consideration for RSIC use. In particular, a terminal which can access both the IBM 360 and the PDP 10, with its time-sharing capabilities, is desirable.

3.1.4.2 BIRS program. The Michigan State University Basic Information Retrieval System (BIRS),[4] version 4.0, is a general-purpose file maintenance, indexing, and retrieval system, having more than 100 commands available which control the operations. The program and information data files are stored on private disk. BIRS jobs are easily set up and submitted through CRBE, normally processing text data stored on CRBE disk files. The main use of BIRS by RSIC is to produce indices to newly created data or other files not available in the SARIS data base. It will not replace SARIS because of the many SARIS features which continue to be needed, but it is useful as an additional tool. It uses a delimiter to identify data elements and therefore can process the data in the ORNL "general external format."[5]

3.1.4.3 ORCHIS project. The ORNL Mathematics Division, supported by various programs, is developing a comprehensive information system called ORCHIS (Oak Ridge Computerized Hierarchical Information System).[5] Several components of the system are being evaluated for possible RSIC routine use. For example, the cathode ray tube RECON terminal, located at the computer facility, is used to search *Nuclear Science Abstracts* when searches are required such as those in areas at the periphery of RSIC scope. By another ORCHIS program, the *Nuclear Science Abstracts* tapes are processed routinely to provide RSIC (and others) with citations of interest.

The ORLOOK program offers the capability of using a deallocated CRBE terminal for conversational search of text. Text in "generalized external format" is processed by the ADSEP[6,7] program for on-line data cell storage. Experience will be obtained in the coming year in the use of this program, which could give immediate response to search questions and the possibility of sharpening one's questions for more effective results.

3.1.5 Computer Code Collections

The computer code collection continues to grow. Those packaged as CCC's[8] are defined to be shielding codes, and the PSR's[9] are defined to be useful peripheral-to-shielding routines. Since last reporting, 29 new CCC packages and 12 new PSR packages have been added to the collection. In addition, 26 new hardware versions to existing code packages have been returned to RSIC, tested, and packaged, and updates have been made to a total of 28 code packages.

The term "code package" is used by RSIC to describe a miscellaneous grouping of materials which, when interpreted and used correctly in connection with a digital computer, enables the scientist-user to solve technical problems in the area for which the material was designed. In general, an RSIC "code package" consists of: (*a*) written material – reports, instructions, data sheets, listings of data, and any other useful material; (*b*) other materials – IBM card decks, or, more often, a reel of magnetic tape on which the IBM source card decks, sample problem input, including any available libraries of data, and the BCD output from the sample problem are written. Not only is the main code of interest included in the package, but any auxiliary routine which has been made available to RSIC is also included. Included in the 178 computer code packages (CCC's) are 725 separate stand-alone computer codes, and in the 37 peripheral-to-shielding packages (PSR's) are 79 separate computer codes.

3.1.6 The Data Library Collection (DLC)

Two new data libraries were added, and several existing ones were updated and improved during the past year. A total of 176 separate shipments of these data sets were made, and abstracts of the current series were published.[10]

The philosophy behind the packaging and distributing of these data libraries is to preserve and make available

in an easily usable form data which may be useful to those utilizing or performing radiation transport calculations. Since this usually involves the use of large computer programs, several of these libraries are multigroup cross sections in the format utilized by many such programs. In addition, a data library may consist of voluminous results from particular calculations or input data that can be used to reproduce bench-mark calculations.

Data libraries on magnetic tape or in other forms are packaged, maintained, and distributed in a manner analogous to computer code distribution. Each library carries a Data Library Collection (DLC) number and is packaged as a unit. In addition to the data, the package contains a handling program and documentation, including an RSIC-prepared abstract. Additions to and revisions of the DLC's are announced in the RSIC newsletter.

During the next year it is expected that we will acquire and package neutron and gamma-ray cross-section data sets which have proved useful for analyzing bench-mark experiments in important shielding materials, such as nitrogen, oxygen, sodium, and iron.

3.1.7 Defense Nuclear Agency Cross-Section Library[11]

RSIC began serving as a depository for the DNA cross-section data, which is a working library (in ENDF format)[12] subject to modification and revision at as fast a rate as necessary. The key to this approach is the selected evaluator, a person responsible who will authorize and document changes in evaluations for particular elements. The evaluations are for those materials of interest to DNA, and emphasis is apt to be placed on neutron energies up to 20 MeV and on secondary gamma-ray production.

The clearinghouse for the program is RSIC. Initial versions of evaluations are received, processed through checking codes to eliminate obvious format errors, and modified as necessary in collaboration with the evaluator. Next, DNA Phase I data testing is performed, whereby selected reviewers will be provided with listings, output from checking codes, graphics, etc., and asked to review the data and feed back their comments. These will be relayed to the evaluator, and, upon his instruction, appropriate changes will be made.

The data, along with available documentation, are distributed upon request. The users are asked to feed back any comments they have through using the data.

The official DNA library will be maintained at RSIC. Changes to it will be initiated only by the evaluator, and each change will be documented so that users can at any time refer to an identifiable data set when reporting results of their calculations.

Because the data are apt to be revised with some frequency, each evaluation is designated by a DNA MAT number and a MOD number. The DNA MAT number is equal to the ENDF MAT number plus 3000 for those evaluations which are submitted for inclusion in the ENDF/B library. The MOD number designates the number of times the DNA evaluation has been modified since its initial availability through RSIC.

The current contents of the DNA library are listed in Table 3.1.1. All these were incorporated in the ENDF/B Version III Library except tantalum, which was not available prior to the release of ENDF/B-III. Note that ENDF/B-III has earlier versions for calcium and lead (MOD 1) than are now currently in the DNA library.

Table 3.1.1. Contents of the Defense Nuclear Agency working cross-section library

Material	Evaluators	DNA MAT	MOD	Date of MOD
Nitrogen	Young, Foster – LASL	4133	3	2-72
Oxygen	Young, Foster – LASL	4134	1	2-72
Aluminum	Foster, Young – LASL	4135	2	2-72
Lead	Fu, Perey – ORNL	4136	2	4-72
Hydrogen	Stewart, LaBauve, Young – LASL	4148	1	2-72
Silicon	Drake, Kinsey – BNL	4151	1	2-72
Calcium	Fu, Perey – ORNL	4152	2	5-72
Beryllium	Howerton, Perkins – LLL	4154	0	2-72
Sodium	Paik, Pitterle, Perey – WARD, ORNL	4156	0	2-72
Tantalum	Howerton, Perkins, MacGregor – LLL	4179	0	2-72
Iron	Penny, Kinney, Wright, Perey, Fu – ORNL	4180	0	3-72

3.1.8 Shielding Subcommittee, Cross-Section Evaluation Working Group

RSIC continues to collaborate with the National Neutron Cross Section Center (NNCSC) at Brookhaven National Laboratory (BNL) and the Cross Section Evaluation Working Group (CSEWG) Shielding Subcommittee. The Center's role in this activity is to assist in the acquisition, check-out, and review of "shielding" cross sections in ENDF format which will ultimately be placed in the ENDF/B file. In this context, "shielding" cross sections are evaluations performed in the shielding, radiation effects, or weapons community which are likely to have an emphasis on gamma-ray production cross sections, gamma-ray interaction cross sections, and neutron cross sections in the energy range of interest for shielding with detailed energy and angular distribution resolution.

Twelve evaluations were received by RSIC during the year, processed through checking codes, modified as necessary, and forwarded to NNSCS for inclusion in the ENDF/B library. Version III of ENDF/B, which was distributed in January 1972, thus contained, for the first time, evaluations including secondary gamma-ray production data. A list of these is given in Table 3.1.2.

Future efforts of the CSEWG Shielding Subcommittee will focus on recommending appropriate experiments for Phase II Integral Data Testing of the "shielding" evaluations. Other efforts will involve reviewing photon interaction libraries, devising formats for charged-particle- and gamma-ray-induced reactions, and improving and expanding the ENDF/B library to meet the needs of shielding calculations.

Table 3.1.2. Evaluations in ENDF/B Version III which contain gamma-ray production data

Material	ENDF/B MAT
Nitrogen	1133
Oxygen	1134
Aluminum	1135
Lead	1136
Hydrogen	1148
Chlorine	1149
Potassium	1150
Silicon	1151
Calcium	1152
Beryllium	1154
Sodium	1156
Iron	1180

3.1.9 ORNL Cross Section Steering Committee (ORNL-CSSC)

RSIC plays an active role in the ORNL Cross Section Steering Committee (CSSC), which has as its charter the promotion of information exchange and the reduction of duplication of effort in manipulating and using cross-section data at ORNL. Its membership consists of personnel from the Mathematics, Neutron Physics, and Reactor Divisions. The membership includes ORNL representatives to CSEWG, and thus a substantial portion of the work sponsored by CSSC is related to tasks for CSEWG, described in a following section.

RSIC acts as the local clearinghouse for all ENDF data and codes distributed to ORNL by NNCSC. The Center also promotes, through CSSC, the various computer programming efforts which are useful to the program of the Shielding Subcommittee of CSEWG.

For example, the ENDF checking codes PLOTFB[13] and CHECKER[13] were programmed to accept data in the gamma-ray production files used by ENDF/B.

3.1.10 Annual Summary of Operations and Services

During the 12 months of 1971 a total of 2313 separate letters/telephone calls of request were logged into the Center – an average of 193 per month – resulting in 5766 separate actions to satisfy the requests. General information requests accounted for 847 of the communications, while 1466 were concerned with information about and requests for data and/or code packages.

RSIC shipped 636 separate code packages (including full documentation) – an average of 2.5 per working day – and 176 separate data library packages – an average of 3.5 data shipments per work week. Additional shipments of 79 sets of updating material for computer codes were made during the year.

Other items mailed to requesters include: 455 RSIC publications, 1459 shielding documents (1196 code documents not counted in code package shipments), and 117 packets of RSIC introductory literature.

A total of 136 calls were serviced in which staff members assisted a requester as he was learning to use a specific program. Research was done and advice and descriptive material were given to help in the selection of computer codes to fit the requester's problem and his local computer environment in 1021 instances.

In 1565 instances, time was spent by RSIC staff members in assisting the requester to solve his shielding problem – giving general advice and counsel. Of these, at least 461 research efforts were nontrivial, requiring technical expertise, considerable time, and occasionally

a need to use the computer to find solutions to the requester's difficulty.

During CY 1971, RSIC performed 122 separate data-handling activities involving the use of the computer in connection with the National Neutron Cross Section Center (NNCSC) and the Shielding Subcommittee of the Cross Section Evaluation Working Group (CSEWG). No effort was made to record and analyze RSIC's clearinghouse activities associated with the DNA Cross Section Working Library.

In addition to the attendance at the DNA-sponsored air transport seminar-workshop held during the year, RSIC received 140 visitors for orientation and/or to use the Center's facilities. Twenty-five visitors were from foreign countries: nine from Germany; one each from Brazil, India, Sweden, Japan, Hungary, Denmark, Italy, and Australia; one from IAEC, Vienna; one from ENEA in Paris and three from the ENEA Computer Programme Library in Italy; and three from EURATOM, Italy.

Most recent statistics (1972) indicate that RSIC processes about 200 letters of request per month on an average, requiring about 460 separate actions to satisfy the requests. The actions range from the trivial – for example, mailing a document – to sending a code and/or a data package, to requests for technical information requiring time spent by a senior technical research staff member, and sometimes requiring the use of a computer to do calculations. On an average, 2.5 code packages are currently shipped each working day, and approximately three data packages per week.

Two areas given priority within RSIC operations are (1) effective and expeditious review of all relevant published technical information, and selection and processing of that pertinent to shielding research or design; and (2) quick response to customer inquiry with a serious effort to supply the best information and advice available.

3.1.11 Shielding Standards

Previous work on shielding standards has been associated with the American Nuclear Society (ANS) Standard Subcommittees ANS-6, Shielding, and ANS-10, Mathematics and Computation. The goal of ANS-6 is to establish standards in connection with radiation shields, to provide shielding information to other standards groups, and to prepare recommended sets of shielding data and test problems. Previous work has been reported in ref. 14.

In February, D. K. Trubey was appointed chairman of ANS-6. The immediate work was to reorganize the committee, since nearly all previous members have resigned.

In April, the American Nuclear Society forwarded to the American National Standards Institute (ANSI) the proposed standard "Program for Testing of Biological Shielding in Nuclear Reactor Plants" (ANS-6.3). The ANSI Nuclear Technical Advisory Board Committee N-18, Nuclear Design Criteria, approved the proposed standard in late 1971 with no negative ballots. In response to N-18 comments, a revised draft was prepared in May and forwarded to ANS.

Comments by ANS-6 on the draft standard "Concrete Radiation Shields" (ANS 11.13) were forwarded to the standard writer for use in preparing a revision.

The purpose of ANS-10 is to recommend practices which will facilitate the exchange of computer programs among the users and simplify the conversion of existing programs at a given laboratory when there is a change in computers. Specifically, the intent is to provide standards for documentation, programming practices, and test problems. An RSIC staff member has worked with this effort since its inception. Two working group meetings were held during the year. ANS-STD.3-1971, "Recommended Programming Practices to Facilitate the Interchange of Digital Computer Programs," was published. Progress was made toward revising and updating ANS-STD.2-1967, "A Code of Good Practices for the Documentation of Digital Computer Programs."

Work has also begun in preparing a standard on LMFBR radiation analysis which would document the experience gained in the analysis of the Fast Test Reactor (FTR), especially by the ORNL Neutron Physics Division. This work has initially taken the form of writing a proposal to prepare the standard. The proposal will briefly outline the problems of radiation analysis and describe recommended practices and data which have been developed to deal with these problems.

References

1. Work partially supported by the Defense Nuclear Agency (DNA) under Subtask PB052-03 and by National Aeronautics and Space Administration (NASA) under NASA Order H-79272A.

2. J. G. Jones, D. K. Trubey, and J. Gurney, *RSIC Storage and Retrieval Information System (SARIS)*, ORNL-TM-2719 (1969); J. G. Jones and R. O. Green, *Radiation Shielding Information Center Program Set-Up Instruction Manual*, CTC-INF-1017 (1971); and J. G. Jones, R. O. Green, and S. L. Young, *RSIC User Documentation*, CTC-48 (1971).

3. D. K. Trubey, J. G. Jones, and R. O. Green, Jr., *The 1971 EIS Directory Program: A Synopsis,* ORNL-EIS-71-4 (1972).

4. John F. Vinsonhaler, John M. Hafterson, and Stuart W. Thomas, Jr. (eds.), *BIRS Technical Manual, Basic Information Retrieval System,* vols. I–XII, Information Systems Laboratory, College of Education, Michigan State University (1970).

5. C. J. Oen, N. F. Sollins, and D. K. Trubey, *Guide to the Generalized Bibliographic Format for the Environmental Information System,* ORNL-EIS-71-3 (1972).

6. A. A. Brooks, *ADSEP – an Automated Data Set Editing Program,* CTC-34 (May 1970).

7. A. A. Brooks, *ADSEP Text Input,* ORNL-CF-71-9-3 (September 1971).

8. Betty F. Maskewitz, *Abstracts of Digital Computer Code Packages Assembled by the Radiation Shielding Information Center,* ORNL-RSIC-13, vols. I, II, and III.

9. Betty F. Maskewitz, *Abstracts of the Peripheral Shielding Code Packages Assembled by the Radiation Shielding Information Center,* ORNL-RSIC-31 (1971).

10. R. W. Roussin, *Abstracts of the Data Library Packages Assembled by the Radiation Shielding Information Center,* ORNL-RSIC-30 (Vol. I) (March 1972).

11. R. W. Roussin, *Defense Nuclear Agency Working Cross Section Library: Description and Contents,* ORNL-RSIC-34, to be published.

12. M. K. Drake (ed.), *Data Formats and Procedures for the ENDF Neutron Cross Section Library,* BNL-50274 (ENDF-102, Vol. I) (October 1970); and Donald J. Dudziak (compiler), *ENDF Formats and Procedures for Photon Production and Interaction Data,* LA-4549 (ENDF-102, Rev., Vol. II) (July 1971).

13. Odelli Ozer (ed.), *Description of the ENDF/B Processing Codes and Retrieval Subroutines,* BNL-50300 (ENDF-110) (September 1967) (revised April 1969, September 1970, and June 1971).

14. H. Clyde Claiborne, D. J. Dudziak, and N. M. Schaeffer, *Activities of the ANS-6 Subcommittee on Radiation Shielding Standards,* ORNL-TM-3251 (1970).

3.2 SHIELDING OF MANNED SPACE VEHICLES AGAINST PROTONS AND ALPHA PARTICLES[1]

R. G. Alsmiller, Jr. H. C. Claiborne
R. T. Santoro J. Barish[2]

Preparation of a space shielding handbook, which will summarize the available information on the shielding of manned space vehicles against protons and alpha particles in space, has continued. The handbook is intended primarily for nonexperts and is expected to be most useful to mission planners who must decide with little effort whether a radiation hazard is likely to exist during a specific mission. It will also serve as a useful starting point for obtaining more adequate information about the shielding required when a radiation hazard is thought to exist on a specific mission.

Many space shielding calculations have been published and are available, but to ensure uniformity and consistency throughout the handbook, a large majority of the calculated results that will be contained in the handbook are being generated specifically for the handbook. The calculational model that is being used is that of a 300-cm-ID spherical shell shield of a specified material and thickness with a 30-cm-diam tissue sphere at the center. This configuration simulates only very approximately a manned space vehicle, but it does serve to illustrate many of the significant features in spacecraft shield design.

Typical results for inclusion in the handbook are shown in Fig. 3.2.1. In the figure the dose-equivalent rate as a function of depth in the tissue sphere is shown as a function of shield thickness for a variety of incident Van Allen belt spectra, shield thicknesses, and shield materials. The incident spectra in all cases correspond to spacecraft in circular orbits with specific altitudes and orbital inclinations. Calculated results obtained with two different transport codes, NMTC[3,4] and MEVDP,[5] are shown in the figure. The nucleon-meson transport code NMTC takes into account the production and transport of all particles produced by nuclear reactions and is designed to treat the shielding problem as accurately as possible. Results obtained with NMTC have been compared with a variety of experimental data, and, in general, good agreement has been attained.[4,6–8] The code MEVDP neglects particle production from nuclear reactions and makes other simplifying assumptions. It is designed primarily to carry out space shielding calculations with very complex spacecraft geometries. In general, the MEVDP results are in good agreement with the NMTC results, and therefore the approximations used in MEVDP are quite justified. It is perhaps worth noting, however, that for the thickest shield considered (75 g/cm^2 of polyethylene) MEVDP gives an overestimate of the dose-equivalent rate.

References

1. Research funded by the National Aeronautics and Space Administration under Orders H-38280A and H-79272A.

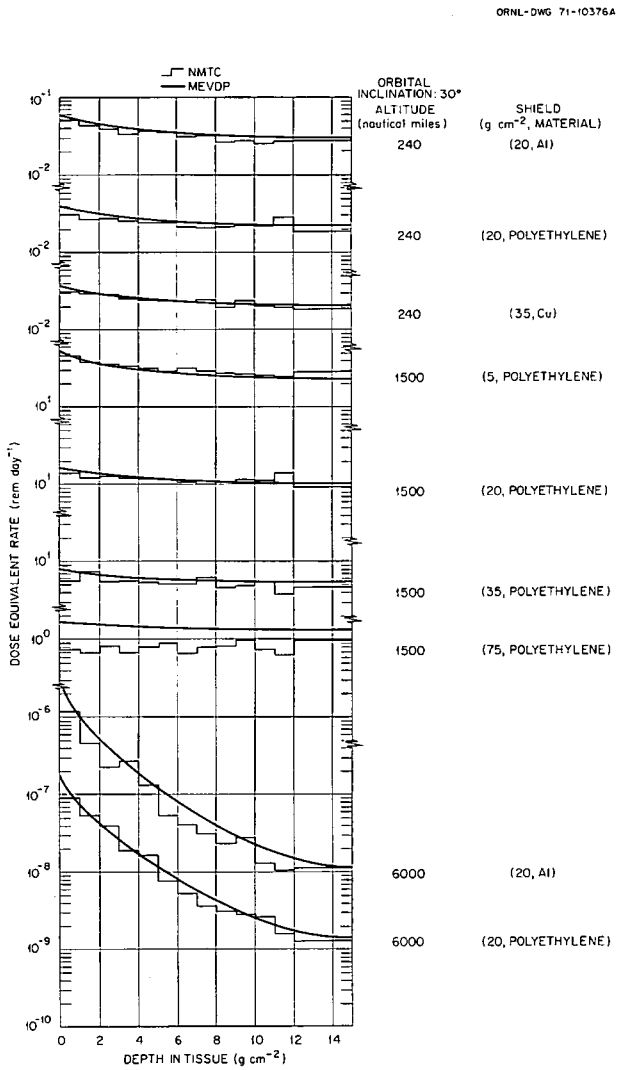

Fig. 3.2.1. Dose-equivalent rate vs depth in tissue for Van Allen belt proton spectra isotropically incident on spherical shell shields of various thicknesses.

2. Mathematics Division.

3. W. A. Coleman and T. W. Armstrong, "The Nucleon-Meson Transport Code NMTC," ORNL-4606 (1970); code abstract, *Nucl. Sci. Eng.* **43**, 353–54 (1971).

4. W. A. Coleman and R. G. Alsmiller, Jr., *Nucl. Sci. Eng.* **34**, 104 (1968).

5. B. Liley and S. C. Hamilton, *Modified Elemental Volume Dose Program (MEVDP)*, AFWL-TR-69-68, Space Division, North American Rockwell Corp. (1971).

6. T. W. Armstrong and R. G. Alsmiller, Jr., *Nucl. Sci. Eng.* **33**, 391 (1968).

7. T. W. Armstrong and B. L. Bishop, *Rad. Res.* **47**, 581 (1971).

8. T. W. Armstrong and K. C. Chandler, *Monte Carlo Calculations of the Dose Induced by Charged Pions and Comparison with Experiment*, ORNL-TM-3678 (1972); submitted for journal publication.

3.3 EXTENSIONS TO PLOTFB, A PLOTTING PROGRAM FOR ENDF/B DATA

R. Q. Wright[1] J. L. Lucius[1]

PLOTFB, a plotting program for ENDF/B cross-section data, has been extended and improved. The program now processes the photon production data (ENDF/B files 12–16), and the plotting of ENDF/B file 5 (secondary energy distributions) has been implemented. A modified version of the program, PLOTFC, utilizes the Calcomp pen plotter (rather than the CRT). The programs have been forwarded to the National Neutron Cross Section Center (NNCSC).

Reference

1. Mathematics Division.

3.4 MODIFICATION OF PLOTFB FOR DNA PHASE I DATA TESTING PROGRAM[1]

J. E. White[2] R. Q. Wright[2]

The PLOTFB program has been extended and improved for the Defense Nuclear Agency (DNA) Phase I data testing of its working cross-section library. Plots of evaluated data of interest to DNA are needed to assist various reviewers assessing the completeness of an evaluation. The primary aim of the present work was to plot quantities more directly related to experimental results. As a consequence, the following features have been incorporated in the program:

1. The differential cross section is now plotted from ENDF/B files 4, 5, 14, and 15. The units used are millibarns per steradian and millibarns per keV.
2. The reaction Q value has been added to the heading in file 3.
3. An identification number is now associated with each plot.
4. The simple fission spectrum (LF=7) has been included in the file 5 routines.
5. Tick marks are made on all axes.

6. For logarithmic plots of matrices containing zeros, the number of decades required is minimized to best represent the nonzero elements. (The previous version arbitrarily replaced the zeros with 10^{-10}.)
7. A modification number is used to distinguish between different versions of the same ENDF/B evaluation.

In addition to its normal role, the modified version of PLOTFB has proven to be a very useful tool in spotlighting inconsistencies in the neutron energy representation for threshold reactions in files 4 and 5.

References

1. Work funded under Defense Nuclear Agency (DNA) Subtask PB052-03.
2. Mathematics Division.

3.5 COUPLED CALCULATIONS OF THE TRANSPORT OF NEUTRONS AND SECONDARY GAMMA RAYS THROUGH CONCRETE FOR NEUTRON SOURCES WITH ENERGIES BETWEEN 15 AND 75 MeV[1]

R. W. Roussin R. G. Alsmiller, Jr.
J. Barish

Coupled neutron and gamma-ray transport calculations have been performed for monoenergetic neutrons normally incident on an infinite slab shield of concrete with 5.5% water content by weight. The production of gamma rays from interactions of neutrons with energy greater than 15 MeV was ignored. For the 50- and 75-MeV incident neutron energies, the gamma-ray dose equivalent was found to be no more than 5% of the total dose equivalent. For the 15- and 25-MeV incident neutron energies, the gamma-ray dose equivalent dominates at greater depths into the slab. A conservative estimate of the effect of including gamma rays produced by interactions of neutrons having energies greater than 15 MeV indicates that the calculated total dose equivalent would increase by less than 6%.

References

1. Abstract of paper submitted for publication in *Nuclear Engineering and Design;* also abstract of report entitled *Shielding against Neutrons in the Energy Range 15 to 75 MeV,* ORNL-TM-3659 (December 1971).
2. Mathematics Division.

3.6 REVISIONS TO UKE – A COMPUTER PROGRAM FOR TRANSLATING NEUTRON CROSS-SECTION DATA FROM THE UKAEA NUCLEAR DATA LIBRARY TO THE EVALUATED NUCLEAR DATA FILE

R. Q. Wright[1]

The UKE[2] program, which translates neutron cross-section data from the UKAEA Nuclear Data Library to the Evaluated Nuclear Data File, has been extensively revised to conform with the ENDF/B version II format. The translation of some of the United Kingdom Atomic Energy Authority Nuclear Data Library secondary energy distributions was also revised. Translation of 91 materials in the UK library to the ENDF/B version II format was completed and transmitted to the National Neutron Cross Section Center. Of particular interest at ORNL were the ^{6}Li and ^{7}Li cross sections, because these materials were not available in the officially released ENDF/B-II library.

References

1. Mathematics Division.
2. R. Q. Wright, S. N. Cramer, and D. C. Irving, *UKE – a Computer Program for Translating Neutron Cross Section Data from the UKAEA Nuclear Data Library to the Evaluated Nuclear Data File Format,* ORNL-TM-2880 (March 1970).

3.7 REVISION TO VIXEN – A COMPUTER PROGRAM FOR PERFORMING PHYSICS CHECKS OF GAMMA-RAY PRODUCTION DATA IN ENDF FORMAT

J. B. Wright R. Q. Wright[1]
W. E. Ford III[1]

The VIXEN[2] computer code was obtained from Los Alamos and made operational at ORNL for use in Phase I data testing by RSIC in conjunction with both the DNA Working Cross Section Library and the ENDF/B Library. The VIXEN code checks data files in ENDF format for consistency and physical realism. Improvements were made to allow processing of more than one evaluation in a single run. In the course of utilizing the code, several errors were discovered and corrected.

References

1. Mathematics Division.
2. D. J. Dudziak and J. M. Romero, *VIXEN, a Code to Check Physical Consistency of Photon-Production Data in Revised ENDF Format,* LA-4739 (ENDF-155) (October 1971).

3.8 CDC VERSION OF SUPERTOG, A MULTIGROUP NEUTRON CROSS-SECTION GENERATOR

R. Q. Wright[1]

SUPERTOG,[2] a multigroup neutron cross-section generator, was implemented on a CDC-6400 computer at Kaman Nuclear Corporation, Colorado Springs, Colorado, by ORNL and Kaman Nuclear Corporation staff members. This effort was sponsored by the Radiation Shielding Information Center, which distributes versions of SUPERTOG operational on both IBM and CDC computing equipment.

References

1. Mathematics Division.
2. R. Q. Wright, N. M. Greene, J. L. Lucius, and C. W. Craven, Jr., *SUPERTOG: A Program to Generate Fine Group Constants and* P_n *Scattering Matrices from ENDF/B,* ORNL-TM-2679 (September 1969).

3.9 ABSTRACTS OF THE DATA LIBRARY PACKAGES ASSEMBLED BY THE RADIATION SHIELDING INFORMATION CENTER (RSIC)[1]

Robert W. Roussin

Data libraries are now being packaged and organized by RSIC in a manner analogous to the RSIC code collection. Each data set carries a Data Library Collection (DLC) number and is packaged as a unit. As with the code packages, a particular data package will not remain static, but will be subject to revision, updating, and expansion as required. ORNL-RSIC-30 is a loose-leaf binder in which currently 16 abstracts of data sets are published.

Reference

1. Abstract of ORNL-RSIC-30, vol. 1 (March 1972); work partially funded under DNA Subtask PB052-03 and NASA Order H-79272.

3.10 CHECKER CODE MODIFICATION

R. Q. Wright[1] J. L. Lucius[1]

A new version of the CHECKER program was obtained from the National Neutron Cross Section Center, Brookhaven National Laboratory, and is now operational on ORNL computers. The purpose of CHECKER is to check the data on an ENDF/B BCD card-image tape. CHECKER has been used to process the ENDF/B-III preliminary tapes.

Reference

1. Mathematics Division.

3.11 CALCULATION OF NEUTRON FLUENCE-TO-KERMA CONVERSION FACTORS BASED ON THE ENDF/B NEUTRON CROSS SECTION LIBRARY

Mohamed Abdou[1]. R. Q. Wright

A computer code is under development to read the ENDF/B library and calculate neutron fluence-to-kerma conversion factors. The computer code will be made available by RSIC as a PSR, and a library of kerma factors, along with a suitable retrieval program, will be packaged as a DLC.

Reference

1. Nuclear Engineering Department, University of Wisconsin, Madison.

3.12 THE MAINTAIN CODE FOR USE IN MAINTAINING CRBE FILES ON TAPE[1]

D. K. Trubey

The Conversational Remote Batch Entry (CRBE) system is useful for on-line creating, editing, and storing text data on disk via the ORNL IBM 360/75. The on-line storage space is limited, however, and it is therefore necessary to copy data on tape for off-line longer-term storage. The MAINTAIN code was written for this purpose. Commands, similar to those of CRBE, control the operations of the program. Each command consists of $$ plus three more characters in columns 1–5. Additional characters may be added if desired. These commands and their uses are:

Command	Result
(1) $$NEW	Add new data to tape from a CRBE file, initializing the tape
(2) $$ADD	Copy old tape and add a new file to the new tape
(3) $$PRINT	Use line printer to print a particular tape file or the whole tape
(4) $$FETCH	Copy a tape file to an on-line disk for CRBE editing
(5) $$REPLACE	Copy old tape but replace a particular file with new data on the new tape

(6) $$PURGE	Copy old tape but delete a particular file
(7) $$COPY	Copy selected files of old tape to a new tape
(8) $$CADSEP	Copy selected files of old tape to a new tape in ADSEP format[2]
(9) $$CHECK	Check first record of old tape to be sure of data

References

1. Summary of ORNL-CF-72-5-24 (May 1972).
2. A. A. Brooks, *ADSEP Text Input*, ORNL-CF-71-9-3 (September 1971).

3.13 MULTIGROUP NEGATIVE FLUXES IN REFLECTION GEOMETRY

R. W. Roussin D. K. Trubey

It is known that the Legendre expansion is not a good one for the Klein-Nishina formula. Multigroup cross-section data produced by the MUG[1] and GAMLEG[2] codes result in negative cross-section values at some angles. The problem persists even with rather high-order expansion such as P_{12}. As a result, codes such as ANISN[3] will compute negative fluxes for certain points in phase space. The problem is particularly acute in cases of gamma-ray reflection problems.

The ^{14}N decay gamma ray of 6.2 MeV is troublesome in water-cooled reactor plants.[4] If one is evaluating the problem of such gamma rays scattered from concrete, for example, the energy-angular distribution of reflected gamma rays must be known. The discrete ordinates codes would be useful to determine these quantities, but the accuracy of the results, when negative fluxes are observed, is questionable.

Consequently, a study is being undertaken to compare results from ANISN, MORSE[5] (Monte Carlo but using multigroup cross sections as in ANISN), and OGRE[6] (Monte Carlo, energy point cross sections). The transport of the photons by MORSE is done using the usual multigroup cross sections, but there are several options in the estimator. The following ones are used: (1) boundary crossings, (2) statistical (next event) estimation based on the multigroup cross sections, (3) statistical estimation based on the basic Klein-Nishina distribution, which is never negative. The OGRE estimators used were (1) boundary crossing estimator from each flight and (2) estimated reflection in various directions from each collision, a form of statistical estimation also used in MORSE for this problem. Annihilation radiation from pair production was treated.

It was found that the overall MORSE, ANISN, and OGRE albedos were in good agreement, although the OGRE results were slightly lower. At the higher reflected energies, above 1 MeV for a 6.2-MeV source and normal incidence, the OGRE values were zero, while the ANISN fluxes had small negative or positive values.

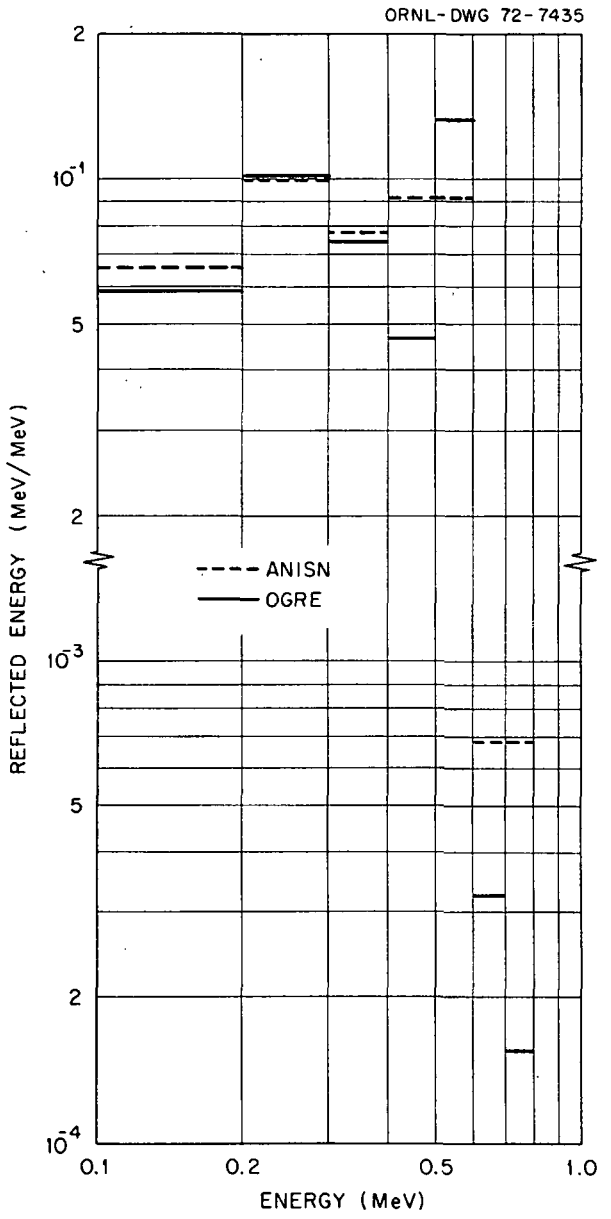

Fig. 3.13.1. Reflected photon energy spectrum per 6.2-MeV photon normally incident on a concrete slab two mean free paths thick.

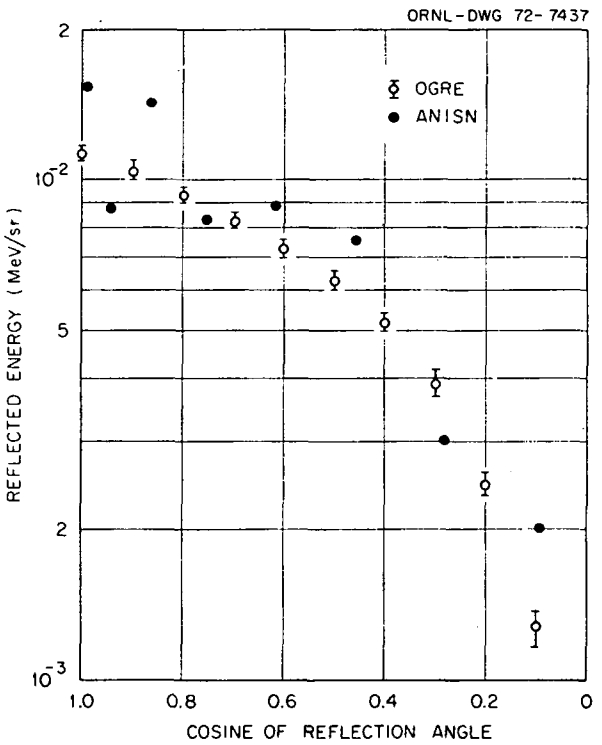

Fig. 3.13.2. Reflected energy per 6.2-MeV photon normally incident on a concrete slab two mean free paths thick as a function of reflection angle cosine.

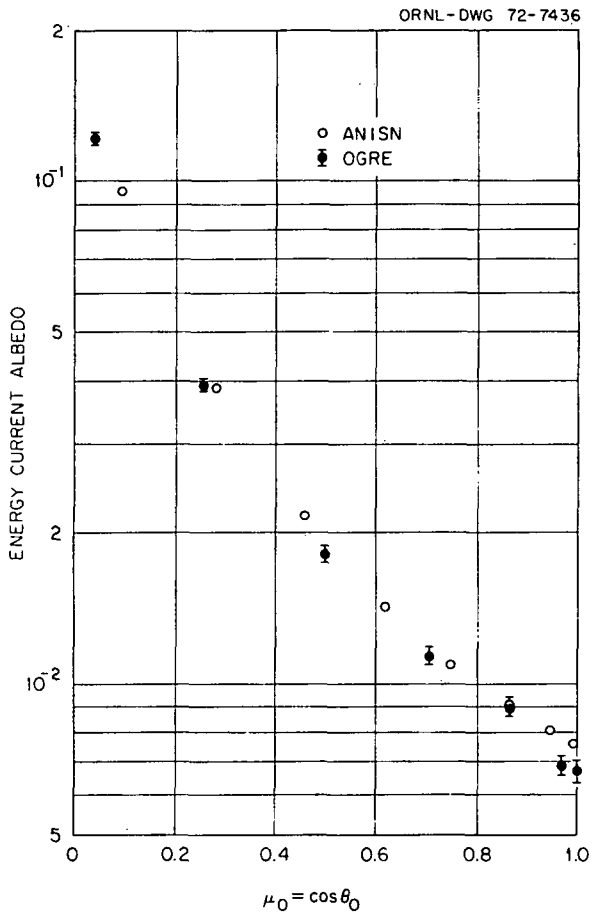

Fig. 3.13.3. Energy albedo for 6.2-MeV incident photons on a concrete slab two mean free paths thick as a function of incident angle cosine.

Typical results for essentially normal incidence are shown in Figs. 3.13.1 and 3.13.2. The albedo as a function of incident angle is shown in Fig. 3.13.3.

References

1. J. R. Knight and F. R. Mynatt, *MUG – a Program for Generating Multigroup Photon Cross Sections* CTC-17 (1970); RSIC Code Package PSR-7.

2. K. D. Lathrop, *GAMLEG – a FORTRAN Code to Produce Multigroup Cross Sections for Photon Transport Calculations,* LA-3267 (April 1965); available from RSIC.

3. W. W. Engle, Jr., *A User's Manual for ANISN,* K-1694 (1967); RSIC Code Package CCC-82.

4. W. M. Lowder, P. D. Raft, and C. V. Gogolak, *Environmental Gamma Radiation from Nitrogen-16 Decay in the Turbine of a Large Boiling Water Reactor,* HASL TM-72-1.

5. E. A. Straker, P. N. Stevens, D. C. Irving, and V. R. Cain, *The MORSE Code – a Multigroup Neutron and Gamma-Ray Monte Carlo Transport Code,* ORNL-4385 (1970); RSIC Code Package CCC-127.

6. S. K. Penny and D. K. Trubey, *OGRE, a Monte Carlo System for Gamma-Ray Transport Studies, Including an Example (OGRE-P1) for Transmission through Laminated Slabs* (1966); RSIC Code Package CCC-46.

3.14 A REVIEW OF CALCULATIONS OF RADIATION TRANSPORT IN AIR – THEORY, TECHNIQUES, AND COMPUTER CODES

Proceedings of a seminar, November 15–17, 1971[1]

D. K. Trubey H. E. Comolander
Compilers

Summaries are presented of papers given at a seminar-workshop on radiation transport in air held at Oak Ridge, Tennessee, November 15–17, 1971. The papers,

in their review of the state of the art, show the various approaches to computing the transport of neutrons and gamma rays in the atmosphere. Reviews are given of the recent evaluations of nitrogen and oxygen neutron cross sections, and descriptions are presented of the many computer codes and data libraries available.

Among the computer codes discussed, the newly developed ATR (Air Transport of Radiation) code is being placed with the Radiation Shielding Information Center for distribution. The ATR code, using parametric models, provides neutron and gamma-ray transport data for the atmosphere and includes corrections for exponential density and the ground interface.

Reference

1. Abstract of ORNL-RSIC-33 (CONF-711125) (May 1972); work funded by Defense Nuclear Agency under Subtask PB052-03.

3.15 A COMPUTER CODE CENTER – EXPERIENCE AND OPERATIONS[1]

Betty F. Maskewitz

The history of the codes activities of the Radiation Shielding Information Center (RSIC) is traced from 1962 to present. Emphasis is placed on advances in hardware and software as they have facilitated code exchange. The paper's thesis is that computer technology information, including computer codes, is an integral part of all information processed by an information analysis center such as RSIC.

Reference

1. Abstract of a paper published in *Proceedings of Symposium on Sharing of Computer Programs and Technology in Nuclear Medicine,* CONF-710425 (April 1971).

3.16 THE MAINTENANCE OF EDITOR: AN ENDF/B PROCESSING CODE

J. E. White[1] S. K. Penny[1]

The ENDF/B processing code EDITOR[2] has been improved and updated in accordance with the revised ENDF/B formats and procedures. Most of the modifications were made to improve the edit portion and to make the code operational on the CDC machines. EDITOR will now print the literal information used to identify the ENDF/B file and reaction type on each page. This feature is especially useful when editing very large arrays. In addition, some of the quantities previously represented by FORTRAN variables have been replaced by more familiar physics terms. For example, consider the case where multiplicities are given in file 12, section 102. The variables ES and EG(I) have been changed to LEVEL ENERGY and PHOTON ENERGY respectively.

Table 3.16.1. Changes in Hollerith data string

Section	From	To
	Neutron interaction and photon production files	
4	INELASTIC	(N,N*)TOTAL
51–90	(N,N*)MT-40	(N,N*)LEVEL
91	(N,N*)MT-40	(N,N*)CONT
	Photon interaction files	
501	TOTAL	TOTAL PHOTON
502	ELASTIC	COHERENT
504	INELASTIC	INCOHERENT
516	PAIR PROD	PAIR PRD TOT

Table 3.16.1 summarizes the changes that have been made to the Hollerith information used to identify the ENDF/B reaction types in the BLOCK DATA statement. EDITOR will now process the following ENDF/B formats: (1) the revised formats for radioactive decay data (MT=453), fission product yield data (MT=454), and delayed neutron data (MT=455); (2) Reich-Moore and Adler-Adler resolved resonance parameters; (3) the new formats for the average number of prompt neutrons per fission and the LR flag.

These extensions have not affected the core size required to execute the program.

References

1. Mathematics Division.
2. C. L. Thompson, J. R. Stockton, L. M. Petrie, R. Q. Wright, and S. K. Penny, *EDITOR, a Processing Code for ENDF/B Format Data,* ORNL-TM-3266 (ENDF-142) (February 1971).

3.17 COMPUTER CODES FOR SHIELDING AND RELATED CALCULATIONS – 1972[1]

Betty F. Maskewitz Francis H. Clark[2]
D. K. Trubey

The Radiation Shielding Information Center (RSIC)[3] maintains and distributes an extensive library of computer codes useful in radiation shielding and related calculations. Summary descriptions of available codes have been published in the past. This paper brings these prior summaries[4–6] up to date.

References

1. Abstract of article to be published in *Nuclear Engineering and Design.*

2. Instrumentation and Controls Division.

3. Work partially funded under DNA Subtask PB052-03 and NASA Order H-79272A.

4. D. K. Trubey, "The Radiation Shielding Information Center – a Technical Information Service for Nuclear Engineers," *Nucl. Eng. Des.* **9**, 392–395 (1969).

5. D. K. Trubey and Betty F. Maskewitz, "Computer Codes for Shielding Calculations – 1969," *Nucl. Eng. Des.* **10**, 505–517 (1969).

6. Betty F. Maskewitz and D. K. Trubey, "Computer Codes for Shielding Calculations – 1970," *Nucl. Eng. Des.* **13**, 448–449 (1970).

4. Theoretical Studies of Medium- and High-Energy Radiation Transport

4.0 INTRODUCTION

R. G. Alsmiller, Jr.

Theoretical studies of medium- and high-energy radiation transport are pursued on a continuing basis. The work is primarily directed at the shielding of manned space vehicles and high-energy accelerators, but the transport methods developed for shielding purposes are also applicable in areas other than shielding, and some results in these peripheral areas are presented.

One of the fundamental difficulties in the study of medium- and high-energy nucleon transport is the lack of differential particle-production cross-section data, so a portion of the program is directed at obtaining these needed data. The basis of essentially all of the cross-section work is the intranuclear-cascade model of nuclear reactions. This model has also been used extensively at the Brookhaven National Laboratory, at Columbia University, and at the Joint Institute for Nuclear Research, Dubna, U.S.S.R., and during the past year a paper comparing the results of the various institutions and written jointly by authors from all of the facilities has been published. The most recent effort in the area of cross-section development is an attempt to adapt the intranuclear-cascade model to obtain estimates of differential particle-production cross sections from high-energy heavy-nucleus, heavy-nucleus collisions. These data are needed to carry out shielding studies involving the heavy nuclei component of galactic cosmic rays and to carry out theoretical studies on the use of high-energy heavy nuclei in cancer radiotherapy.

In the area of particle transport, the major effort has continued to be an exploitation of the capabilities of the high-energy transport code HETC, which is capable of treating nucleons and pions at energies of the order of several hundred GeV. A variety of applications of this code in the areas of accelerator shielding, instrumentation to measure high-energy hadrons, space shielding, and space physics have been carried out and are reported.

A small effort has continued on carrying out theoretical studies related to the use of negatively charged pions in cancer radiotherapy. During the past year, very good agreement has been obtained between calculated and experimental energy-deposition data for negatively charged pions of approximately 175 MeV/c incident on a water phantom.

The transport of low-energy (of the order of a few MeV) electrons through matter is important in the shielding of manned space vehicles against Van Allen belt electrons. For some time efforts have been in progress to treat the transport of such electrons by the method of discrete ordinates. During the past year, the work reached a sufficient degree of completion to allow the publication of a paper showing the results that have been obtained.

4.1 NONELASTIC INTERACTIONS OF NUCLEONS AND π-MESONS WITH COMPLEX NUCLEI AT ENERGIES BELOW 3 GeV[1,2]

Hugo W. Bertini Miriam P. Guthrie
Arline H. Culkowski[3]

Nonelastic interactions corresponding to continuum state transitions are calculated using the intranuclear-cascade-evaporation approach. Spallation yields, energy- and angular-dependent spectra, particle multiplicities, and nonelastic cross sections are calculated for incident nucleons and π-mesons with energies below 3 GeV on complex nuclei. Comparisons with experimental data are made, and, in general, the agreement is good. Discrepancies in these comparisons are discussed with respect to the deficiencies in the model.

References

1. Work partially funded by the National Aeronautics and Space Administration under Order H-38280A.

2. Abstract of ORNL-TM-3148 (Mar. 28, 1972); to be published in the *Physical Review.*
3. Mathematics Division.

4.2 MEDIUM-ENERGY INTRANUCLEAR-CASCADE CALCULATIONS: A COMPARATIVE STUDY[1,2]

V. S. Barashenkov[3] G. D. Harp[4]
Hugo W. Bertini A. S. Iljinov[3]
K. Chen[4,5] J. M. Miller[5]
G. Friedlander[4] V. D. Toneev[3]

Comparisons are reported among the Monte Carlo simulations of proton-induced intranuclear cascades as carried out by three different sets of investigators. The three sets of results for interactions of 150- and 300-MeV protons with ^{27}Al and ^{181}Ta are in excellent agreement for observable quantities such as energy spectra of emitted protons and mass-yield curves for spallation reactions.

References

1. Brookhaven National Laboratory and Columbia University work funded by U.S. Atomic Energy Commission; ORNL work partially by National Aeronautics and Space Administration under Order H-38280A.
2. Abstract of a joint paper, BNL-16429, and to be published in *Nuclear Physics.*
3. Joint Institute for Nuclear Research, Dubna, U.S.S.R.
4. Brookhaven National Laboratory, Upton, N.Y.
5. Columbia University, New York, N.Y.

4.3 RESULTS FROM MEDIUM-ENERGY INTRANUCLEAR-CASCADE CALCULATION[1,2]

Hugo W. Bertini Miriam P. Guthrie

An appreciable quantity of data has been generated using a medium-energy intranuclear-cascade calculation. Reactions were calculated for incident neutrons, protons, and charged pions on five elements ranging from oxygen to lead. The energy range of the incident nucleons was from 500 to 3000 MeV in 500-MeV steps, and, similarly, the energy range of the incident pions was from 500 to 2500 MeV. Data from the cascade and evaporation phases are available. A preliminary version of the computer programs used to generate the data is also available. The final version of the programs will be made available in the near future.

References

1. Work partially funded by the National Aeronautics and Space Administration under Order H-38280A.
2. Abstract of *Nucl. Phys.* **A169**, 670 (1971); included in last year's annual as abstract of ORNL-TM-3336 (1970).

4.4 CALCULATION OF HEAVY-ION INTERACTIONS[1]

Hugo W. Bertini R. T. Santoro
T. A. Gabriel J. D. Hunt[2]

The interactions of energetic nucleons ($E \gtrsim 100$ MeV) with complex nuclei have been shown to be reasonably well represented by the method of intranuclear cascades followed by evaporation.[3] In this method the life histories of each incident nucleon and all nucleons that interact with it are followed until they escape from the nucleus or are captured. Every interaction is assumed to be a free-particle-type interaction with the individual nucleons of the nucleus. These interactions are modified to include the effects of the Fermi motion of the bound nucleons, the changing nucleon density and changing nuclear potential with nuclear radius, and the exclusion principle. After the life histories of all of the particles involved in these collisions (for each incident particle) are followed, the remaining nucleus is made to lose its residual excitation energy by particle evaporation.[4]

This approach and the associated computer programs are being adapted to the calculation of heavy-ion interactions. The underlying assumption is that at sufficiently high interaction energies (MeV per nucleon $\gg$ binding energy per nucleon) the heavy-ion reaction can be represented in large part as the high-energy interaction of two Fermi gas clouds. As the clouds merge, cascades develop simultaneously in both, with nucleons being knocked out of both, until they separate. Each cloud (nucleus), now generally reduced in mass and in a highly excited state, moves away from the other, losing its excitation energy by the "boil off" of particles.

As a first step in these calculations, the simultaneous development of the cascade in each nucleus is approximated in the following manner: if the incident heavy ion consists of A_p nucleons ($p \equiv$ projectile), then $A_p - Z_p$ neutrons and Z_p protons are sent into a stationary target nucleus one at a time, and the cascades for each of these nucleons are allowed to develop in the target, independently of the other incident nucleons. The nucleons of the projectile that interact in the target are removed from the projectile, leaving holes therein. The nucleons of the projectile that miss or simply pass through the target are considered to form a residual projectile (with the holes), and hence this fragment is in an excited state. The direction of the fragment is

altered slightly from the initial projectile direction to account for the fact that the vector momentum of the particles (due to the Fermi motion) removed from the projectile does not, in general, add to zero. It is assumed that prior to the reaction the vector momenta of the Fermi motion of all of the particles within the projectile add to zero. When particles are removed, the vector momentum of the remaining particles is not zero, and hence the residual projectile is allowed recoil in the direction of the resultant momentum. Both the residual target and the projectile are in excited states, and they are made to lose this excitation energy by particle evaporation.[4]

For this first step in the calculation, the cascade is allowed to take place in the target only, but this accounts for only half of the reaction; that is, the weight of this event is $1/2$. The other half of the reaction is calculated by letting A_t ($t \equiv$ target) nucleons with appropriate energy strike the projectile (which is now assumed to be stationary) and by letting the cascade develop in the projectile. This calculation is carried out in the same manner described above, but at the end of the interacting process the results are transformed back to the laboratory frame. Each forward and corresponding "backward" calculation is repeated, using Monte Carlo techniques, until a sufficient number of samples representing the heavy-ion interactions has been taken.

It is acknowledged that there are many deficiencies in this approach; the most notable is probably the need to include the reduction in nuclear density as the cascade proceeds. However, the calculation of heavy-ion reactions is an extremely complicated problem that has heretofore defied formulation. The method being tried is our first attempt at penetrating the bulwarks of these reactions where existing programs need only be modified and not developed. Comparisons of the predicted results with experimental data will be made, but the supply of available data is extremely meager.

A somewhat similar approach was tried for alpha particles on complex nuclei, where the alpha particle was assumed to consist of four nucleons impinging on a target.[5] The "backward" calculation was not included. The agreement of the calculated results with experimental data was fair.

References

1. Work funded by the National Aeronautics and Space Administration under Order H-38280A.

2. Present address: Sioux Falls College, Sioux Falls, S.D. 57101.

3. Hugo W. Bertini, Miriam P. Guthrie, and Arline H. Culkowski, *Nonelastic Interactions of Nucleons and π-Mesons with Complex Nuclei at Energies Below 3 GeV*, ORNL-TM-3148 (Mar. 28, 1972) (to be published in the *Physical Review*); Hugo W. Bertini, *Phys. Rev.* **188**, 1711 (1969); and Hugo W. Bertini, *Phys. Rev.* **131**, 1801 (1963), with erratum *Phys. Rev.* **138**, AB2 (1965).

4. Miriam P. Guthrie, *EVAP-4: Another Modification of a Code to Calculate Particle Evaporation from Excited Compound Nuclei*, ORNL-TM-3119 (Sept. 10, 1970).

5. T. A. Gabriel, R. T. Santoro, and R. G. Alsmiller, Jr., *An Approximate High-Energy Alpha-Particle–Nucleus-Collision Model*, ORNL-TM-3153 (Oct. 1, 1970).

4.5 MONTE CARLO CALCULATIONS OF HIGH-ENERGY NUCLEON-MESON CASCADES AND COMPARISON WITH EXPERIMENT[1,2]

T. W. Armstrong K. C. Chandler[3]
R. G. Alsmiller, Jr. B. L. Bishop[4]

A Monte Carlo transport code for calculating high-energy nucleon-meson cascades in thick targets is described. The calculational method uses an intranuclear-cascade-extrapolation-evaporation model for treating nonelastic collisions $\gtrsim$ 3 GeV. Calculated results for the development of the cascade induced in thick iron targets by 10-, 19.2-, 29.4-, and 200-GeV/c protons are presented. For the cases of 10-, 19.2-, and 29.4-GeV/c incident protons, comparisons are made with experimental data, and, in general, good agreement is obtained.

References

1. Work partially funded by National Aeronautics and Space Administration under Order H-38280A.

2. Abstract of ORNL-TM-3667 (Jan. 5, 1972); to be published in *Nuclear Science and Engineering.*

3. Mathematics Division.

4. Civil Defense Research Project.

4.6 CALCULATION OF THE LONG-LIVED ACTIVITY IN SOIL PRODUCED BY 500-GeV PROTONS[1]

T. A. Gabriel R. T. Santoro

Calculations have been made to estimate the time and spatial dependence of the long-lived ($\tau_{1/2} \geqslant 1$ day)

activity in the soil surrounding a semi-infinite beam target tunnel. The activity distributions are given for 500-GeV protons incident on a Be target positioned in the tunnel for an irradiation time of 25 years at 10^{13} protons per second and at a time after shutdown of one month. The distributions are presented as a function of the radial distance from the tunnel axis for the spatial regions along the tunnel and at the end of the tunnel. The activity arising from selected nuclides is given for selected spatial points. Curves showing the decrease in activity as a function of shutdown time are given. Included is the calculated integrated activity along the tunnel axis.

Reference

1. Abstract of *Nucl. Instrum. Methods* **95**, 275 (1971); included in last year's annual as abstract of ORNL-TM-3262 (1970).

4.7 NUCLEON AND CHARGED-PION ALBEDO SPECTRA IN AN ACCELERATOR CAVE FROM 200-GeV PROTON INTERACTIONS IN IRON[1]

T. A. Gabriel R. T. Santoro

Nucleon and charged-pion albedo flux distributions in an accelerator cave resulting from the interaction of 200-GeV protons have been calculated. The spectra are given as a function of secondary-particle energy and of radial position and distance from the point where the beam is dumped into the iron. Comparisons between the omnidirectional and "backward" flux distributions are presented.

Reference

1. Abstract of ORNL-TM-3437 (Aug. 27, 1971) and of *Nucl. Instrum. Methods* **99**, 5 (1972).

4.8 ENERGY DEPOSITION IN IONIZATION SPECTROMETERS AND TANC COUNTERS FOR INCIDENT HIGH-ENERGY HADRONS

T. A. Gabriel T. W. Armstrong
K. C. Chandler[1]

Ionization spectrometers, which consist basically of thin plastic scintillators embedded in thick absorbers, have been found to be useful instruments for measuring the energy of high-energy hadrons (e.g., ref. 2). In addition, total-absorption nuclear-cascade (TANC) counters (e.g., ref. 3), which are composed entirely of a scintillating material, are under investigation as high-energy particle detectors. One advantage of TANC counters is their ability to measure all of the energy deposited by the nuclear-electromagnetic cascade, whereas the ionization spectrometers sample only a portion of the energy deposited. A disadvantage, however, is that because of the relative low density of most scintillating materials, the counters must be substantially larger (relative to ionization spectrometers) in order to contain a sizable portion of the energy of the incident hadron.

Detailed information on the energy deposited by the induced nuclear and electromagnetic cascades is required to properly design such instruments and to evaluate their response for energy determination. In the present work, the energy deposition in TANC counters and ionization spectrometers is determined by means of calculation, and the calculated results are compared with available experimental data.

The description of the nuclear cascade and the source distribution for the electromagnetic cascade were obtained using the Monte Carlo code HETC.[4] This code allows for the three-dimensional transport of nucleons, charged pions, and muons. It takes into account the slowing down of charged particles via the continuous slowing-down approximation; the decay of charged pions and muons, nonelastic nucleon- and charged-pion–nucleus (excluding hydrogen) collisions via the intranuclear-cascade-evaporation model[5,6] ($E \lesssim 3$ GeV) and extrapolation-evaporation model[7] ($E \gtrsim 3$ GeV); nonelastic nucleon- and charged-pion-hydrogen collisions via the isobar model[8] ($E \lesssim 3$ GeV) and phenomenological fits to experimental data[9] ($E \gtrsim 3$ GeV); and elastic nucleon- and charged-pion-collisions with hydrogen. The electromagnetic cascade calculations were carried out using a slightly modified version of the Monte Carlo code developed by Beck.[10] This code takes into account all of the significant electron, positron, and photon interaction processes. The source for the electromagnetic cascade calculation, that is, photons from neutral-pion decay, and electrons and positrons from muon decay, is provided by HETC.

Some calculated and experimental results for 8-GeV/c negative pions incident on one end of a TANC counter with average dimensions of $11\frac{1}{2} \times 56$ in. are shown in Fig. 4.8.1. The experimental data, indicated by the jagged curve, are taken from ref. 3. This figure shows the frequency distribution for the energy deposition, that is, the relative number of incident pions that will produce a given energy deposition in the scintillator. The calculated and experimental data are normalized to equal area between 2 and 7 GeV. In the experimental data, the large peak at approximately 900 MeV is due

mainly to muon contamination, and the peak at 8 GeV results from incident 8-GeV electrons used for energy calibration. Since only incident negative pions are considered in the calculations, these two peaks are not reproduced in the calculated results. The solid-lined histogram represents the calculated results when the electron-photon cascade is not included; that is, it was assumed that electrons and positrons from muon decay and neutral pions deposited all of their energy at their point of origin. The dashed-lined histogram represents the calculated results when the electron-photon cascade is included. The average experimental energy deposition is 49% of the incident energy, while the calculated average energy deposition for the cases described above is 49% and 45%, respectively. Overall, the agreement with the experimental data is quite good.

The energy deposition in an ionization spectrometer due to 28-GeV/*c* incident protons has also been calculated and compared with the measurements of Jones et al.[2] In this case, the agreement between calculation and experiment is only fiar.

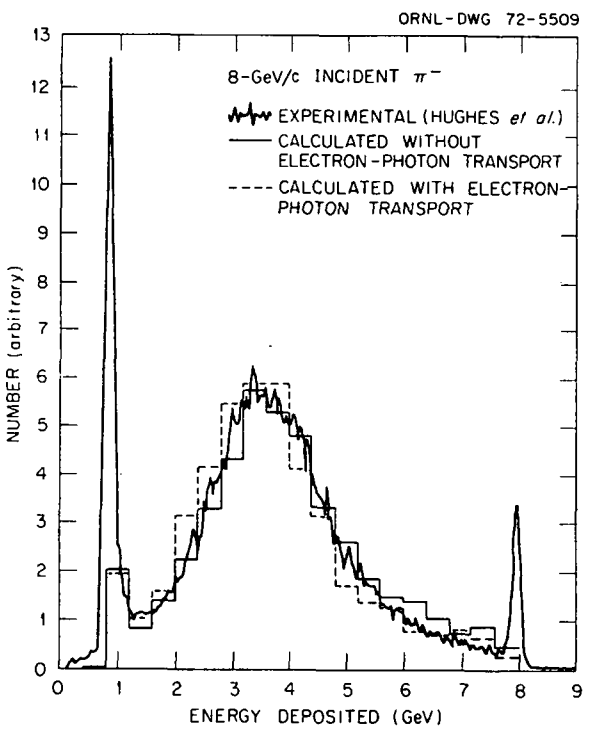

Fig. 4.8.1. Energy-deposition fluctuations by 8-GeV/*c* negative pions in a large NaI(Tl) scintillator. The calculated and experimental data are normalized to equal area between 2 and 7 GeV.

References

1. Mathematics Division.
2. W. V. Jones et al., *Nucl. Instrum. Methods* **72**, 173 (1969).
3. E. B. Hughes et al., *Nucl. Instrum. Methods* **75**, 130 (1969).
4. K. C. Chandler and T. W. Armstrong, *Operating Instructions for the High-Energy Nucleon-Meson Transport Code HETC,* ORNL-4744 (1972).
5. H. W. Bertini et al., *Instructions for the Operation of Codes Associated with MECC-3, a Preliminary Version of an Intranuclear-Cascade Calculation for Nuclear Reactions,* ORNL-4564 (1971).
6. H. W. Bertini and M. P. Guthrie, *Nucl. Phys.* **A169**, 670 (1971).
7. T. A. Gabriel et al., *An Extrapolation Method for Predicting Nucleon and Pion Differential Production Cross Sections from High-Energy (>3 GeV) Nucleon-Nucleus Collisions,* ORNL-4542 (1970).
8. H. W. Bertini et al., *Phenomenologically Determined Isobar Angular Distributions for Nucleon-Nucleon and Pion-Nucleon Reactions below 3 GeV,* ORNL-TM-3132 (1970).
9. T. A. Gabriel et al., *A Calculational Method for Predicting Particle Spectra from High-Energy Nucleon and Pion Collisions (≥3 GeV) with Protons,* ORNL-TM-3615 (1971).
10. Harold L. Beck, *A Monte Carlo Simulation of the Transport of High-Energy Electrons and Photons in Matter,* Health and Safety Laboratory, USAEC, report HASL-213 (1969).

4.9 CALCULATION OF COSMOGENIC RADIONUCLIDES IN THE MOON AND COMPARISON WITH APOLLO MEASUREMENTS[1,2]

T. W. Armstrong R. G. Alsmiller, Jr.

Calculations have been carried out to determine the time and spatial dependence of the production of various radionuclides in the moon from solar and galactic proton bombardment. The calculational method utilizes Monte Carlo techniques to obtain a detailed description of the induced nucleon-meson cascade. All required spallation cross sections are computed using the intranuclear-cascade-evaporation model. The calculated depth dependence of ^{26}Al and ^{22}Na is in good agreement with Apollo 11 and 12 measurements. The depth-dependent neutron spectra are also directly available from the calculations. The calculated thermal-neutron flux is in good agreement with the flux obtained from measured ^{60}Co concentra-

tions. Irradiation ages obtained from the calculated thermal flux and the thermal fluence based on measured gadolinium concentrations are consistent with the ages determined by other methods.

References

1. Work funded by National Aeronautics and Space Administration under Order T-85613.

2. Abstract of *Geochim. Cosmochim. Acta Suppl. 2, vol. 2, Proc. Second Lunar Science Conf.*, pp. 1729–45, M.I.T. Press (1971); included in last year's annual as abstract of ORNL-TM-3267 (1970).

4.10 CALCULATION OF THE LUNAR PHOTON ALBEDO FROM GALACTIC AND SOLAR PROTON BOMBARDMENT[1,2]

T. W. Armstrong

The lunar photon albedo due to cosmogenic and primordial photon sources has been calculated. The individual photon leakage spectra from prompt photons produced by galactic cosmic ray (GCR) and solar cosmic ray (SCR) induced nuclear interactions, from the decay of GCR- and SCR-induced radionuclides, and from the decay of naturally occurring radionuclides are given. An approximate estimate of the leakage from the photon-electron cascade initiated by the decay of neutral pions is also given. Monte Carlo methods were used to determine the nucleon-meson cascade, and discrete-ordinates methods were used for the photon and low-energy neutron transport.

References

1. Research funded by National Aeronautics and Space Administration under Order T-85613.

2. Abstract of *J. Geophys. Res.* 77, 524 (1972); included in last year's annual as abstract of ORNL-TM-3268 (1971).

4.11 CALCULATION OF THE NEUTRON SPECTRUM IN THE EARTH'S ATMOSPHERE PRODUCED BY GALACTIC COSMIC RAYS[1]

T. W. Armstrong K. C. Chandler[2]
J. Barish[2]

Some of the neutrons produced in the earth's atmosphere by cosmic-ray bombardment escape and subsequently decay within the magnetosphere into protons and electrons. It was initially suggested by Singer[3] that this neutron albedo supplies at least part of the particles trapped in the Van Allen radiation belts. Previous efforts (e.g., ref. 4) to test this hypothesis have shown serious discrepancies between predicted and measured trapped-proton intensities, but these comparisons have been based on neutron albedo spectra obtained from rather approximate calculations,[5] especially for that portion of the albedo spectra $\gtrsim$ 10 MeV. As part of an experimental[6] and calculational program to better define the magnitude of the neutron albedo, calculations using fewer approximations than previously possible have been carried out to determine the neutron spectrum in the earth's atmosphere due to galactic proton bombardment.

The Monte Carlo code HETC was used[7,8] to compute the production and transport of protons, charged pions, and neutrons (>12 MeV) due to incident galactic protons in the energy range from 30 MeV to 200 GeV. The neutron production $\leqslant$12 MeV from the HETC calculation was used as input to the discrete ordinates code ANISN[9] to obtain the low-energy ($\leqslant$12 MeV) portion of the neutron spectrum. The basic input for this method of calculation is the incident proton spectrum. This differs from most methods used previously to calculate the neutron albedo[5,10,11] in which the low-energy ($\lesssim$10 MeV) neutron production was estimated from rather sparse experimental data, and only the low-energy ($\lesssim$10 MeV) transport calculations were carried out in detail.

Figure 4.11.1 shows the calculated neutron albedo spectrum (0 g/cm^2) and, for comparison, the albedo spectrum calculated by Lingenfelter[5] that has been used in previous estimates of the proton intensity in the Van Allen belt. Also shown in Fig. 4.11.1 are the spectra at 200- and 1033-g/cm^2 depths which have been calculated to compare with the measurements of Hess et al.[12] All of the comparisons are absolute. The calculated and measured spectra differ somewhat at low energies but are in very good agreement at high energies. Although the albedo spectra are in good agreement at low energies, for neutrons >10 MeV the present calculations give an albedo flux ~8 times higher than that calculated by Lingenfelter. This difference is in the right direction to reduce some of the present discrepancies between calculated and measured trapped-proton intensities.

Calculations are in progress to determine the contribution of incident galactic alpha particles to the neutron albedo.

References

1. Work partially funded by National Aeronautics and Space Administration under Order H-38280A; paper presented at June 18–22 meeting of American Nuclear Society, Las Vegas, Nev.

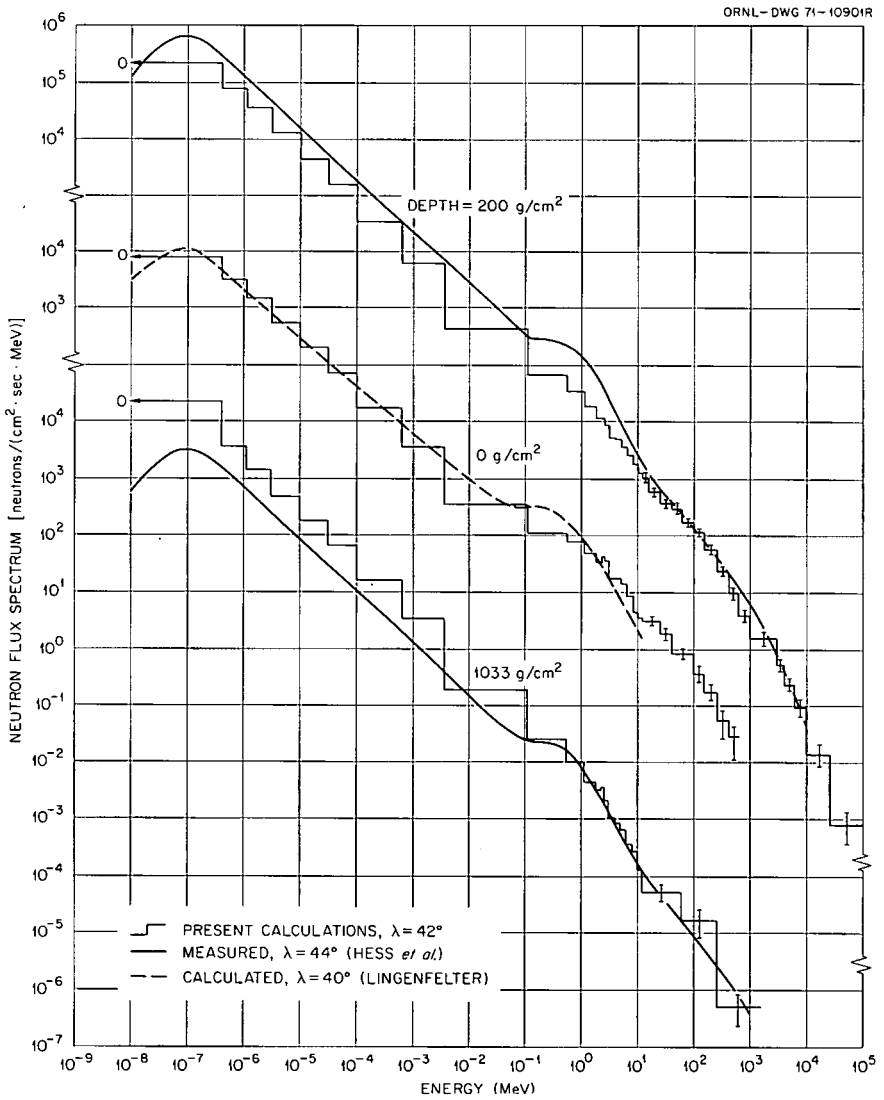

Fig. 4.11.1. Neutron flux spectra at various depths in the earth's atmosphere produced by galactic protons near solar minimum. The present calculations are compared with the calculations of Lingenfelter (ref. 5) and with the measurements of Hess et al. (ref. 12). λ = geomagnetic latitude.

2. Mathematics Division.

3. S. F. Singer, "Trapped Albedo Theory of the Radiation Belt," *Phys. Rev. Lett.* **1**, 181 (1958).

4. A. J. Dragt, M. M. Austin, and R. S. White, "Cosmic Ray and Solar Proton Albedo Neutron Decay Injection," *J. Geophys. Res.* **71**, 1293 (1966).

5. R. E. Lingenfelter, "The Cosmic-Ray Neutron Leakage Flux," *J. Geophys. Res.* **68**, 5633 (1963).

6. W. Zobel, T. A. Love, J. T. Delorenzo, and C. O. McNew, "Neutron Spectral Measurements in the Upper Atmosphere," paper presented at the National Symposium on Natural and Manmade Radiation in Space, Las Vegas, Nevada, March 1–5, 1971 (to be published in the proceedings).

7. T. W. Armstrong, R. G. Alsmiller, Jr., K. C. Chandler, and B. L. Bishop, *Monte Carlo Calculations of High-Energy Nucleon-Meson Cascades and Comparison with Experiment,* ORNL-TM-3667 (1972).

8. K. C. Chandler and T. W. Armstrong, *Operating Instructions for the High-Energy Nucleon-Meson Transport Code HETC,* ORNL-4744 (1972).

9. W. W. Engle, Jr., *A Users Manual for ANISN, a One-Dimensional Discrete Ordinates Transport Code with Anisotropic Scattering,* K-1693, Computing Technology Center, Union Carbide Corporation (1967).

10. W. N. Hess, E. H. Canfield, and R. E. Lingenfelter, "Cosmic-Ray Neutron Demography," *J. Geophys. Res.* **66**, 665 (1961).

11. L. L. Newkirk, "Calculation of Low-Energy Neutron Flux in the Atmosphere by the S_n Method," *J. Geophys. Res.* **68**, 1825 (1963).

12. W. N. Hess, H. W. Patterson, and R. Wallace, "Cosmic-Ray Neutron Energy Spectrum," *Phys. Rev.* **116**, 445 (1959).

4.12 DEPTH-DOSE DISTRIBUTIONS IN A TISSUE PHANTOM SHIELDED FROM GALACTIC COSMIC-RAY PROTONS[1]

R. T. Santoro R. G. Alsmiller, Jr.

Calculations have been performed using the high-energy nucleon-meson transport code HETC[2] to estimate the absorbed-dose rate and the dose-equivalent rate as a function of depth in a tissue phantom shielded from galactic cosmic-ray protons. Depth-dose distributions that arise from the incident protons and from the reaction products produced by high-energy nuclear collisions in the shield and in the tissue are given; they reflect the large contribution to the depth dose from the reaction products.

The transport of the incident protons and the secondary reaction products through the shield and tissue is accomplished using Monte Carlo techniques. Differential particle-production cross sections for nucleon-nucleus and pion-nucleus collisions are obtained with an intranuclear-cascade-evaporation model[3] for energies $\lesssim 3$ GeV and with an extrapolation model for higher energies.[4] Particle production from nucleon- and pion-proton collisions is obtained by sampling from phenomenological fits to experimental data.[5] The calculational procedures are described in refs. 2 and 6. The validity of HETC in high-energy calculations has previously been demonstrated by favorable comparisons between calculated and experimental results.[6,7]

The geometry used to simulate a spacecraft-astronaut configuration is a spherical shell shield having an inner radius of 150 cm and a 30-cm-diam tissue sphere at its center. Calculations have been carried out for a solar-minimum proton spectrum[8] (energies from 30 MeV to 200 GeV) isotropically incident on aluminum shields of thicknesses of 5, 20, and 35 g/cm^2 and a solar-maximum proton spectrum[9] (energies from 30 MeV to 200 GeV) isotropically incident on an aluminum shield of thickness 35 g/cm^2.

The results reported here include the absorbed-dose rate and the dose-equivalent rate as a function of depth in the tissue sphere produced from primary and secondary protons, heavy nuclei ($A > 1$), charged pions, photons from neutral pions, electrons, positrons, photons, and muons. In all cases considered, the primary proton and total absorbed-dose rates and the primary proton and total dose-equivalent rates are approximately constant as a function of depth in the tissue sphere. The primary proton and total absorbed-dose rates and the primary proton and total dose-equivalent rates at the center of the tissue sphere are shown in Table 4.12.1. The errors given represent one standard deviation. The significant point to be noted is the relatively large contribution to the total dose rates from

Table 4.12.1. Absorbed-dose rate and dose-equivalent rate at the center of the tissue sphere from galactic cosmic-ray protons incident on aluminum shields

Shield thickness (g/cm^2)	Absorbed-dose rate[a]		Dose-equivalent rate[a]	
	Primary protons (rads/sec) (10^{-7})	Total (rads/sec) (10^{-7})	Primary protons (rems/sec) (10^{-7})	Total (rems/sec) (10^{-7})
		Solar-minimum spectrum		
5	1.10 ± 0.05	2.10 ± 0.18	1.15 ± 0.06	4.10 ± 1.43
20	0.92 ± 0.05	2.21 ± 0.38	0.96 ± 0.06	4.66 ± 0.89
35	0.73 ± 0.05	1.58 ± 0.16	0.75 ± 0.05	3.0 ± 0.58
		Solar-maximum spectrum		
35	0.29 ± 0.02	1.15 ± 0.17	0.28 ± 0.02	3.80 ± 1.13

[a]The absorbed-dose rate and dose-equivalent rate are obtained by averaging over a 3-cm radius around the center of the tissue sphere.

particles produced by nuclear reactions, that is, from particles other than primary protons.

References

1. Work funded by National Aeronautics and Space Administration under Order H-38280A; paper presented at June 18–22 meeting of American Nuclear Society, Las Vegas, Nev.

2. K. C. Chandler and T. W. Armstrong, *Operating Instructions for the High-Energy Nucleon-Meson Transport Code HETC,* ORNL-4744 (1972).

3. H. W. Bertini, "Intranuclear-Cascade Calculation of the Secondary Nucleon Spectra from Nucleon-Nucleus Interactions in the Energy Range 340 to 2900 MeV and Comparisons with Experiment," *Phys. Rev.* **188**, 1711 (1969).

4. T. A. Gabriel, R. G. Alsmiller, Jr., and M. P. Guthrie, *An Extrapolation Method for Predicting Nucleon and Pion Differential Production Cross Sections from High-Energy (>3 GeV) Nucleon-Nucleus Collisions,* ORNL-4542 (1970).

5. T. A. Gabriel, R. T. Santoro, and J. Barish, *A Calculational Method for Predicting Particle Spectra from High-Energy Nucleon and Pion Collisions (⩾3 GeV) with Protons,* ORNL-TM-3615 (1971).

6. T. W. Armstrong et al., *Monte Carlo Calculations of High-Energy Nucleon-Meson Cascades and Comparison with Experiment,* ORNL-TM-3667 (1972).

7. T. W. Armstrong and R. G. Alsmiller, Jr., "Calculation of Cosmogenic Radionuclides in the Moon and Comparison with Apollo Measurements," Proc. Apollo 12 Lunar Science Conf., *Geochim. Cosmochim. Acta* 2, Suppl. 2, 1729–45, M.I.T. Press, Cambridge (1971).

8. F. B. McDonald, "IQSY Observations of Low-Energy Galactic and Solar Cosmic Rays," in *Annals of the IQSY,* vol. 4, ed. A. C. Strickland, M.I.T. Press, Cambridge (1969), p. 187.

9. N. Durgaprasad, C. E. Fichtel, and D. E. Guss, "Solar Modulation of Cosmic Rays and Its Relationship to Proton and Helium Fluxes, Interstellar Travel, and Interstellar Secondary Production," *J. Geophys. Res.* **72**, 2765 (1967).

4.13 CALCULATION OF THE ABSORBED DOSE AND DOSE EQUIVALENT FROM NEUTRONS AND PROTONS IN THE ENERGY RANGE FROM 3.5 GeV TO 1.0 TeV[1,2]

T. W. Armstrong K. C. Chandler[3]

Nucleon-meson cascade calculations have been carried out for monoenergetic neutrons and protons in the energy range from 3.5 GeV to 1.0 TeV normally incident on a semi-infinite slab of tissue 30 cm thick. The absorbed dose and dose equivalent as a function of tissue depth are presented, and analytic expressions for the resulting maximum and average fluence-to-absorbed-dose and fluence-to-dose-equivalent factors are given as a function of incident neutron or proton energy. The calculations were performed by using Monte Carlo methods in conjunction with theoretical nuclear interaction models.

References

1. Work partially funded by National Aeronautics and Space Administration under Order H-38280A.

2. Abstract of ORNL-TM-3758 (1972); submitted for journal publication.

3. Mathematics Division.

4.14 A CALCULATIONAL METHOD FOR PREDICTING PARTICLE SPECTRA FROM HIGH-ENERGY NUCLEON AND PION COLLISIONS (⩾3 GeV) WITH PROTONS[1,2]

T. A. Gabriel R. T. Santoro
J. Barish[3]

A calculational method for predicting the spectra from high-energy nucleon and pion collisions (⩾3 GeV) with protons is described. The determination of nucleon-proton and pion-proton total, elastic, and nonelastic cross sections from experimental data is discussed, and procedures for obtaining nucleon and charged-pion spectra from the Ranft-Borak distributions are presented. A brief discussion of the computer program logic is also included.

References

1. Work partially funded by National Aeronautics and Space Administration under Order H-38280A.

2. Abstract of ORNL-TM-3615 (Nov. 1, 1971).

3. Mathematics Division.

4.15 OPERATING INSTRUCTIONS FOR THE HIGH-ENERGY NUCLEON-MESON TRANSPORT CODE HETC[1,2]

K. C. Chandler[3] T. W. Armstrong

The high-energy nucleon-meson transport code HETC computes the transport of nucleons, charged pions, and muons through matter for energies up to several hundred GeV by using Monte Carlo methods. This

report is primarily concerned with the programming aspects of HETC. Instructions for operating the code are given, and the code input is described. HETC is written in FORTRAN IV for the IBM 360/75 and IBM 360/91 computers.

References

1. Work partially funded by National Aeronautics and Space Administration under Order H-38280A.
2. Abstract of ORNL-4744 (January 1972); also code abstract submitted for journal publication.
3. Mathematics Division.

4.16 MUON TRANSPORT AND THE SHIELDING OF HIGH-ENERGY (≤500 GeV) PROTON ACCELERATORS[1]

R. G. Alsmiller, Jr. J. Barish[2]
F. S. Alsmiller Y. Shima[3]

Calculated results on the muon shielding required around high-energy (200 GeV and 500 GeV) proton accelerator targets are presented. The calculations differ from those presented previously in that, in addition to the angular scattering of the muons due to Coulomb elastic collisions, an estimate of the angular scattering of the muons due to bremsstrahlung production, pair production, and nonelastic nuclear collisions is included. It is found that the angular scattering of the muons due to bremsstrahlung production, pair production, and nonelastic nuclear collisions does not have a pronounced effect on the shield dimensions and therefore for many design purposes may be neglected.

The calculations also differ from those presented previously in that the case of laminated shields is considered.

References

1. Abstract of p. 601 in *Proc. International Congress on Protection against Accelerator and Space Radiation, CERN, Geneva, Switzerland, April 26–30, 1971,* CERN 71-16, vol. 2, July 1, 1971; included in last year's annual as abstract of ORNL-TM-3353 (Apr. 12, 1971).
2. Mathematics Division.
3. Present address: Soreq Nuclear Research Center, Yavne, Israel.

4.17 LOW-ENERGY ELECTRON TRANSPORT BY THE METHOD OF DISCRETE ORDINATES[1,2]

D. E. Bartine[3] F. R. Mynatt
R. G. Alsmiller, Jr. W. W. Engle, Jr
J. Barish[3]

The one-dimensional discrete ordinates code ANISN has been adapted to simulate the transport of low-energy (on the order of a few MeV) electrons. Two different calculational techniques have been utilized for the treatment of electron-electron collisions that result in a small energy transfer. One method treats such collisions by a continuous slowing-down approximation, while the other method treats these collisions by the use of a very approximate cross section. Calculated results obtained with ANISN are compared with experimental data for the transmitted energy and angular distributions for 1-, 2.5-, 4-, and 8-MeV electrons normally incident on aluminum slabs of various thicknesses and for 1-MeV electrons normally incident on a gold slab. The calculated and experimental results are in reasonably good agreement for the aluminum slabs but are in poor agreement for the gold slab. Calculated results obtained with ANISN are also compared with calculated results obtained with Monte Carlo methods.

References

1. Work funded by National Aeronautics and Space Administration under Order H-38280A.
2. Abstract of ORNL-TM-3438 (Aug. 18, 1971); to be published in *Nuclear Science and Engineering.*
3. Mathematics Division.

4.18 CALCULATED RESPONSE OF THE TLND PERSONNEL DOSIMETER TO NEUTRONS WITH ENERGIES ≤400 MeV

R. G. Alsmiller, Jr. J. Barish[1]

The TLND is an albedo-type neutron dosimeter designed by Hoy.[2] Awschalom[3] compared dose-equivalent data obtained with the TLND with dose-equivalent data obtained with a Bonner spectrometer and found the TLND to be quite accurate. To further test the reliability of this dosimeter, its response to monoenergetic neutron fluences with energies between thermal energies and 400 MeV has been calculated, and the results have been compared with the available low-energy (<10 MeV) experimental data.

A schematic diagram of the geometry considered is shown as an inset in Fig. 4.18.1. The steel-encased object represents the TLND. In principle, the neutron dose equivalent D is obtained with the TLND from the equation

$$D = K(R_B - R_A)\,, \tag{1}$$

where

K = a constant that is considered to be independent of the incident neutron energy spectrum,

R_A, R_B = the neutron-absorption reactions in the ^{6}LiF cylinders labeled A and B in Fig. 4.18.1.

The relative response of the TLND is defined to be the dose equivalent obtained with the TLND divided by the dose equivalent calculated from the fluence-to-dose-equivalent conversion factors recommended by the International Commission on Radiation Units and Measurements;[4] that is, the relative response R is given by

$$R = \frac{D}{\int F(E)\,\phi(E)\,dE} = \frac{K(R_B - R_A)}{\int F(E)\,\phi(E)\,dE}\,, \tag{2}$$

where

$F(E)$ = the fluence-to-dose-equivalent conversion factor for neutrons with energy E,

$\phi(E)$ = the incident particle fluence per unit energy,

and the indicated integrations are to be carried out over all incident energies. If K is independent of energy, then for any incident fluence per unit energy the relative response should be unity. In particular, for monoenergetic incident neutrons the relative response should be unity for all incident neutron energies.

Calculations have been carried out for very broad beams of neutrons both normally and isotropically incident on the face of the tissue which contains the TLND. The calculations were carried out using the discrete ordinates code DOT in the adjoint mode.[5] For neutron energies of <15 MeV, differential cross-section data were taken from ref. 6 for H, C, N, O, and Fe, from Joanou and Dudek[7] for Cd and F, and from Norton[8] for Li. For neutron energies of >15 MeV, differential elastic cross-section data were taken from the O5R[9] master cross-section tape,[10] and differential nonelastic cross-section data were taken from the work of Bertini.[11,12]

The calculated and measured[2] relative response of the TLND from monoenergetic incident neutrons is shown in Fig. 4.18.1 as a function of neutron energy. The value of K in Eq. (2) has been determined by making the calculated and measured values for normal incidence agree at approximately 1 MeV.

The shape of the solid histogram in Fig. 4.18.1 is very approximately the same as that of the experimental data at energies between 10^{-1} and 10 MeV. At thermal energies, however, there is a large discrepancy between the calculated and experimental data since for normally

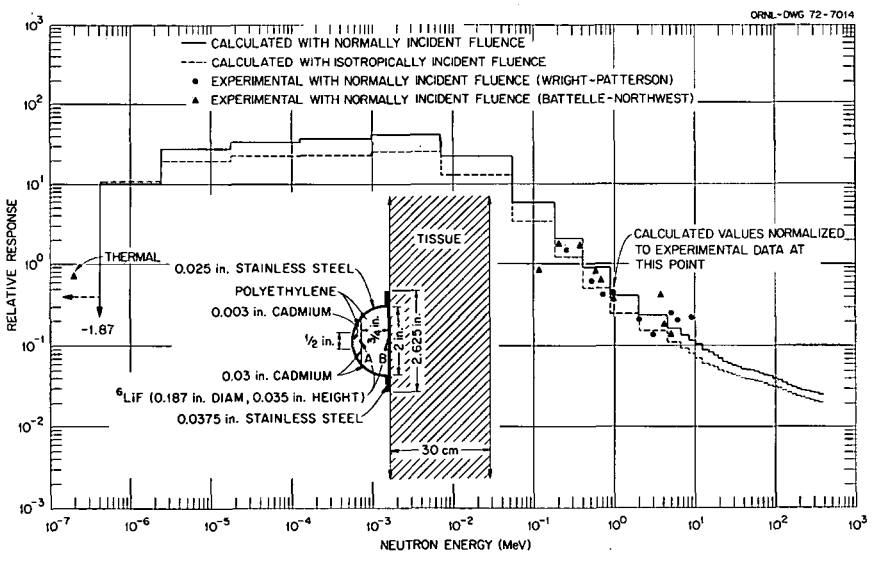

Fig. 4.18.1. Relative response of TLND as a function of neutron energy.

incident neutron fluences the measured relative response is positive, while the calculated relative response is negative; that is, in the calculations for this case $R_B < R_A$. This discrepancy may not be significant since there is a large difference in the calculated relative response for isotropically and normally incident thermal-neutron fluences, and the extent to which the experimental thermal neutrons were normally incident is not precisely known. The shapes of the calculated relative response histograms for normally and isotropically incident neutron fluences are approximately the same except at very low energies. The calculated relative response histograms are not at all constant with energy, as they would be if K in Eq. (2) were independent of energy. Over very limited energy ranges, however, the TLND, by an appropriate choice of K for the energy range, can be used to obtain approximate values of the dose equivalent. Also, it seems possible that the dose equivalent from various classes of incident continuous spectra could be obtained approximately with the TLND by an appropriate choice of K. Calculations to determine the extent to which the latter is possible are in progress.

References

1. Mathematics Division.
2. J. Hoy, *Personnel Albedo Neutron Dosimeter with Thermoluminescent ^{6}LiF and ^{7}LiF,* DP-1277, E. I. du Pont de Nemours and Co., Savannah River Plant (January 1972).
3. M. Awschalom, "The Radiation Safety Philosophy and Its Implementation at NAL," *Proc. International Congress on Protection against Accelerator and Space Radiation, CERN, Geneva, Switzerland, April 26–30, 1971,* CERN 71-16, vol. 2 (1971), p. 1050.
4. International Commission on Radiation Units and Measurements, *Radiation Protection Instrumentation and Its Application*, ICRU report 20 (1971).
5. F. R. Mynatt, F. J. Muckenthaler, and P. N. Stevens, *Development of Two-Dimensional Discrete Ordinates Transport Theory for Radiation Shielding,* CTC-INF-952, Computing Technology Center, Union Carbide Corporation (1969).
6. M. K. Drake (ed.), *Data Formats and Procedures for the ENDF Neutron Cross Section Library,* BNL-50274 (T-601), vol. 1 of ENDF-102, Brookhaven National Laboratory (1970).
7. G. D. Joanou and J. S. Dudek, *GAM-II, a B_3 Code for the Calculation of Fast-Neutron Spectra and Associated Multigroup Constants,* GA-4265, General Atomic (1963).
8. D. S. Norton, *The U.K.A.E.A. Nuclear Data Library, February 1968,* AEEW-M824, U.K.A.E.A., Winfrith (1968).
9. D. C. Irving et al., *O5R, a General-Purpose Monte Carlo Neutron Transport Code,* ORNL-3622 (1965).
10. The master cross-section tape for use in the O5R Monte Carlo code, together with references to the source of the cross sections, is available on request from the Radiation Shielding Information Center of the Oak Ridge National Laboratory.
11. H. W. Bertini, *Nucl. Phys.* 87, 138 (1966).
12. R. G. Alsmiller, Jr., M. Leimdorfer, and J. Barish, *Analytic Representation of Nonelastic Cross Sections and Particle-Emission Spectra from Nucleon-Nucleus Collisions in the Energy Range 25 to 400 MeV,* ORNL-4046 (1967).

4.19 CALCULATION OF THE ABSORBED DOSE AND DOSE EQUIVALENT INDUCED BY MEDIUM-ENERGY NEUTRONS AND PROTONS AND COMPARISON WITH EXPERIMENT[1,2]

T. W. Armstrong B. L. Bishop[3]

Monte Carlo calculations have been carried out to determine the absorbed dose and dose equivalent for 592-MeV protons incident on a cylindrical phantom and for neutrons from 580-MeV proton-Be collisions incident on a semi-infinite phantom. For both configurations, the calculated depth dependence of the absorbed dose is in good agreement with experimental data.

References

1. Work partially funded by National Aeronautics and Space Administration under Order H-38280A.

2. Abstract of *Rad. Res.* 47, 581 (1971); included in last year's annual as abstract of ORNL-TM-3304 (Feb. 5, 1971).

3. Civil Defense Research Project.

4.20 CALCULATION OF THE DOSE, RADIONUCLIDE PRODUCTION, AND DELAYED PHOTON LEAKAGE DUE TO SOLAR-PROTON BOMBARDMENT OF TISSUE WITH APPLICATION TO ASTRONAUT DOSIMETRY[1,2]

T. W. Armstrong K. C. Chandler[3]

Calculations have been carried out to determine the dose (absorbed dose and dose equivalent), induced radionuclides, and time-dependent photon-leakage spec-

trum due to solar-proton bombardment of a slab of tissue 30 cm thick. Proton spectra with characteristic rigidities of P_0 = 50, 100, and 200 MV were considered. The induced nucleon-meson cascade and the photon transport were calculated using Monte Carlo methods. The radionuclide production was determined by using calculated nucleon spectra and available production cross sections. The purpose of the calculations is to investigate the possibility of determining the whole-body dose received by astronauts in case of solar-flare exposure from measurement of the photons from the decay of radionuclides induced in the astronauts' bodies.

References

1. Work funded by National Aeronautics and Space Administration under Orders H-38280A and T-85613.
2. Abstract of paper published in *Health Phys.* (1972); included in last year's annual as abstract of ORNL-TM-3452 (June 30, 1971).
3. Mathematics Division.

4.21 MONTE CARLO CALCULATIONS OF THE DOSE INDUCED BY CHARGED PIONS AND COMPARISON WITH EXPERIMENT[1]

T. W. Armstrong K. C. Chandler[2]

A calculational method that utilizes Monte Carlo techniques in conjunction with the intranuclear-cascade-evaporation model for treating nuclear interactions is applied to study the dose induced in matter by charged pions. To test the validity of the calculational method for pion dose calculations, calculated results are compared with experimental data for the absorbed dose induced in water phantoms by a π^- beam of mean momentum 175 MeV/c and by π^- and π^+ beams of mean momentum 150 MeV/c. The calculated and experimental results are in good general agreement, but the comparisons are not completely definitive because precise descriptions of the incident beams used in the experiments are not available. The calculations indicate the importance of secondary particles in determining the spatial dependence of the absorbed dose and dose equivalent. Information on the spatial dependence of the neutron current produced by the 175-MeV/c π^- beam is also calculated.

References

1. Abstract of ORNL-TM-3678 (Feb. 4, 1972); submitted for journal publication.
2. Mathematics Division.

4.22 CALCULATIONS FOR PRODUCING DESIRED DEPTH-DOSE DISTRIBUTIONS USING NEGATIVELY CHARGED PIONS[1]

T. W. Armstrong R. G. Alsmiller, Jr.
K. C. Chandler[2]

At the present time a major reason for the failure of cancer treatment by radiotherapy is the inherently large ratio of normal tissue dose to tumor dose delivered by those radiations routinely used in radiotherapy. Negatively charged pions have physical properties which, in principle, will allow large, well-confined doses to be delivered to the tumor with relatively little damage to the skin and surrounding tissue. In planning the treatment of patients using negatively charged pions, it is necessary to be able to accurately predict the energy spectrum of the incident pion beam needed to produce a uniform dose over a specified volume (representing a tumor) at a given position in the body. A general computational method for this purpose has not yet been developed. In the present work, an idealized case is considered whereby available calculated results[3] for the depth-dose distributions produced by monoenergetic pions incident on a slab of tissue are used to synthesize the energy spectrum of a pion beam to approximate a uniform dose-equivalent distribution over a specified depth interval in tissue.

The depth dependence of the absorbed dose and dose equivalent produced by monoenergetic pion beams of 53, 82, and 108 MeV (corresponding to ranges in tissue of approximately 10, 20, and 30 cm, respectively) incident normally on a 60-cm-thick slab of tissue has been previously calculated.[3,4] These calculations were carried out using the nucleon-meson transport code NMTC,[5] and all significant physical processes, including the effect of all secondary particles produced by nuclear interactions, multiple Coulomb scattering by the primary pions, and, in an approximate manner, range straggling, were taken into account. This calculational method has been shown to give good agreement with measured dose distributions produced by pions.[6]

The depth dependence of the dose equivalent calculated previously for monoenergetic beams having ranges of approximately 20 and 30 cm were used to synthesize the energy spectrum of an incident pion beam that would produce a uniform dose-equivalent distribution over a depth interval of 20 to 30 cm. Since this synthesis procedure involved several approximations, the spectrum obtained was used as input for a detailed dose calculation (using the same calculational method as used previously for the monoenergetic cases) to check the uniformity of the dose-equivalent distribution.

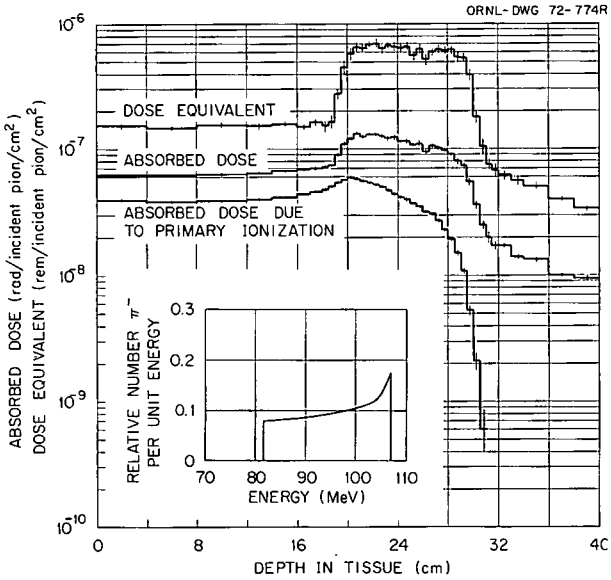

Fig. 4.22.1. Calculated dose distributions produced by an incident π^- beam having an energy spectrum (shown in inset) synthesized to produce a uniform dose-equivalent distribution between 20 and 30 cm.

The results obtained using the synthesized spectrum are shown in Fig. 4.22.1. Since monoenergetic pions produce a slightly different spatial distribution for the dose equivalent than for the absorbed dose and since the incident spectrum was synthesized on the basis of a constant dose equivalent, the dose equivalent obtained is relatively uniform over the desired interval, but the absorbed dose shows more variation. Thus, the incident pion spectrum is somewhat dependent upon whether a uniform dose equivalent or a uniform absorbed dose is requested.

In principle, the dose equivalent should provide a better criterion than the absorbed dose for specifying the beam spectrum, since the dose equivalent reflects the LET dependence of the energy deposited by the various particle types. However, it should be realized that the dose-equivalent distribution shown is only approximately related to biological damage, because the LET-dependent quality factors used[7] are designed for radiation protection purposes and because of fundamental objections in using LET as a measure of biological damage (e.g., ref. 8).

References

1. Work funded by Los Alamos Scientific Laboratory under Order CMI-7364-1.
2. Mathematics Division.
3. T. W. Armstrong, R. G. Alsmiller, Jr., and K. C. Chandler, *Trans. Amer. Nucl. Soc.* **14**(2), 523 (1971).
4. T. W. Armstrong, R. G. Alsmiller, Jr., and K. C. Chandler, *Neutron Phys. Div. Annu. Progr. Rep. May 31, 1971*, ORNL-4705, p. 89.
5. W. A. Coleman and T. W. Armstrong, *Nucl. Sci. Eng.* **43**, 353–54 (1971).
6. T. W. Armstrong and K. C. Chandler, *Monte Carlo Calculations of the Dose Induced by Charged Pions and Comparison with Experiment*, ORNL-TM-3678 (Feb. 4, 1972); submitted for journal publication.
7. R. G. Alsmiller, Jr., T. W. Armstrong, and B. L. Bishop, *Nucl. Sci. Eng.* **43**, 257–66 (1971).
8. R. Katz et al., *Rad. Res.* **47**, 402–25 (1971).

4.23 RADIATION TRANSPORT CODES FOR POTENTIAL APPLICATIONS RELATED TO RADIOBIOLOGY AND RADIOTHERAPY USING PROTONS, NEUTRONS, AND NEGATIVELY CHARGED PIONS[1,2]

T. W. Armstrong

In connection with long-term programs in space-vehicle, accelerator, and reactor shielding, the Oak Ridge National Laboratory has developed rather sophisticated calculational methods for determining the transport in matter of protons, neutrons, pions, muons, electrons, and photons. This work has resulted in several Monte Carlo radiation-transport computer codes which are quite general with respect to allowable source-particle descriptions, geometries, material compositions, etc. Recently, a limited study has been directed toward applying some of these computer codes to predict quantities of interest in the fields of radiotherapy and radiobiology, such as depth-dose patterns, and toward assessing the accuracy of the codes for applications in these fields. In this paper, the calculational methods are described, and comparisons of calculated and experimental results are presented for dose distributions produced by protons, neutrons, and negatively charged pions. Comparisons of calculated and experimental cell-survival probabilities are also presented.

References

1. Work partially funded by National Aeronautics and Space Administration under Order H-38280A.
2. Abstract of ORNL-TM-3816 (in press).

4.24 VALIDITY OF USING PRIMARY PROTONS ONLY IN VAN ALLEN BELT AND SOLAR-FLARE PROTON SHIELDING STUDIES[1,2]

R. T. Santoro R. G. Alsmiller, Jr.
J. Barish[3]

The validity of the approximations of neglecting proton attenuation due to nuclear collisions and all reaction products from nuclear collisions in space vehicle shielding studies is tested. Comparisons of absorbed-dose and dose-equivalent results obtained with the production and transport of nuclear-reaction products included with similar results obtained using the approximations are presented. The use of the approximations is found to lead to a slight overestimation of the absorbed dose and dose equivalent for a wide range of incident Van Allen belt and solar-flare proton spectra and for a variety of shield thicknesses and shield materials.

References

1. Work funded by National Aeronautics and Space Administration under Order H-38280A.
2. Abstract of ORNL-TM-3785 (Apr. 25, 1972); submitted for journal publication.
3. Mathematics Division.

4.25 ANALYSIS SUBROUTINES FOR THE NUCLEON-MESON TRANSPORT CODE NMTC[1,2]

T. W. Armstrong K. C. Chandler[3]

Several subroutines for analyzing the transport data generated by the nucleon-meson transport code NMTC are described. The principal subroutines compute: (1) flux and current from boundary crossing, (2) flux from collision densities, (3) residual nuclei distributions, and (4) star densities in emulsions. Various auxiliary subroutines are also described.

References

1. Work partially funded by National Aeronautics and Space Administration under Order H-38280A.
2. Abstract of ORNL-4736 (November 1971).
3. Mathematics Division.

4.26 TRAPP, A COMPUTER PROGRAM FOR THE TRANSPORT OF ALPHA PARTICLES AND PROTONS WITH ALL NUCLEAR-REACTION PRODUCTS NEGLECTED[1,2]

J. Barish[3] F. S. Alsmiller
R. T. Santoro R. G. Alsmiller, Jr.

TRAPP is a FORTRAN IV program primarily intended for carrying out studies of the shielding required to protect astronauts against Van Allen belt protons and against solar-flare protons and alpha particles. The program treats the transport of protons and alpha particles through a homogeneous shield and tissue with the assumptions that all nuclear-reaction products may be neglected and all particles travel in a straight line and undergo a continuous slowing down. The geometry considered is that of a spherical shell shield with a tissue sphere at its center. For an isotropically incident proton or alpha-particle flux per unit energy with maximum energy $\leqslant 3$ GeV, the program gives the particle flux per unit energy, the absorbed-dose rate, and the dose-equivalent rate at the center of the tissue sphere as a function of the spherical-shell-shield thickness.

References

1. Work funded by National Aeronautics and Space Administration under Order No. H-38280A.
2. Abstract of ORNL-4763 (in press).
3. Mathematics Division.

5. Medium-Energy Nucleon Spectroscopic Studies

5.0 INTRODUCTION

R. W. Peelle

The last abstract in this section covers the final report on a measurement of the fast-neutron spectrum near the top of the atmosphere using a scintillation spectrometer with sensitivity nearly independent of angle. The results reflect the considerable difficulties associated with such spectroscopy, but no such spectrum now in the literature spans the neutron energy region 5–50 MeV. We have tentatively abandoned efforts to obtain funding to place an instrument of this type onto a satellite to determine the neutron spectrum near the earth but above the atmosphere, largely because the sponsoring agencies seem to have little interest in the use of such a nondirectional instrument even though its relative simplicity would tend to assure obtaining some meaningful results. We frankly question whether complex instruments required for directional response to >10-MeV neutrons would be as likely to yield in space the spectra they are designed to determine.

After a decade of working to determine characteristics of the particle spectra from medium-energy reactions, our space shielding experimental program sponsored by Langley Research Center is expected to terminate within the next year. The prime justification has been to assess the validity of the intranuclear cascade model used to treat nuclear reaction secondaries in space shielding analysis (and other practical applications). This model yields correct secondary spectra within typically 30%, and our results have led to an extension of the model's range of plausible applicability. Extensive comparisons with experimental data do indicate some systematic trends for incident proton energies below 100 MeV which may lead to improvements in such models should further critical applications be identified.

This section includes the first final results for differential neutron production cross sections from nuclear reactions of 60-MeV protons. The results for this case indicate that at least the local version of the intranuclear cascade model predicts within 30% the correct overall secondary intensity at energies above 20 MeV, but the model predicts far too few nucleons at backward angles and too sharp a quasifree scattering distribution at small angles. The similarity of these findings to those for secondary protons, though only the results for aluminum are yet available, already goes far to restrict the types of modifications to the model which may be considered. As expected, although the neutron results will not have the broad coverage which was possible for charged particles, they will prove to be of great importance in defining the reaction mechanisms.

We have hoped in this work to obtain sufficiently interesting results that scientific interest would be regenerated in the continuum regions of the outgoing particle spectra. Such interest has rarely been visible among nuclear physicists, for they have used nuclear reactions primarily to gain insights about nuclear structure. Some interest among physicists has been generated by our work, because it has examined reactions to higher residual excitation levels than have usually been studied. For instance, an awkward but distinct bump in the small-angle (p,p') spectra from several elements now appears to reflect excitation of a giant quadrupole resonance not previously identified. (We had long puzzled why the energy position of the bump did not agree with the position of the known dipole resonance!) Future work which will likely be done at higher energy to study this resonance will almost have to clear up long-standing questions about the behavior of quasifree scattering in the 100- to 200-MeV range.

But it is primarily the nuclear chemists who now seem excited by the profuse secondary particle spectra we have generated for several targets! We should have guessed, for it is the chemists who must be concerned with the whole sweep of reactions which induce transmutations, and this concern logically should lead to interest in particle spectra as well as radiochemical yields. Two or three groups of nuclear chemists are now

actively engaged in working over our data using several versions of cascade and other (Griffin) preequilibrium decay models. If they find success, one can again anticipate further experiments elsewhere which will bear on the applied goals of interest to our sponsors (NASA). This sequence of events may provide an interesting example of "reverse spinoff" of basic knowledge from applied or programmed research which was quite unlikely to be performed as "basic research." By the criterion of value to adjacent disciplines, our group's studies of continuum reactions promise to prove successful.

5.1 FAST FORWARD NEUTRON PRODUCTION IN THE ^{7}Li(p,n)^{7}Be REACTION FOR 40.6- AND 63.8-MeV PROTONS[1,2]

J. W. Wachter T. A. Love
R. T. Santoro W. Zobel

Measurements have been made by the time-of-flight technique of the neutron energy spectra observed at zero degrees from the ^{7}Li(p,n)^{7}Be reaction using 40.6- and 63.8-MeV incident protons. The neutron production cross sections for the fast forward peak are compared with those reported elsewhere, and the suitability of such ^{7}Li targets as a source of monoenergetic neutrons is discussed.

References

1. Work funded by the National Aeronautics and Space Administration under Order L-12,186.
2. Abstract of ORNL-TM-3853.

5.2 DIFFERENTIAL CROSS SECTIONS FOR THE PRODUCTION OF NEUTRONS FROM THE BOMBARDMENT OF C AND Al BY 63.8-MeV PROTONS[1,2]

J. W. Wachter T. A. Love
R. T. Santoro W. Zobel

Differential cross sections in energy and angle have been obtained using time-of-flight spectroscopy for secondary neutrons produced in the reactions of 63.8-MeV protons with C and Al. Neutron energy spectra are given for laboratory angles of 20, 45, 60, and 135° for neutrons with energy above ~10 MeV. The experimental apparatus, neutron detector, electronic instrumentation, and methods of data analysis are described. Comparisons are made between the Al cross sections and the predictions of the intranuclear cascade model of Bertini.

References

1. Work funded by the National Aeronautics and Space Administration under Order L-12,186.
2. Abstract of ORNL-TM-3851.

5.3 MEASUREMENT AND CALCULATION OF RESPONSE FUNCTIONS OF AN NE-213 NEUTRON DETECTOR FOR 15–61.5 MeV[1]

J. W. Wachter T. A. Love
R. T. Santoro W. Zobel

We are presently measuring neutron energy spectra in the range between 10 and 61.5 MeV with a time-of-flight neutron spectrometer utilizing an NE-213 neutron detector. The efficiency of such detectors has been successfully calculated by Monte Carlo techniques. The 05S code of Textor and Verbinski[2] has been used to calculate response functions for a 1.8-in. by 1.8-in.-diam NE-213 scintillator which match those found experimentally in the energy range between 0.2 and 22 MeV.[3] Cohen et al.[4] extended the calibration to 37.4-MeV neutrons and found that the integral efficiency predicted by the 05S computation agreed with experiment when modified cross-section values and an extrapolated proton light curve were used. However, comparison of the response functions calculated with this revised 05S program and responses derived from the pulse-height distributions for 40- to 61.5-MeV neutrons showed poor agreement. In this paper we describe experiments leading to a new estimate of the proton light curve at high energies for use in calculating the efficiency of our detector.

The experimental apparatus has been described in detail previously,[5] and typical energy spectra are presented in ref. 6. In deriving the proton light curve, attention was directed to three spectra from 63.8-MeV proton bombardments which showed readily identifiable peaks: the 61.5-MeV ground-state peak of the ^{7}Li(p,n)^{7}Be reaction as observed at zero degrees; the ^{12}C(p,n)^{12}N ground-state reaction viewed at 20° (neutron peak energy of 44 MeV); and the ^{12}C(p,n)^{12}N reaction observed at 45° (peak energy of 40 MeV). The energy identification of these peaks is independent of the efficiency of the detector and depends only on the flight time–to–amplitude converter and the identification of the prompt gamma flash from the target.

Experimental response functions for 61.5, 44, and 40 MeV were found by obtaining the distribution in pulse height of the neutrons whose time of flight fell within the ground-state peaks. For each such run, a similar

response function was obtained for 15-MeV neutrons, and the pulse-height gain was renormalized by comparison of the experimental 15-MeV response with the computed 15-MeV response. The maximum gain adjustment was 4%. This energy was selected for the normalization because the 05S calculation has been well established at this energy and because the corresponding experimental pulse height lies well within the range of the measurement system.

The curve defined by the X's in Fig. 5.3.1 shows the response function obtained by analysis of the $^7Li(p,n)^7Be$ reaction and is typical of those found in the other runs. At each neutron energy the response shows a shoulder at the high-energy edge which results from (n,p) elastic collisions in the scintillator. In these events the proton is given the full energy of the neutron, recoils in the same direction as the incident neutron, and loses all its energy within the scintillator. The kinematics of the reaction are known, so that the accuracy in predicting the light emitted is dependent only upon the correctness of the relation between the energy deposited by the proton and the consequent light emitted: that is, the "proton light curve."

The experimental estimates of the proton light emitted for these absorbed energies were obtained at the half-height of the distribution edges. The light curve was obtained by extending the Textor and Verbinski curve from 10 MeV so as to pass through the experimental points. The extrapolation of the curve was constrained to conform to Birks'[7] formula for the rate of light emission for absorbed energies above 10 MeV:

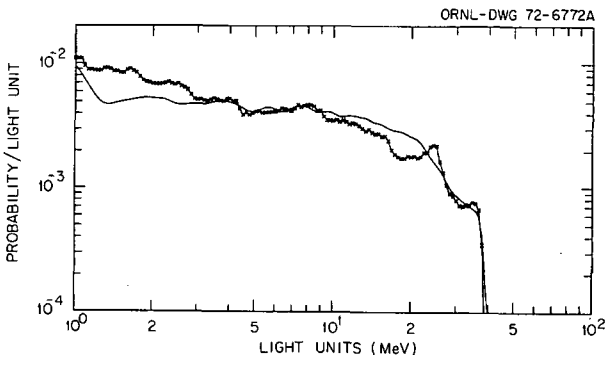

Fig. 5.3.1. Comparison of theoretical and measured response functions for a 3-in.-thick by 3-in.-diam NE-213 liquid scintillator irradiated by monoenergetic 61.5-MeV neutrons. The theoretical curve was calculated using the O5S Monte Carlo code. The experimental results (X's) were inferred using the appropriate time intervals from the secondary-neutron measurements of ^7Li bombarded by 63.8-MeV protons and observed at 0°. The data were normalized to the O5S results in the range between 2 and 30 light units.

the light emitted by the scintillator is then related to the energy absorbed by the expression

$$L = 4.55 + A\int_{10}^{E_p}\left(1 + B\left|\frac{dE}{dx}\right|\right)^{-1} dE\,,$$

where L is the total light, in the Textor and Verbinski light units, emitted by a proton of energy E_p, and dE/dx is the rate of energy deposition along the proton path length. Values of dE/dx as a function of E for the NE-213 scintillator were those of Peelle.[8] The integral is performed from 10 MeV, at which the Textor and Verbinski curve is 4.55. The derived constants were A = 0.69 and B = 0.0025 cm^2/g. Figure 5.3.2 shows the resulting proton light curve with the fitted line shown as a solid line.

Figure 5.3.1 shows the fit obtained between experiment and theory when the revised proton light curve is incorporated into the 05S code. The two curves have been superimposed by normalizing the vertical scale of the experimental curve so as to minimize the value of

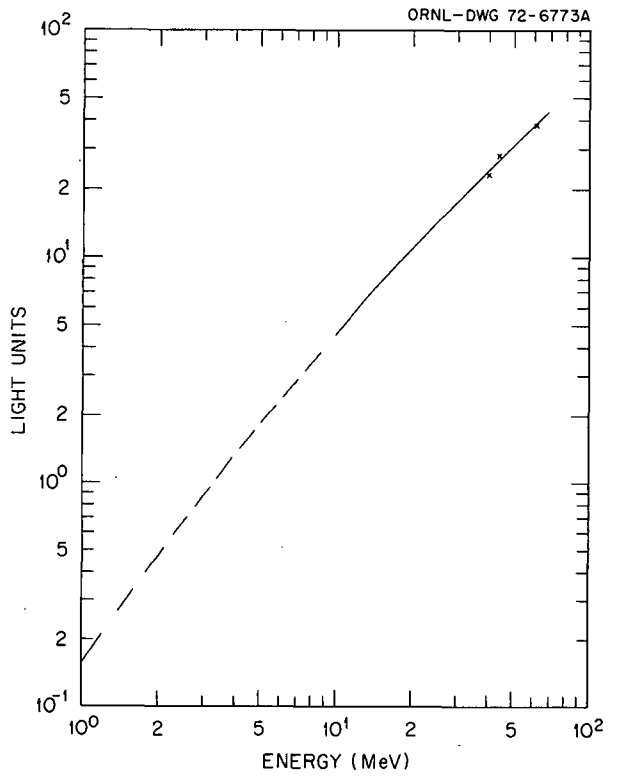

Fig. 5.3.2. Proton light curve for NE-213 inferred from this experiment. The curve has been extrapolated from the data of Textor and Verbinski from 10 to 61.5 MeV using a Birks' law fit to the experimental point (the X's).

χ^2 over the range between 2 and 30 light units. The integrals under the two curves for this same range differ by only 7%, although the curves themselves differ by almost a factor of 2 at some points in the region above 10 light units. While the characteristic peak at the edge of the distribution is reproduced by the calculation, the small peak below this point appears to be distributed into adjacent energy regions.

References

1. Work funded by the National Aeronautics and Space Administration under Order L-12,186.
2. R. E. Textor and V. V. Verbinski, *05S: A Monte Carlo Code for Calculating Pulse-Height Distributions Due to Monoenergetic Neutrons Incident on Organic Scintillators,* ORNL-4160 (1968).
3. V. V. Verbinski et al., *Nucl. Instr. Methods* **65**, 8 (1968).
4. L. D. Cohen et al., *Neutron Phys. Div. Annu. Progr. Rep. May 31, 1969,* ORNL-4433, p. 108.
5. J. W. Wachter et al., *Neutron Phys. Div. Annu. Progr. Rep. May 31, 1970,* ORNL-4592, p. 104.
6. J. W. Wachter et al., *Neutron Phys. Div. Annu. Progr. Rep. May 31, 1971,* ORNL-4705, p. 101.
7. J. B. Birks, *Proc. Phys. Soc.* **A64**, 74 (1952).
8. R. W. Peelle, *Rapid Computation of Specific Energy Losses for Energetic Charged Particles,* ORNL-TM-977 (April 1965).

5.4 DIFFERENTIAL CROSS SECTIONS FOR HYDROGEN AND HELIUM PARTICLES FROM 30- TO 60-MeV PROTONS ON NUCLEI

R. W. Peelle F. E. Bertrand[1]

Analysis is nearing conclusion of data from our cyclotron experiments on charged particles from 30- to 60-MeV protons on nuclei. The last of the nuclear data reports, that for carbon and oxygen targets, is now being drafted while summarizing studies are being made in preparation for final overall publication. Some spinoff research by Lewis and Bertrand, under other sponsorship, has identified a (isoscalar quadrupole) giant resonance excitation in the small-angle (p,p') spectra from several targets bombarded by 60-MeV protons.[2] Similar excitation spectra were seen long ago for incident 182-MeV protons, but were identified to be from dipole excitation.[3]

Figure 5.4.1 illustrates some of the observed differential cross sections for protons from 61-MeV protons on carbon, compared with the predictions of the Bertini version of the intranuclear cascade model.[4] Excitation of discrete residual states plays the marked role expected for this target. Data for oxygen are similar, except that excitations of discrete states are less strong and the experimental data are less precise, because the effects of carbon reactions had to be subtracted from data obtained with targets which contained both carbon and oxygen.

Figure 5.4.2 shows a summary of observed angle-integrated particle yields for secondaries with kinetic energy greater than 20 MeV in the laboratory system. Observed integral cross sections were divided by the nonelastic cross section predicted by the Bertini calculation.[4,5] The proton yields given by the cascade calculation are shown for comparison. This method of presentation eliminates effects of variable evaporation contributions but risks some inequity of treatment induced by the differences among the Q values for the various targets. Note the similar behavior of cross sections for protons and deuterons, and the widely divergent behavior of cross sections for production of ^{3}H and ^{3}He. If the observed integral cross sections for protons are divided by $A^{1/3}$ (a length proportional to the nuclear perimeter), a constant value is obtained for all the targets as heavy as aluminum. Similar results were previously shown for cross sections observed at 30°.[6]

References

1. Physics Division.
2. M. B. Lewis and F. E. Bertrand, submitted to *Nuclear Physics.*
3. H. Tyren and Th. A. J. Maris, *Nucl. Phys.* **4**, 637 (1957); **6**, 446 (1958); **7**, 24 (1958).
4. H. W. Bertini, *Phys. Rev.* **131**, 1801 (1963).
5. H. W. Bertini, *Phys. Rev. C,* to be published in June 1972.
6. R. W. Peelle and F. E. Bertrand, *Neutron Phys. Div. Annu. Progr. Rep. May 31, 1970,* ORNL-4592, p. 101.

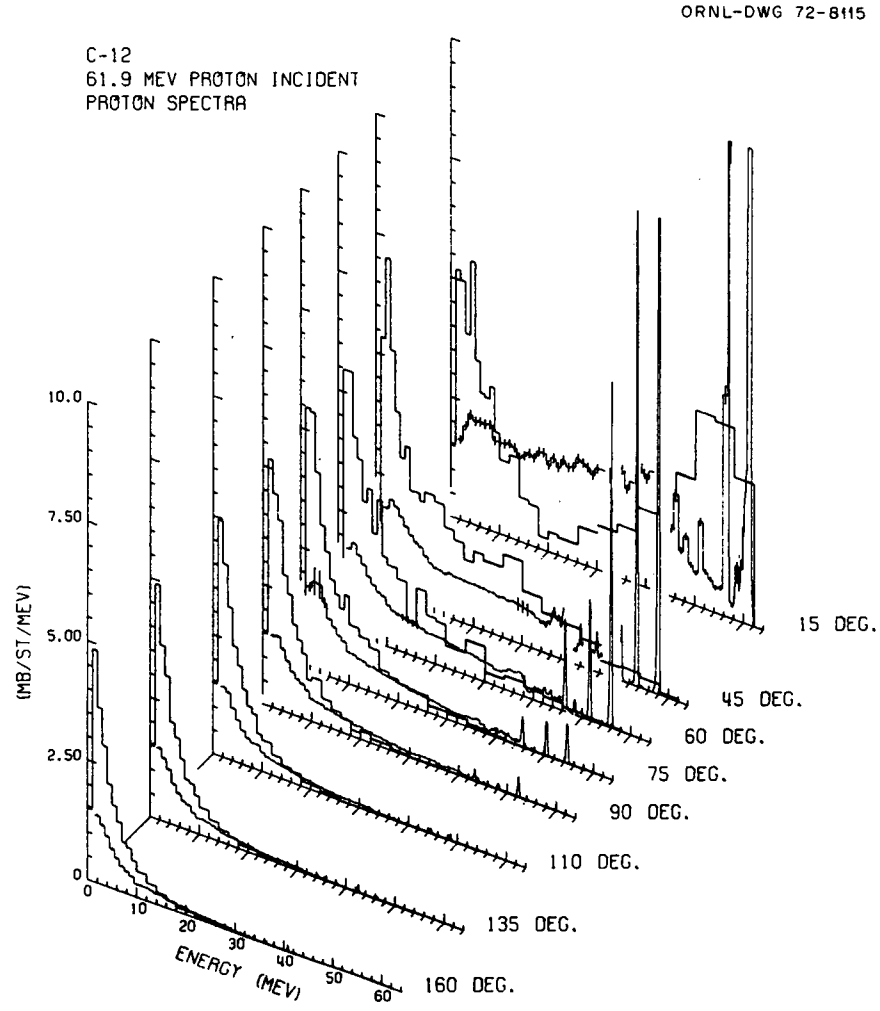

Fig. 5.4.1. Selected differential cross sections for the $^{12}C(p,xp)$ reaction at 61.9 MeV incident energy. In the continuum region the experimental spectra have been averaged over 1-MeV bins. For comparison the predictions of the Bertini intranuclear cascade (plus evaporation) model are plotted with somewhat broader bins. The calculation predicts too much evaporation strength and too much peaking of the quasifree scattering at small angles.

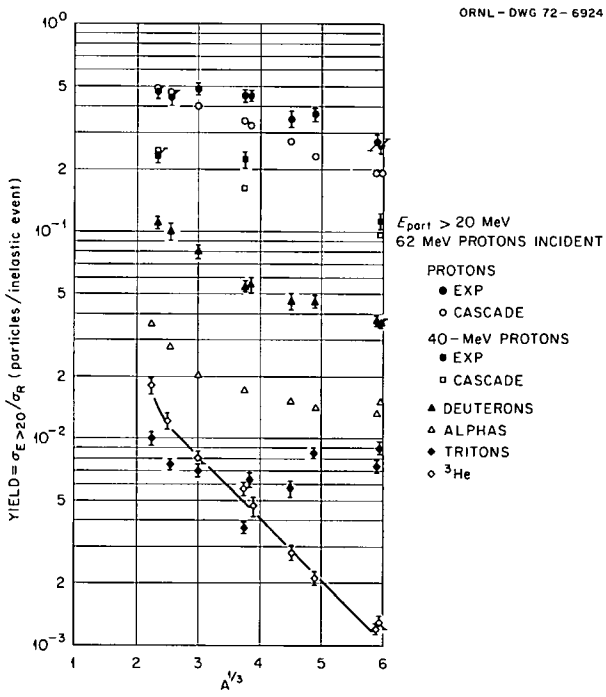

Fig. 5.4.2. Yields per nonelastic reaction of particles with energy >20 MeV produced by 61-MeV protons. For secondary protons some analogous results for incident 39-MeV protons are also shown, as are the predictions of the Bertini intranuclear cascade for both incident energies.

5.5 A HIGH-RESOLUTION SPECTROMETER SYSTEM WITH PARTICLE IDENTIFICATION FOR 1- THROUGH 60-MeV HYDROGEN AND HELIUM PARTICLES[1,2]

F. E. Bertrand[3] N. W. Hill[5]
W. R. Burrus[4] T. A. Love
R. W. Peelle

A coincidence semiconductor spectrometer system based on a Ge(Li) total-absorption detector has been applied to the simultaneous spectroscopy of all charge 1 and 2 particles from targets bombarded with protons with energy up to 62 MeV. Output spectra cover the range from the full energy down to a 1- to 5-MeV threshold which depends on particle type. The method for choosing the thicknesses for the two ΔE detectors is discussed, and unusual features of the system are described. Particles too slow to penetrate the first ΔE counter were sorted according to mass using the flight-time vs E discrimination, while the more energetic particles were separated using two sets of $\Delta E \times E$ discrimination. Germanium detectors thick enough to stop 60-MeV protons were used with particles entering perpendicular to or parallel to the field lines, and in either case the only significant inactive region in the path of the detected particles was the protective foil over the Ge(Li) detector. The typical pulse-height resolution of the system was about 200 keV for 60-MeV protons, although a germanium detector used alone gave 55-keV resolution at this energy. Analysis was performed after the experiments, using magnetic tapes written by an on-line computer; corrections to the pulse-height spectra for reaction and collimator tails are discussed. The electronic logic system is described, including portions for event characterization, for use on an "active" detector collimator, and for pileup pulse rejection based on timing information.

References

1. Research sponsored by National Aeronautics and Space Administration under Order L-12,186.
2. Abstract of ORNL-TM-3669; also to be published in *Nuclear Instruments and Methods.*
3. Physics Division.
4. Present address: Tennecomp, Inc., Oak Ridge, Tennessee.
5. Instrumentation and Controls Division.

5.6 ELASTIC SCATTERING OF 40-MeV PROTONS FROM ^{48}Ti, ^{nat}Cr, AND ^{64}Zn: TABULATED DIFFERENTIAL CROSS SECTIONS[1]

J. K. Dickens F. G. Perey
E. E. Gross[2] A. Van der Woude[2]
A. Zucker[3]

Numerical values of differential cross sections for elastic scattering of 40-MeV protons from targets of ^{48}Ti, ^{nat}Cr, and ^{64}Zn for scattering angles between 10 and 145° are reported in tabular form.

References

1. Abstract of ORNL-TM-3591 (October 1971).
2. Physics Division.
3. National Academy of Sciences, 2101 Constitution Ave., Washington, D.C. 20418.

5.7 MEASUREMENT OF THE NEUTRON ENERGY SPECTRUM AT 9-g/cm^2 RESIDUAL ATMOSPHERE[1,2]

W. Zobel C. O. McNew[3]
T. A. Love R. H. Baldry[4]
J. T. DeLorenzo[3] H. W. Parker[5]

An experiment to measure the neutron energy spectrum at an altitude corresponding to 9-g/cm^2 residual

atmosphere was performed near solar maximum. The nondirectional spectrometer employed was flown at geomagnetic latitude 40° N from Palestine, Texas, on June 17, 1969. The experimental arrangement is described, the data reduction scheme is discussed, and the results are presented for the neutron spectrum in the energy range 3 to 60 MeV. The spectrum is compared with those from other experiments and from calculations. The spectrum is consistent with the calculation of Lingenfelter after application of an altitude correction, but is lower than the measurement of Preszler, Simnett, and White or the calculations of Armstrong, Chandler, and Barish. Except for an apparent but likely spurious peak at 20 MeV of intensity ~0.04 neutron cm^{-2} sec^{-1}, the spectrum between 4 and 50 MeV is approximated quite well by $\phi(E) = 0.6\ E^{-1.54}$ neutrons cm^{-2} sec^{-1} MeV^{-1} with E expressed in MeV.

References

1. Work partially supported by National Aeronautics and Space Administration; flight costs and participation by NASA personnel provided by NASA-MSFC (Space Science Laboratory), Huntsville, Alabama.

2. Abstract of ORNL-TM-3877 (to be published); also to be submitted to the *Journal of Geophysical Research.*

3. Instrumentation and Controls Division.

4. Present address: ORTEC, Inc., Oak Ridge, Tennessee

5. Marshall Space Flight Center, Huntsville, Alabama.

Publications and Papers Presented at Scientific Meetings

PUBLICATIONS

ALSMILLER, R. G., JR., F. S. ALSMILLER, J. BARISH, AND Y. SHIMA

"Muon Transport and Shielding of High-Energy (≤500 GeV) Proton Accelerators," in *Proceedings of International Congress on Protection against Accelerator and Space Radiation, CERN, Geneva, Switzerland, April 26–30, 1971,* CERN-71-16, vol. 2, p. 601. (4.16)*

ARMSTRONG, T. W.

"Calculation of the Lunar Photon Albedo from Galactic and Solar Proton Bombardment," *J. Geophys. Res.* **77**, 525 (1971). (4.10)

"Radiation Transport Codes for Potential Applications Related to Radiobiology and Radiotherapy Using Protons, Neutrons, and Negatively Charged Pions," ORNL-TM-3816 (1972). (4.23)

ARMSTRONG, T. W., AND R. G. ALSMILLER, JR.

"Calculation of Cosmogenic Radionuclides in the Moon and Comparison with Apollo Measurements," *Geochim. Cosmochim. Acta, Suppl. 2, Vol. 2, Proc. Second Lunar Science Conf.*, 1729–1745, M.I.T. Press (1971). (4.9)

ARMSTRONG, T. W., R. G. ALSMILLER, JR., K. C. CHANDLER, AND B. L. BISHOP

"Monte Carlo Calculations of High-Energy Nucleon-Meson Cascades and Comparison with Experiment," ORNL-TM-3667 (Jan. 5, 1972). (4.5)

ARMSTRONG, T. W., AND B. L. BISHOP

"Calculation of the Absorbed Dose and Dose Equivalent Induced by Medium-Energy Neutrons and Protons and Comparison with Experiment," *Radiat. Res.* **47**, 581 (1971). (4.19)

ARMSTRONG, T. W., AND K. C. CHANDLER

"Monte Carlo Calculations of the Dose Induced by Charged Pions and Comparison with Experiment," ORNL-TM-3678 (Feb. 4, 1972). (4.21)

"Analysis Subroutines for the Nucleon-Meson Transport Code NMTC," ORNL-4736 (1971). (4.25).

"Calculation of the Absorbed Dose and Dose Equivalent from Neutrons and Protons in the Energy Range from 3.5 GeV to 1.0 TeV," ORNL-TM-3758 (May 1972). (4.13)

BARISH, J., R. T. SANTORO, F. S. ALSMILLER, AND R. G. ALSMILLER, JR.

"TRAPP, a Computer Program for the Transport of Alpha Particles and Protons with All Nuclear-Reaction Products Neglected," ORNL-4763 (1972). (4.26).

BARTINE, D. E., R. G. ALSMILLER, JR., F. R. MYNATT, W. W. ENGLE, JR., AND J. BARISH

"Low-Energy Electron Transport by the Method of Discrete Ordinates," *Nucl. Sci. Eng.* **48**, 159–178 (1972). (4.17)

---

*Abstract of paper published in this report under this number.

BERTINI, H. W.

"Reaction Cross Sections for 30- to 60-MeV Protons on Various Elements: Comparison of Theoretical Results with Experiment," *Phys. Rev.* **C(5)**, 2118 (1972).

BERTINI, H. W., A. H. CULKOWSKI, M. P. GUTHRIE, AND O. W. HERMANN

"MECC-3, a Monte Carlo Intranuclear-Cascade Code for Medium-Energy (<3500 MeV) Particle-Nucleus Collisions," Computer Code Abstract, *Nucl. Sci. Eng.* **46**, 437 (1971).

BERTINI, H. W., AND M. P. GUTHRIE

"Results from Medium-Energy Intranuclear-Cascade Calculation," *Nucl. Phys.* **A169**, 670 (1971). (4.3)

BERTINI, H. W., MIRIAM P. GUTHRIE, AND ARLINE H. CULKOWSKI

"Nonelastic Interactions of Nucleons and π-Mesons with Complex Nuclei at Energies below 3 GeV," ORNL-TM-3148 (Mar. 28, 1972). (4.1)

BERTRAND, F. E., W. R. BURRUS, N. W. HILL, T. A. LOVE, AND R. W. PEELLE

"A High Resolution Spectrometer System with Particle Identification for 1- through 60-MeV Hydrogen and Helium Particles," ORNL-TM-3669 (January 1972). (5.5)

BOOTH, R. S., AND F. J. MUCKENTHALER

"The Total Gamma-Ray Energy Spectrum above 1 MeV from Neutron Interactions in ^{235}U and ^{238}U," ORNL-4691 (August 1971).

BOOTH, R. S., J. E. WHITE, S. K. PENNY, AND K. J. YOST

"A Comparison of Calculated and Measured Energy-Dependent Capture Gamma-Ray Yields in ^{238}U," *Nucl. Sci. Eng.* **47**, 8 (1972). (2.36)

BURGART, C. E.

"MORSE Monte Carlo Shielding Calculations for the Zirconium Hydride Reference Reactor," ORNL-TM-3366 (Aug. 26, 1971). (2.50)

"Capabilities of the MORSE Multigroup Monte Carlo Code in Solving Reactor Eigenvalue Problems," ORNL-TM-3662 (Dec. 17, 1971). (2.26)

"Neutron and Gamma-Ray Fluence Transmitted through a Slab of Borated Polyethylene – a Milestone Calculation," ORNL-TM-3517 (Mar. 22, 1972). (2.17)

BURGART, C. E., AND M. B. EMMETT

"Monte Carlo Calculations of the Response Functions of Bonner Ball Neutron Detectors," ORNL-TM-3739 (Apr. 3, 1972). (2.6)

BURGART, C. E., AND E. A. STRAKER

"XCHEKR – a Multigroup Cross-Section Editing and Checking Code," ORNL-TM-3518 (Aug. 13, 1971). (2.23)

CHANDLER, K. C., AND T. W. ARMSTRONG

"Operating Instructions for the High-Energy Nucleon-Meson Transport Code HETC," ORNL-4744 (January 1972). (4.15)

CLAIBORNE, H. C., AND W. W. ENGLE, JR.

"Bracketing the Peak Primary Gamma-Ray Dose Rate from Nuclear Devices by Steady-State Transport Calculations," *Nucl. Sci. Eng.* **13**, 209 (1972). (2.25)

CLIFFORD, C. E., F. R. MYNATT, P. N. STEVENS, F. J. MUCKENTHALER, R. M. FREESTONE, JR., M. L. GRITZNER, K. M. HENRY, L. B. HOLLAND, J. L. HULL, J. LEWIN, J. J. MANNING, AND J. N. MONEY

"Experimental Investigation of Neutron Streaming through the Grid-Plate Shield of the Fast Flux Test Facility," ORNL-TM-3514 (Oct. 5, 1971). (2.2)

DICKENS, J. K.

"Al($n,x\gamma$) Reactions for $5.3 \leqslant E_n \leqslant 9.0$ MeV," *Phys. Rev.* **C(5)**, 100 (January 1972). (2.37)

"Self-Absorption of Gamma Rays Produced in Large Cylindrical Samples," *Nucl. Instrum. Methods* **98**, 451 (1972). (2.31)

"Energies and Intensities of Gamma Rays Emitted by a ^{226}Ra Source," ORNL-TM-3509 (Aug. 13, 1971). (2.29)

"The ^{23}Na($n,x\gamma$) Reaction for $4.85 \leqslant E_n \leqslant 7.5$ MeV," ORNL-TM-3737 (Mar. 3, 1972). (2.39)

"Level Structure of ^{54}Mn," ORNL-TM-3674 (Jan. 14, 1972). (2.40)

"Ca($n,x\gamma$) Reactions for $4.85 \leqslant E_n \leqslant 8.05$ MeV," ORNL-TM-3584 (Oct. 4, 1971). (2.33)

"The Neutron-Induced Gamma-Ray Reactions in Calcium in the Energy Range $4.85 \leqslant E_n \leqslant 8.5$ MeV," *Nucl. Sci. Eng.* **48**, 78 (1972). (2.33)

DICKENS, J. K., E. E. GROSS, F. G. PEREY, A. VAN DER WOUDE, AND A. ZUCKER

"Elastic Scattering of 40-MeV Protons from ^{48}Ti, ^{nat}Cr, and ^{64}Zn: Tabulated Differential Cross Sections," ORNL-TM-3591 (Oct. 7, 1971). (5.6)

DICKENS, J. K., G. L. MORGAN, AND F. G. PEREY

"Gamma-Ray Production Due to Neutron Interactions with Iron for Incident Neutron Energies between 0.8 and 20 MeV: Tabulated Differential Cross Sections," ORNL-4798 (1972). (2.38)

FORD, W. E., III, AND J. S. GILLEN

"Calculated Perturbations in Threshold Foil Measurements Due to Neutron Interactions in B_4C Shells," ORNL-TM-3519 (Sept. 3, 1971). (2.47)

"The Testing of ^{238}U Secondary Gamma Ray Production Data Sets from the POPOP4 Library," ORNL-TM-3482 (February 1972). (2.41)

FU, C. Y., AND F. G. PEREY

"An Evaluation of Neutron and Gamma-Ray Production Cross Sections for Lead," ORNL-4765 (March 1972). (2.27)

GABRIEL, T. A., M. P. GUTHRIE, AND O. W. HERMANN

"PICA, a Monte Carlo Intranuclear-Cascade Code Package for Medium-Energy (30 to 400 MeV) Photon-Induced Nuclear Reactions," Computer Code Abstract, *Nucl. Sci. Eng.* **47**, 243 (1972).

GABRIEL, T. A., AND R. T. SANTORO

"Nucleon and Charged-Pion Albedo Spectra in an Accelerator Cave from 200-GeV Proton Interactions in Iron," *Nucl. Instrum. Methods* **99**, 5 (1972); also ORNL-TM-3437 (Aug. 27, 1971). (4.7)

"Calculation of the Long-Lived Activity in Soil Produced by 500 GeV Protons," *Nucl. Instrum. Methods* **95**(2), 275 (1971). (4.6)

GABRIEL, T. A., R. T. SANTORO, AND J. BARISH

"A Calculational Method for Predicting Particle Spectra from High-Energy Nucleon and Pion Collisions ($\geqslant$3 GeV) with Protons," ORNL-TM-3615 (Nov. 1, 1971). (4.14)

IRVING, D. C.

"Description of the CDC-1604 Version of the O6R Neutron Monte Carlo Transport Code," ORNL-TM-3458 (June 1971).

KINNEY, W. E., AND F. G. PEREY

"Neutron Elastic- and Inelastic-Scattering Cross Sections for Oxygen in the Energy Range 4.34 to 8.56 MeV," ORNL-4780 (April 1972). (1.1)

KUMAR, K.

"Intrinsic Quadrupole Moments and Shapes of Nuclear Ground State and Excited States," *Phys. Rev. Lett.* **28**, 249 (1972).

LEWIN, J.

"A Brief Summary of Dr. Glenn T. Seaborg's Visit to the U.S.S.R., August 1971," ORNL-TM-3860 (June 1972).

MAIENSCHEIN, F. C.

"Neutron Cross Section Measurements of Reactor Interest with the Oak Ridge Electron Linear Accelerator (ORELA)," ORNL-TM-3833 (May 1972).

MASKEWITZ, B. F.

"A Computer Code Center – Experience and Current Operations," *Proceedings of the Symposium on Sharing of Programs and Technology in Nuclear Medicine, April 2–3, 1971,* CONF-710425 (September 1971). (3.15)

McGREGOR, B. J., AND E. A. STRAKER

"A Study of the Effects of Source Asymmetry on Time-Dependent Neutron and Secondary Gamma-Ray Transport in Air," ORNL-4741 (February 1972). (2.13)

MORGAN, G. L., T. A. LOVE, J. K. DICKENS, AND F. G. PEREY

"Gamma-Ray Production Cross Sections of Tantalum and Carbon for Incident Neutron Energies between 0.007 and 20.0 MeV," ORNL-TM-3702 (Feb. 8, 1972). (2.35)

MYNATT, F. R., R. G. ALSMILLER, JR., AND L. R. WILLIAMS

"A Study of Mine Detection by Means of Neutron-Induced Gamma Rays," Technical Note, *Nucl. Appl. Technol.* **12**, 329 (1971).

MYNATT, F. R., et al.

"Fast Reactor Shielding Monthly Progress Report for June, 1971, 189A No. 10028, Activity No. 40 01 61," ORNL-TM-3521 (Aug. 1, 1971).

"Fast Reactor Shielding Monthly Progress Report for July, 1971, 189A No. 10028, Activity No. 40 01 61," ORNL-TM-3538 (Aug. 25, 1971).

"Fast Reactor Shielding Monthly Progress Report for August, 1971, 189A No. 10028, Activity No. 40 01 61," ORNL-TM-3573 (Sept. 17, 1971).

"Fast Reactor Shielding Monthly Progress Report for September, 1971, 189A No. 10028, Activity No. 40 01 61," ORNL-TM-3606 (Oct. 18, 1971).

"Fast Reactor Shielding Monthly Progress Report for October, 1971, 189A No. 10028, Activity No. 40 01 61," ORNL-TM-3639 (Nov. 24, 1971).

"Fast Reactor Shielding Monthly Progress Report for November, 1971, 189A No. 10028, Activity No. 40 01 61," ORNL-TM-3666 (Dec. 31, 1971).

"Fast Reactor Shielding Monthly Progress Report for December, 1971, 189A No. 10028, Activity No. 40 01 61," ORNL-TM-3695 (Jan. 31, 1972).

"Fast Reactor Shielding Monthly Progress Report for January, 1972, 189A No. 10028, Activity No. 40 01 61," ORNL-TM-3746 (Feb. 25, 1972).

"Fast Reactor Shielding Monthly Progress Report for February, 1972, 189a No. 10028, Activity No. 40 01 61," ORNL-TM-3786 (Apr. 7, 1972).

"Fast Reactor Shielding Monthly Progress Report for March, 1972, 189a No. 10028, Activity No. 40 01 61," ORNL-TM-3800 (May 15, 1972).

MYNATT, F. R., C. E. CLIFFORD, F. J. MUCKENTHALER, R. E. MAERKER, M. L. GRITZNER, L. R. WILLIAMS, AND J. L. RATHBUN

"FFTF Related Studies in the ORNL-LMFBR Shielding Program," ORNL-3705 (Mar. 27, 1972). (2.1)

PACE, J. V., III, F. R. MYNATT, AND L. S. ABBOTT

"The Relative Importance of Neutron Capture and Inelastic Scattering Interactions to the Secondary Gamma-Ray Dose Transmitted through Laminated Tungsten and Lithium Hydride SNAP Reactor Shields," ORNL-TM-3270 (CTC-41) (Apr. 12, 1972). (2.51)

PEELLE, R. W.

"Techniques Used at Oak Ridge National Laboratory for Unfolding Neutron and Gamma-Ray Pulse Height Spectra," ORNL-TM-3463 (August 1971). (1.16)

PEREY, F. G., AND W. E. KINNEY

"On a Possible Resolution of the Nitrogen Nonelastic Cross-Section Discrepancy below 9 MeV," *Nucl. Sci. Eng.* **46**, 428 (1971). (2.28)

PEREZ, R. B.

"A General Formalism for Computing the Transition Matrix of Nuclear Reaction Theory, and Its Application to the Treatment of Coupled Channel Equations," ORNL-TM-3778 (May 1972). (1.14)

PEREZ, R. B., G. de SAUSSURE, E. G. SILVER, R. W. INGLE, AND H. WEAVER

"Simultaneous Measurements of the Neutron Fission and Capture Cross Sections for ^{235}U for Neutron Energies from 8 eV to 10 keV," ORNL-TM-3696 (1972). (1.5)

ROUSSIN, R. W.

"Abstracts of the Data Library Packages Assembled by the Radiation Shielding Information Center," ORNL-RSIC-30, Vol. 1 (March 1972). (3.9)

ROUSSIN, R. W., R. G. ALSMILLER, JR., AND J. BARISH

"Shielding against Neutrons in the Energy Range 15 to 75 MeV," ORNL-TM-3659 (December 1971). (3.5)

SANTORO, R. T., R. G. ALSMILLER, JR., AND J. BARISH

"The Validity of Using Only Primary Protons in Van Allen Belt and Solar-Flare Proton Shielding Studies," ORNL-TM-3785 (May 1972). (4.24)

SANTORO, R. T., AND T. A. GABRIEL

"Nucleon and Pion Star Production from High-Energy (>40 GeV) Protons Incident on Iron," letter to *Nucl. Instrum. Methods* **95**(2), 369 (1971).

"Calculation of the Nucleon- and Pion-Induced Star and Flux Distributions from 400-GeV Proton Interactions in Iron," ORNL-4673 (October 1971).

SOLOMITO, M., P. N. STEVENS, E. A. STRAKER, C. E. BURGART, AND S. N. CRAMER

"Methods of Biasing Secondary Gamma-Ray Production in Coupled Neutron Gamma-Ray Monte Carlo Calculations," ORNL-TM-3530 (Dec. 8, 1971). (2.21)

STEVENS, P. N., AND D. K. TRUBEY

"Methods for Calculating Neutron and Gamma-Ray Attenuation," Chap. 3 Rev. of *Weapons Radiation Shielding Handbook*, L. S. Abbott, H. C. Claiborne, and C. E. Clifford, eds., DNA-1892-3 Rev. 1 (formerly DASA-1892-3) (March 1972).

STRAKER, E. A.

"The Effect of the Ground on the Steady-State and Time-Dependent Transport of Neutrons and Secondary Gamma Rays in the Atmosphere," *Nucl. Sci. Eng.* **46**, 334 (1971); also ORNL-TM-3754 (Mar. 21, 1972). (2.10)

STRAKER, E. A., C. E. BURGART, T. A. LOVE, AND R. M. FREESTONE, JR.

"Simultaneous Determination of Fast-Neutron Spectra by Time-of-Flight and Pulse-Height Unfolding Techniques," *Nucl. Instrum. Methods* **97**, 275 (1971).

STRAKER, E. A., AND M. B. EMMETT

"Collision Site Plotting Routines and Collision Density Fluence Estimates for the MORSE Monte Carlo Code," ORNL-TM-3585 (Oct. 5, 1971). (2.20)

"MORSEC, a Revised Cross-Section Module for the MORSE Multigroup Monte Carlo Code," ORNL-4716 (August 1971). (2.39)

STRAKER, E. A., M. B. EMMETT, B. J. McGREGOR, J. V. PACE III,
R. W. ROUSSIN, H. T. SMITH, AND L. R. WILLIAMS

"Investigation of the Adequacy of Nitrogen Cross-Section Sets: Comparison of Neutron and Secondary Gamma-Ray Transport Calculations with Integral Experiments," ORNL-TM-3768 (1972). (2.14)

STRAKER, E. A., T. A. LOVE, C. E. BURGART, R. M. FREESTONE, JR., AND G. L. MORGAN

"Some Tests Related to the Use of Proton Recoil Proportional Counters for Neutron-Flux Measurements," ORNL-TM-3631 (Nov. 16, 1971). (2.5)

STRAKER E. A., AND B. J. McGREGOR

"A Calculation of Gamma-Ray Production and Transport in Liquid Nitrogen," ORNL-TM-3635 (1971). (2.15)

STRAKER, E. A., J. V. PACE III, M. B. EMMETT, W. W. ENGLE, JR.,
F. R. MYNATT, L. R. WILLIAMS, AND L. S. ABBOTT

"Penetration into a Missile Silo of Neutrons and Secondary Gamma Rays Produced by Point Isotropic Neutron Sources," ORNL-TM-3599 (Dec. 20 1971) (classified). (2.16)

TRUBEY, D. K., AND H. E. COMOLANDER (Compiled by)

"A Review of Calculations of Radiation Transport in Air – Theory, Techniques, and Computer Codes – Proceedings of a Seminar, Nov. 15–17, 1971," ORNL-RSIC-33 (CONF-711125) (May 1972). (3.14)

WHITE, J. E., C. Y. FU, AND K. J. YOST

"A Calculation of Neutron Energy-Dependent Capture Gamma-Ray Yield Spectra for Iron and Comparisons with Experiment," ORNL-TM-3442 (Aug. 30, 1971). (2.48)

YOST, K. J., J. E. WHITE, C. Y. FU, AND W. E. FORD III

"Neutron Energy-Dependent Capture Gamma-Ray Yields in Tantalum and Tungsten," *Nucl. Sci. Eng.* **47**, 209 (1972). (2.43)

ZOBEL, W., AND M. E. HALL, JR.

"GAINCALB – a Program Package to Determine the Gain Used with Organic Scintillation Detectors," ORNL-TM-3598 (Oct. 13, 1971).

PAPERS

American Nuclear Society Meeting, Boston, Massachusetts, June 13–17, 1971.

de SAUSSURE, G., R. B. PEREZ, E. G. SILVER, and R. W. INGLE, "Simultaneous Measurements of the Neutron Fission and Capture Cross Sections of ^{235}U for Energies up to 100 keV."

PEELLE, R. W., "Techniques Used at Oak Ridge National Laboratory for Unfolding Neutron and Gamma-Ray Pulse-Height Spectra." (1.16)

TTCP Working Panel N-6, London, England, September 21–24, 1971.

MYNATT, F. R., "A Review of Progress in the Calculational Capability for Radiation Transport in the Atmosphere."

STRAKER, E. A., "Evaluation of the Adequacy of Nitrogen Cross Section Sets Based on Comparison of Transport Calculations with Integral Experiment Results." (2.14)

American Nuclear Society Winter Meeting, Miami, Florida, October 17–21, 1971; Trans. Amer. Nucl. Soc. **14** (1971).

ARMSTRONG, T. W., "Calculation of the Lunar Photon Albedo," p. 906.

ARMSTRONG, T. W., R. G. ALSMILLER, JR., AND K. C. CHANDLER, "Calculation of Depth-Dose Distributions Produced in Tissue by Negative Pions," p. 523. (4.22)

BURGART, C. E., E. A. STRAKER, T. A. LOVE, G. L. MORGAN, AND R. M. FREESTONE, JR., "Measurements and Calculations of Time-Dependent Gamma-Ray Spectra Emerging from Polyethylene Slabs Pulsed with Neutrons," p. 923.

FORD, W. E., III, F. J. MUCKENTHALER, AND J. S. GILLEN, "The Testing of Uranium Secondary Gamma-Ray Production Data," p. 900.

GABRIEL, T. A., AND R. T. SANTORO, "Calculation of the Long-Lived Activity in Soil Produced by 500-GeV Protons," p. 892.

MAERKER, R. E., AND F. J. MUCKENTHALER, "Comparison of Calculations Using ENDF/B Material 1124 Neutron Data with Experiment," p. 922.

MYNATT, F. R., C. E. CLIFFORD, F. J. MUCKENTHALER, R. E. MAERKER, M. L. GRITZNER, L. R. WILLIAMS, AND J. L. RATHBUN, "FFTF Related Studies in the ORNL-LMFBR Shielding Program," p. 935. (2.1)

ROUSSIN, R. W., E. A. STRAKER, AND G. W. MORRISON, "O6R Calculations of Nitrogen and Iron LRL Pulsed Sphere Experiments," p. 925.

SANTORO, R. T., AND T. A. GABRIEL, "Hadron-Induced Spectra from 200- and 400-MeV Proton Interactions," p. 891.

SILVER, E. G., G. de SAUSSURE, AND R. B. PEREZ, "Averaged ^{238}U Capture Cross Sections between 100 and 1200 eV," p. 808. (1.6)

STRAKER, E. A., AND G. W. MORRISON, "Analysis of Neutron and Gamma-Ray Transport Using the O6R and OGRE Codes," p. 919.

American Physical Society Meeting, Tucson, Arizona, November 4–6, 1971.

DICKENS, J. K., "Ca($n,x\gamma$) Reactions for $4.85 \leqslant E_n \leqslant 8.05$ MeV." (2.33)

RSIC Seminar-Workshop on Radiation Transport in Air, Oak Ridge National Laboratory, November 15–17, 1971.

McGREGOR, B. J., "Effects of Source Asymmetry on Radiation Transport in Infinite Air." (2.13)

PEREY, F. G., "Status of Nitrogen and Oxygen Cross Sections."

STRAKER, E. A., "Comparison of Calculations with Integral Experiments with Emphasis on Secondary Gamma Rays." (2.14)

IAEA Seminar on Numerical Reactor Calculations, Vienna, Austria, January 17–21, 1972.

BURGART, C. E., "Capabilities of the MORSE Multigroup Monte Carlo Code in Solving Reactor Eigenvalue Problems." (2.26)

Second Symposium on the Sharing of Computer Programs and Technology in Nuclear Medicine, April 21–22, 1972; proceedings published as CONF-720430 (July 1972).

ARMSTRONG, T. W., "Radiation-Transport Computer Codes."

MASKEWITZ, B. F., AND W. J. McCLAIN, "Some Guidelines for Documentation Practices as an Aid in the Sharing of Computer Programs and Technology."

Cross Section Evaluation Working Group Meeting, May 9–10, 1972, Brookhaven National Laboratory, Upton, Long Island, New York.

de SAUSSURE, GERARD, "Resonance Reaction Formalisms for Fissile Nuclei." (1.9)

American Nuclear Society Meeting, Las Vegas, Nevada, June 18–22, 1972; Trans. Amer. Nucl. Soc. **15** (1972).

ARMSTRONG, T. W., K. C. CHANDLER, AND J. BARISH, "Calculation of the Neutron Spectrum in the Earth's Atmosphere Produced by Galactic Cosmic Rays," p. 562. (4.11)

BARTINE, D. E., R. G. ALSMILLER, JR., F. R. MYNATT, W. W. ENGLE, JR., AND J. BARISH, "Electron Transport by the Method of Discrete Ordinates," p. 580.

CRAMER, S. N., "Heterogeneous Calculations of ZPR-III Assembly 48 by Monte Carlo," p. 460.

CRAMER, S. N., AND R. W. ROUSSIN, "Cross Section Sensitivity Calculations for the LLL Pulsed Sphere Experiments," p. 529.

GABRIEL, T. A., T. W. ARMSTRONG, AND K. C. CHANDLER, "Energy Deposition in Ionization Spectrometers," p. 536.

GREENE, N. M., AND F. R. MYNATT, "The AMPX Modular Code Systems for Generating Coupled Neutron-Gamma Multigroup Cross Section Sets," p. 568.

GWIN, R., E. G. SILVER, AND R. W. INGLE, "Measurement of Neutron Fission Cross Sections for ^{239}Pu and ^{235}U from 0.02 eV to 200 keV," p. 481. (1.4)

MORRISON, G. W., R. H. ODEGAARDEN, AND E. A. STRAKER, "The Use of the MORSE Monte Carlo Code to Solve Shielding and Criticality Problems of Spent Fuel Casks," p. 547.

MORRISON, G. W., E. A. STRAKER, AND R. H. ODEGAARDEN, "A Coupled Neutron and Gamma-Ray Multigroup Cross Section Library for Use in Shielding Calculations," p. 535.

PEREY, F. G., "Fast Neutron Scattering," p. 490.

PEREZ, R. B., G. de SAUSSURE, AND W. KOLAR, "Multilevel Analysis of the ^{235}U Fission and Capture Cross Sections," p. 476. (1.10)

ROUSSIN, R. W., R. G. ALSMILLER, JR., AND J. BARISH, "Coupled Transport Calculations through Concrete for High Energy Neutron Sources," p. 561.

SANTORO, R. T., AND R. G. ALSMILLER, JR., "Depth-Dose Distributions in a Tissue Phantom Shielded from Galactic Cosmic-Ray Protons," p. 557. (4.12)

SANTORO, R. T., R. G. ALSMILLER, JR., AND J. BARISH, "The Validity of Using Primary Particles Only in Van Allen Belt and Solar-Flare Proton Shielding Studies," p. 556.

WESTON, L. W., AND J. H. TODD, "Neutron Fission and Absorption Cross Section Measurements for ^{239}Pu and ^{241}Pu," p. 480. (1.3)

Informal Session of Reactor Physics Division, American Nuclear Society Meeting, Las Vegas, Nevada, June 19–22, 1972.

PEREZ, R. B., AND G. de SAUSSURE, "The Generation of Kapur-Peierls Parameters from *R*-Matrix Parameters by the Invariant Embedding Techniques." (1.11)

SILVER, E. G., R. W. INGLE, G. de SAUSSURE, R. B. PEREZ, H. WEAVER, AND R. J. ROBSON, "The 150-Meter Time-of-Flight Facility at ORELA." (1.7)

ORNL-4800
UC-34 – Physics

INTERNAL DISTRIBUTION

1. Biology Library
2–4. Central Research Library
5. ORNL – Y-12 Technical Library
Document Reference Section
6–50. Laboratory Records Department
51. Laboratory Records, ORNL R.C.
52. L. S. Abbott
53. F. S. Alsmiller
54. R. G. Alsmiller, Jr.
55. T. W. Armstrong
56. J. Barish
57. D. E. Bartine
58. S. E. Beall
59. H. W. Bertini
60. F. E. Bertrand
61. N. Betz
62. B. L. Bishop
63. R. S. Booth
64. A. R. Buhl
65. H. P. Carter
66. K. C. Chandler
67. R. L. Childs
68. G. T. Chapman
69. F. H. Clark
70. H. C. Claiborne
71. C. E. Clifford
72. W. C. Colwell
73. H. E. Comolander
74. S. N. Cramer
75. A. H. Culkowski
76. F. L. Culler
77. F. T. DeLorenzo
78. G. de Saussure
79. J. K. Dickens
80. M. B. Emmett
81. W. W. Engle, Jr.
82. G. F. Flanagan
83. W. E. Ford III
84. R. M. Freestone, Jr.
85. C. Y. Fu
86. T. A. Gabriel
87. J. S. Gillen
88. F. G. Gillespie
89. N. M. Greene
90. M. L. Gritzner
91. E. E. Gross
92. J. Gurney
93. M. P. Guthrie
94. R. Gwin
95. W. O. Harms
96. J. A. Harvey
97. H. R. Hendrickson
98. K. M. Henry, Jr.
99. R. F. Hibbs
100. N. W. Hill
101. T. J. Hoffman
102. L. B. Holland
103. J. L. Hull
104. R. W. Ingle
105. J. D. Jenkins
106. W. H. Jordan
107. W. E. Kinney
108. D. C. Larson
109. J. Lewin
110. T. A. Lewis
111. J. L. Liverman
112. C. T. Long
113. T. A. Love
114. J. L. Lucius
115. R. L. Macklin
116. R. E. Maerker
117–191. F. C. Maienschein
192. J. J. Manning
193. B. F. Maskewitz
194. J. W. McConnell
195. B. J. McGregor
196. C. O. McNew
197. J. N. Money
198. G. L. Morgan
199. G. W. Morrison
200. F. J. Muckenthaler
201. F. R. Mynatt
202. E. M. Oblow
203. J. V. Pace III
204–205. R. B. Parker
206. R. W. Peelle
207. S. K. Penny
208. A. M. Perry
209. C. M. Perey
210. F. G. Perey
211. R. B. Perez
212. V. Rado

213. W. A. Rhoades
214. R. J. Robson
215. R. W. Roussin
216. R. T. Santoro
217. E. G. Silver
218. M. J. Skinner
219. A. H. Snell
220. P. N. Stevens
221. D. Sundberg
222. H. A. Todd
223. J. H. Todd
224. D. K. Trubey
225. J. W. Wachter
226. D. R. Ward
227. H. Weaver
228. A. M. Weinberg
229. L. W. Weston
230. J. E. White
231. G. E. Whitesides
232. L. R. Williams
233. R. R. Winters
234. A. Van der Woude
235. J. B. Wright
236. R. Q. Wright
237. W. Zobel
238. H. Feshbach (Consultant)
239. H. Goldstein (Consultant)
240. C. R. Mehl (Consultant)
241. H. T. Motz (Consultant)

EXTERNAL DISTRIBUTION

242. P. B. Hemmig, Division of Reactor Development, U. S. Atomic Energy Commission, Washington, D. C. 20545
243. W. H. Hannum, Reactor Physics Branch, U. S. Atomic Energy Commission, Washington, D. C. 20545
244. K. O. Laughon, U. S. Atomic Energy Commission, Oak Ridge, Tennessee 37830
245. C. P. McCallum, Division of Space Nuclear Systems, U. S. Atomic Energy Commission, Washington, D. C. 20545
246. F. A. R. Schmidt, Institute for Kernenergetik, Stuttgart, GERMANY
247. W. Kolar, Central Bureau for Nuclear Measurements, Euratum, Geel, BELGIUM
248. Mohammed Abdow, Nuclear Engineering Department, University of Wisconsin, Madison, Wisconsin
249. V. S. Barashenkov, Joint Institute for Nuclear Research, Dubna, USRR
250. K. Chen, Brookhaven National Laboratory, Upton, New York
251. G. Friedlander, Brookhaven National Laboratory, Upton, New York
252. G. D. Harp, Brookhaven National Laboratory, Upton, New York
253. A. S. Iljinov, Joint Institute for Nuclear Research, Dubna, USRR
254. J. M. Miller, Columbia University, New York, New York
255. V. D. Toneev, Brookhaven National Laboratory, Upton, New York
256. J. D. Hunt, Sioux Falls College, Sious Falls, South Dakota 57101
257. Y. Shima, Soreq Nuclear Research Center, Yavne, ISRAEL
258. W. R. Burrus, Tennecomp, Inc., Oak Ridge, Tennessee
259. A. Zucker, National Academy of Sciences, 2101 Constitution Avenue, Washington, D. C. 20418
260. R. H. Baldry, ORTEC, Inc., Oak Ridge, Tennessee 37830
261. H. W. Parker, Marshall Space Flight Center, Huntsville, Alabama
262. J. L. Rathbun, Westinghouse Electric Corporation, Advanced Reactor Division, Waltz Mill Site, Madison, Pa. 25663
263. E. A. Straker, Science Applications, Inc., Clinton Bldg., Suite 432, 2109 Clinton Avenue West, Huntsville, Alabama 35805
264. C. E. Burgart, Science Applications, Inc., 122 LeVeta Drive, Albuquerque, N. M. 87108
265. H. T. Smith, Science Applications, Inc., 2109 Clinton Avenue West, Huntsville, Alabama 35805
266. M. Solomito, 3699 South Galloway Drive, Memphis, Tennessee
267. B. J. Allen, Australian Atomic Energy Commission, Lucas Heights, AUSTRALIA
268. K. J. Yost, Purdue University, Lafayette, Indiana

269–391. Given DNA Transport Distribution
392–396. Given SNAP Distribution
397–441. Given Special NPD Annual Distribution
442–578. Given NASA/High-Energy Distribution
579. Research and Technical Support Division, AEC, ORO
580. Patent Office, AEC, ORO
581–808. Given distribution as shown in TID-4500 under Physics category (25 copies – NTIS)